Numerical Simulation of Saltwater Upconing at the Siefkes Site, Stafford County, Kansas

Tainshing Ma

Marios Sophocleous

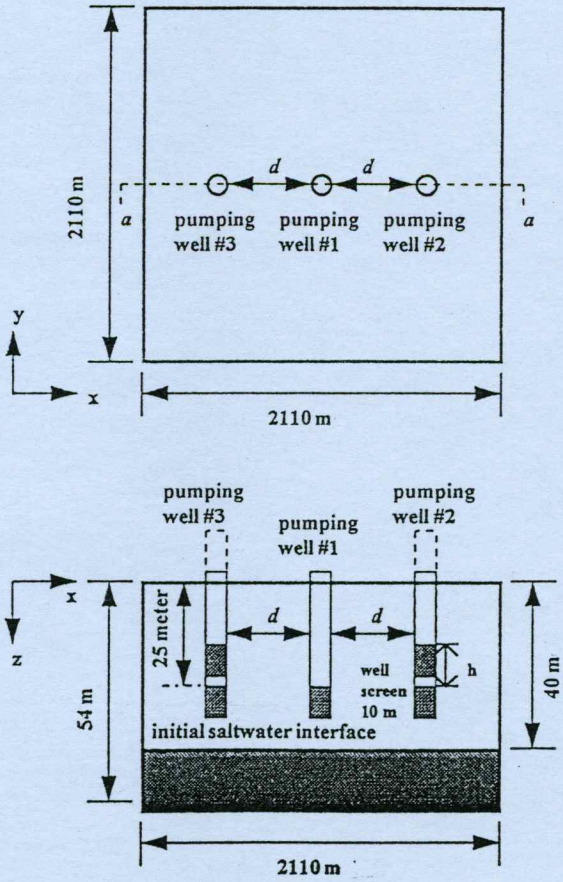

Kansas Geological Survey, Open-File Report 95-40

Lawrence, KS July, 1995

KANSAS GEOLOGICAL SURVEY
OPEN-FILE REPORT 95-40

NUMERICAL SIMULATION OF SALTWATER UPCONING AT THE SIEFKES SITES, STAFFORD COUNTY, KANSAS

by

Tainshing Ma
Marios Sophocleous

Disclaimer

The Kansas Geological Survey does not guarantee this document to be free from errors or inaccuracies and disclaims any responsibility or liability for interpretations based on data used in the production of this document or decisions based thereon. This report is intended to make results of research available at the earliest possible date, but is not intended to constitute final or formal publications.

Kansas Geological Survey
1930 Constant Avenue
University of Kansas
Lawrence, KS 66047-3726

TABLE OF CONTENTS

Executive Summary

The Mineral Intrusion Project is a research effort to understand the hydrologic, water-quality, and water-resource management implications of natural saltwater intrusion into the freshwater Great Bend Prairie aquifer in the eastern portion of Groundwater Management District No. 5 (GMD5). In much of this area a bedrock aquifer of Permian age is in direct hydraulic connection with the base of the Great Bend Prairie (alluvial) aquifer. This connection, which in most other parts of the state is blocked by intervening confining layers of low permeability, permits the brines that are found naturally in the Permian bedrock to move upward and contaminate the freshwater of the overlying aquifer.

In order to support efficient use and management of water resources in the area, the Mineral Intrusion Project includes among its objectives both an understanding of regional controls on the saltwater interface and its responses to ground-water withdrawal, and research into the local effects of high-volume pumping on the depth and characteristics of the saltwater interface. In this progress report we investigate the dynamics of the ground-water system and the saltwater-freshwater interface in response to seasonal irrigation pumping and recharge using numerical modeling. The purpose of this modeling is to obtain an understanding of how the sources and discharges of salt, the aquifer parameters, and surrounding (boundary) conditions interact to cause ground-water flow patterns and consequent brine movement in the system under investigation.

An intensive study site, known as the Siefkes site, was established for detailed investigation; the site is centered on an irrigation well in the southeast quarter of section 27, Township 21S, Range 12W, in northeastern Stafford County that becomes progressively more salty during the pumping season. A sophisticated three-dimensional numerical finite-difference model, known as SWIFT-II, is employed for the numerical modeling using data from the Siefkes field site.

To understand the basic characteristics of the upconing phenomenon and the impact of additional wells on saltwater intrusion, we numerically simulated saltwater upconing under one, two, and three pumping wells. Because of the limited number of field data, we encountered some difficulties in using geostatistical techniques for estimating the aquifer parameters. A sensitivity

analysis was therefore performed to investigate the effect of aquifer and other model input parameters on saltwater upconing. The numerical models were calibrated based on the measured profile of chloride concentration at the Siefkes site, and then projected 10 years into the future to predict the salinity of the discharged ground water in relation to pumping rate and recharge.

In this analysis we first investigate the importance of the following parameters on saltwater intrusion based on the Siefkes site prototype: horizontal (radial) and vertical aquifer hydraulic conductivity, longitudinal and transverse dispersivities (mixing parameters), aquifer porosity, ground-water recharge, ground-water pumping rate, location of well screen, and a number of clay layers interspersed within the aquifer. We also investigated two different sources of salinity: one local source, originating from the aquifer bottom, and one lateral source, originating from the side boundaries of the simulated Siefkes site.

The results of these conceptual simulations indicate that the spatial distribution and continuity of clay layers is the most important factor controlling flow patterns and salinity distribution. The more continuous and extensive the clays, the more protection against brine intrusion they provide. For the clay distribution and geometry at the Siefkes site, these simulations show that the location of the salinity source (bottom or lateral), the aquifer hydraulic conductivity, the location of the well screen relative to the salinity source, and the pumping rate are the most important parameters governing the saltwater intrusion process at the local scale (a radial distance of nearly 4,000 ft from the pumping well). The dispersion mixing parameters and ground-water recharge (which in this case was almost three to seven times smaller than the pumpage) were the least important parameters as regards brine intrusion. However, increasing recharge to the same level as pumpage or higher increases the significance of recharge vis-a-vis brine intrusion. Such analyses quantify the governing factors of saltwater intrusion, provide insights into the dynamic relationships between saltwater and freshwater in a ground-water system, and help guide the calibration of numerical models for management purposes.

Following this sensitivity analysis, we attempted to calibrate the single-well model (representing the Siefkes irrigation well) based on the observed brine concentrations at the Siefkes

site. The size of the study area and mesh of the model adopted in this study was the same as the one used in the sensitivity analysis. The purpose of this model calibration was to reproduce a simulated brine concentration similar to the measured profile. Because of uncertainties in aquifer parameters and distribution of clay layers, and the simplification of pumping schedule and recharge, a near-perfect match of the simulated results to the measured data was not expected. However, the simulated brine-concentration profiles with a local source of brine from the aquifer base are considered to have a satisfactory match with the measured data.

The calibrated model was then projected 10 years into the future using different recharge and pumping rates, so that the relationship of pumping rate and discharged brine concentration could be obtained. For these simulations, pumping was assumed continuous from May to October in each year, and discontinued during the rest of each year. The results of these 10-year simulations show that high recharge and low pumping rate will alleviate the problem of saltwater intrusion, and that the recovery from saltwater intrusion will be significant because of ground-water recharge during the nonpumping season.

We next investigated the interactions of water salinity under a multi-well pumping system. We again confirmed that clay layers, especially continuous ones over the scale of investigation (approximately 7,000 ft in this case), greatly retard the upward movement of saltwater under a pumping stress. Without the protection of a clay layer, the upconing of saltwater will be highly significant. The impact of two or more wells on saltwater upconing is inversely proportional to their separation distance; as the separation distance approaches 1,600 ft, the interactions become insignificant. This implies that as the separation distance increases to a critical distance, each well behaves independently. As expected, the saltwater upconing on the three-well system is more significant than the two-well system. The increase in the separation distance or the decrease in the pumping rate of nearby irrigation wells will reduce the saltwater problem.

It is important to note that in these multi-well simulations (as well as the ones employed in the sensitivity analysis mentioned earlier), the pumpage employed was continuous during the simulation period, even if the water pumped was highly saline, in order to test system responses.

However, although the single- or two- or three-well simulations by themselves may not correspond exactly to real world pumping schedules, if one considers the large number of wells in the area pumping at different times, the cumulative result would be similar to the simulations presented here.

The three-dimensional simulation of the migration of saltwater under the influence of regional ground-water flow, multiple well-pumpage, and recharge at a larger spatial scale (of the order of miles) is currently underway and will be reported, along with additional modeling analyses, in our next report.

Introduction

The major source of freshwater in the Big Bend Groundwater Management District #5 (GMD5) is provided by the Great Bend Prairie aquifer. The demand for ground water has increased steadily since 1960, a fact which raises a concern that the increasing withdrawal of ground water may cause the decline in the available ground-water supply and the deterioration of water quality in the GMD5.

In this progress report we investigate the dynamics of the ground-water system and the saltwater interface in response to seasonal irrigation pumping and recharge in order to determine 1) the minimum total pumpage which can satisfy the water demand and 2) the discharged ground-water salinity which will meet the requirement for general uses.

The Siefkes site, located in the southeast quarter of section 27, Township 21S, Range 12W, is chosen for detailed study. The ground-water flow at the Siefkes site is stratified with freshwater in the upper region and saltwater near the bedrock. The source of the saltwater is the highly mineralized water of the Permian bedrock. The discharged water from an irrigation well at the Siefkes site encounters increasing salinity problems during the pumping season. The well locations and measurements around the Siefkes site are shown in Fig. 1 and Table 1, respectively. In this report, studies of the basic characteristics of the saltwater upconing phenomenon in response

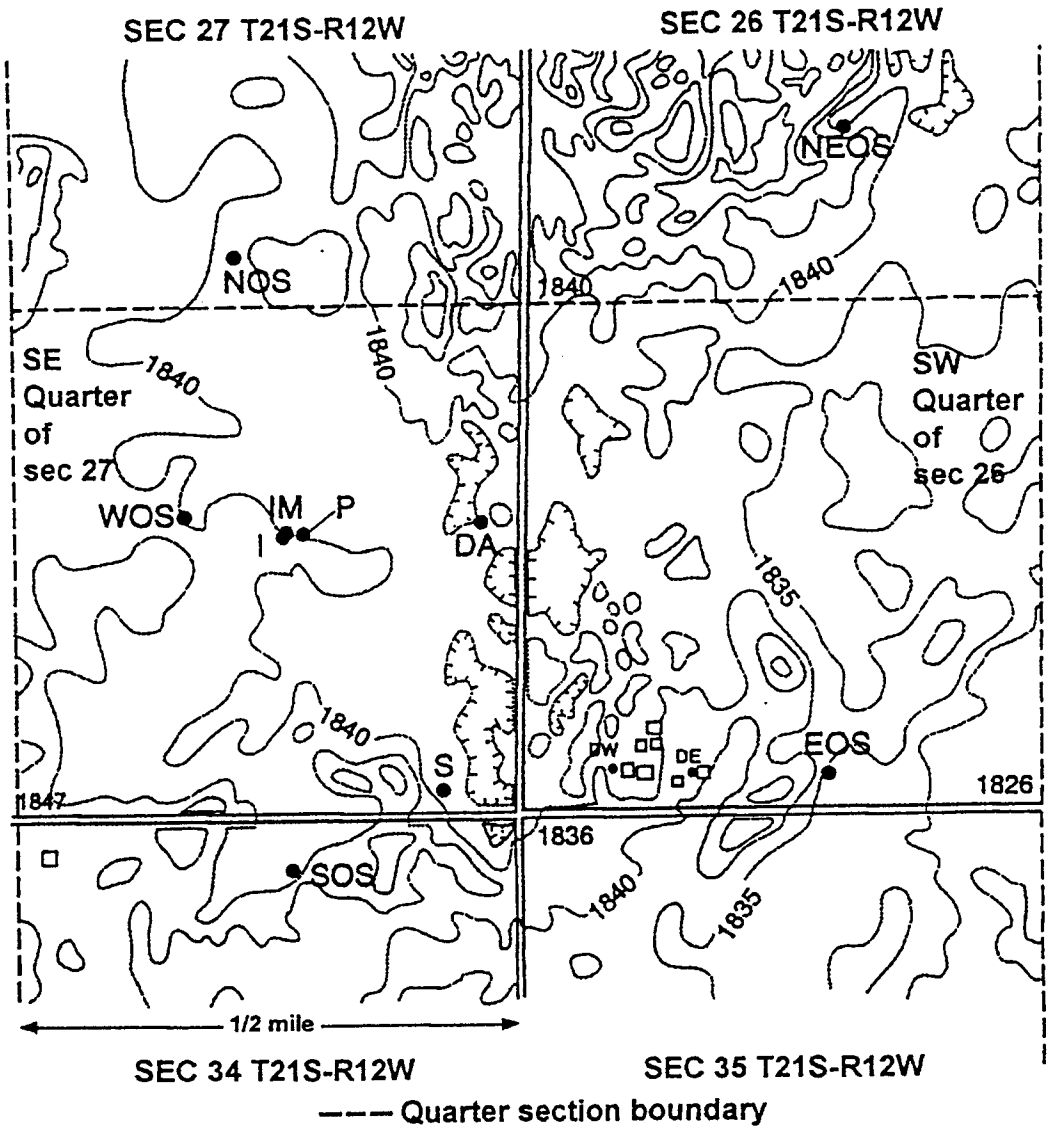

Figure 1. Wells in the Siefkes intensive study area. Contours indicate approximate elevation of land surface (feet above mean sea level).

Table 1. Well locations, characteristics, and measurements around the Siefkes site.

Legal location	Well	Description	Land surface elevation (ft)	Water level elevation (ft)	Date
21-12-27DACC	I	Irrigation well near center of SE Sec. 27 T21S-R12W	1840.7		
21-12-27DBDC	WOS	Oil-field supply well west of irrigation well	1839.4	1825.2 1828.2	3/24/93 5/25/93
21-12-27DACC	IM	2" monitoring well near irrigation well	1840.7	1825.5 1827.9	3/24/93 5/25/93
21-12-27ACDD	NOS	Oil-field supply well north of irrigation well	1839.0	1822.2 1825.2	3/24/93 5/25/93
21-12-27DDDC	S	Stock well southeast of irrigation well	1836.3	1820.3	3/26/93
21-12-34AAB	SOS	Oil-field supply well south of irrigation well	1841.0		
21-12-26CDCC	EOS	Oil-field supply well east of irrigation well	1832.9	1814.3 1816.9	3/26/93 5/25/93
21-12-27DACC	P	KGS Permian monitoring well	1839.6	1816.6 1817.4 1817.6	4/17/93 5/20/93 5/25/93
21-12-27DADD	DA	KGS deep aquifer monitoring well	1839.8	1817.2 1818.9 1819.1	4/17/93 5/20/93 5/25/93
21-12-26BDB	NEOS	Oil-field supply well north-east of irrigation well	1840*	1812.8* 1815.6*	3/27/93 5/25/93

to model input parameters using a single-well model and the behavior of water salinity using multi-well model are conducted using axisymmetrical and three-dimensional numerical models. Two governing differential equations, the ground-water flow equation and the transport equation, are used to describe the saltwater intrusion in aquifers with a freshwater-saltwater transition zone. The finite difference model SWIFT-II (Reeves et al., 1986) is employed to solve these two governing equations. The mathematical model will be calibrated based on the data collected at the Siefkes site, and the calibrated model will be used to simulate a number of management options to provide technical support for management policies promoting the long-term sustainable ground-water supply.

Purpose of Study

The main task in this report is to use a mathematical model, based on the Siefkes site, to study the saltwater upconing in the heterogeneous and unconfined Great Bend Prairie aquifer considering the uncertainties of aquifer parameters and water demand. The specific objectives of this study are:

1. To perform a sensitivity analysis to study the effect of aquifer parameters on predictions of saltwater upconing in a single-well system by using an axisymmetrical model.
2. To study the behavior of saltwater upconing under two- and three-well systems using a three-dimensional finite-difference model, known as SWIFT-II.
3. To calibrate the numerical models employed.
4. To project the results of the calibrated models for a 10-year period to develop preliminary predictions of the salinity of the irrigation-discharged ground water.

Governing Equations for Numerical Model

Saltwater intrusion is a typical density-dependent problem and two approaches are generally employed in analyzing such a problem. One assumes that there exists a sharp interface between saltwater and freshwater without mixing of these two fluids; in this case the assumption is made that

the thickness of the transition zone is small compared to the aquifer thickness. The other is the diffusion-dispersion approach which accounts for a transition zone with continuous variability of salinity created by the mixing of saltwater and freshwater and its dispersion. The latter approach is closer to reality and is adopted in this report.

Density-Dependent Solute-Transport Approach

In this approach, two nonlinear partial differential equations (the ground-water flow equation and the advection-diffusion equation) must be solved simultaneously by iteration. The governing equations are expressed in terms of pressure (p) and intrinsic permeability (κ) because the total head (h) and hydraulic conductivity (K) are functions of density (ρ).

The density-dependent flow is governed by Darcy's law, the conservation of mass balance of fluid and the conservation of solute mass balance in a porous medium. The governing equations, the initial and boundary conditions, are described as follows:

Conservation of Mass Balance of Fluid

The conservation of mass expresses the balance of water and solute mass in a solid matrix. The ground-water equation is based on the conservation of mass coupled with Darcy's law for flow in a porous medium. The general equation is

$$-\nabla \cdot (\rho \underline{u}) - Qw + Rc' = \frac{\partial}{\partial t}(\phi \rho) \qquad (1)$$

where

ρ : fluid density (ML^{-3}).

$\underline{u}$: fluid velocity vector (LT^{-1}).

Qw : sink or source [$(M(L^3T)^{-1}$], a positive sign denotes a sink, a negative sign denotes a source.

ϕ : porosity.

Rc′ : salt dissolution [$(M(L^3T)^{-1}$].

$$\nabla = \left(\frac{\partial}{\partial x}\right) i + \left(\frac{\partial}{\partial x}\right) j + \left(\frac{\partial}{\partial x}\right) k \ .$$

i, j, and k are unit vectors in Cartesian coordinates.

The scalar product of ∇ operator and $\rho \underline{u}$ gives the mass flux per unit volume at each point. The term on the right-hand side of Eq. 1 is an unsteady term which states the rate of change of fluid mass per unit volume. Sinks or sources are used to represent the recharge or discharge wells in the interior grid of the model.

The flow equation is Darcy's law:

$$\underline{u} = \left(\frac{\kappa}{\mu}\right) \cdot (\nabla p - \rho g \nabla z) \qquad (2)$$

where

κ : solid matrix permeability (L^2), a vector quantity.

μ : fluid viscosity [$M(LT)^{-1}$].

g : gravitational acceleration (L/T^2).

z : potential head (L).

Eq. 2 can be written in three principal directions, x, y, and z:

$$u_x = -\frac{k_{xx}}{\mu} \frac{\partial p}{\partial x}$$

$$u_y = -\frac{k_{yy}}{\mu} \frac{\partial p}{\partial y} \qquad (3)$$

$$u_z = -\frac{k_{zz}}{\mu} \left(\frac{\partial p}{\partial z} + \rho g\right)$$

As can be seen in Eq. 3, the specific discharge in x and y directions is caused by a pressure gradient and the specific discharge in the z direction is caused by both a pressure gradient and gravity.

Fluid density is assumed to be a function of salt concentration and pressure, the equation of fluid density is given as

$$\rho = \rho_o \left[1 + C_w(p - p_0) + C_c\hat{C}\right] \tag{4}$$

and

$$C_c = \frac{(\rho_I - \rho_N)}{\rho_0} \tag{5}$$

where

ρ_I : fluid density at reference temperature and pressure at unit brine concentration (M /L^{-3}).

ρ_N : freshwater density at reference temperature and pressure (M /L^{-3}).

ρ_0 : the fluid density for the initial conditions (M /L^{-3}).

$\hat{C}$: local salt concentration (M /L^3).

C_W : compressibility of the water [M/(LT^2)]$^{-1}$.

p : local pressure in the aquifer [M/(LT^2)].

p_0 : reference pressure [M/(LT^2)].

The fluid viscosity depends on the salinity concentration and the temperature of the fluid and is expressed as

$$\mu = \mu_R(\hat{C})\exp\left[B(\hat{C})(T^{-1} - T_R^{-1})\right] \tag{6}$$

where T_R is the reference temperature of rock surrounding the wellbore; the relationship between $\mu_R(C)$ and B(C) is determined from the available viscosity, μ, temperature, T, and concentration, $\hat{C}$, data. The determination of fluid viscosity is discussed by Reeves et al. (1986) and internally included in the SWIFT II code.

Porosity ϕ is a function of pressure p:

$$\phi = \phi_0 \left[1 + C_R(p - p_0)\right] \tag{7}$$

where

ϕ_0 : the dimensionless porosity at the reference pressure.

C_R : the compressibility of the pores (Pa^{-1}).

Conservation of Solute Mass Balance

The solute mass balance is expressed as

$$-\nabla\cdot\left(\rho\,\hat{C}\,\underline{u}\right) + \nabla\cdot\left[\rho\left(D_{i,j} + D_m I\right)\nabla\hat{C}\right] - Q_W\hat{C}_I = \frac{\partial}{\partial t}\left(\phi\,\rho\,\hat{C}\right) \tag{8}$$

where

D_m : molecular diffusivity (L^2T^{-1})

$D_{i,j}$: dispersion tensor (L^2T^{-1})

I : identity tensor

The above equation describes the rate of change of solute in the fluid phase in terms of the net dispersive and diffusive flux, the net advective flux, and the solute source or injection rate.

The dispersion coefficient is originally from Bear (1961) and Scheidegger (1961). For an isotropic porous medium, the dispersion tensor $D_{i,j}$ is a function of velocity of ground-water flow and can be expressed by the longitudinal dispersivity α_L (m) and the transverse dispersivity α_T (m):

$$D_{ij} = (\alpha_L - \alpha_T)\frac{u_i u_j}{u} + \alpha_T u \delta_{ij} \qquad (9)$$

where

$u_i(x,y,t)$: velocity in the i direction.

δ_{ij} :Kronecker delta function.

$u = \left(u_1^2 + u_2^2 + u_3^2\right)^{1/2}$

i and j are unit vectors in the Cartesian coordinates.

Initial and Boundary Conditions

For the problem of interest, supplementary information (initial and boundary conditions) has to be provided in order to obtain a solution of the above equations. The boundary and initial conditions specify that the dependent variables are known functions of space and time in the simulated domain. The boundary conditions can be generally classified into three types: Dirichlet, Neumann, and Cauchy.

The hydrostatic equilibrium is assumed for the initial pressure distribution. However, if the constant Darcy flux is specified as the initial condition, Eq. 2 will be employed to adjust the hydrostatic pressure. In addition, brine concentration is initially specified at appropriate locations to represent the initial saltwater distribution.

The initial and boundary conditions and the above two partial differential equations (Eq. 1 & Eq. 8) are solved by the finite-difference scheme to determine the piezometric heads and the concentrations at nodes inside the aquifer boundary.

The numerical algorithm and its associated computer code employed in this study is referred to as SWIFT II (Reeves et al., 1986). Numerical procedures for solving the governing equations

require an appropriate mesh in space, as well as time, steps. The set of linear equations generated by spatial discretization have to be solved repeatedly as the simulation time advances. To solve the partial differential equations (Eqs. 1 & 8) by using the finite difference technique, the two-line, successive overrelaxation method (Varga, 1962) is employed. It is a block-iterative method; an optimal overrelaxation factor is firstly estimated to increase convergence, then two neighboring lines of nodes are oriented and solved together by direct elimination. Once the optimal relaxation parameters and the optimal directions are determined at the time step for each transport equation, a convergent solution can be achieved. Although this matrix solver is efficient, numerical dispersion and oscillations will occur and accumulate at each time step due to the truncation of the high order derivatives of the Taylor series. The finite difference equations are considered to be stable if the numerical dispersion and oscillations are less than a certain tolerance. The numerical instability comes mainly from the diffusion-convection equation (Price et al., 1966); therefore, stability analysis is preferable before the numerical simulation is initiated.

A general guide to avoid numerical problems is to check the Courant number (Co) that controls numerical oscillations from the discrete approximation of the time derivative, and the Peclet number (Pe) that controls oscillations from spatial discretization. These two constraints provide a general guide for the selection of the local grid spacing in x, y, and z directions and for the time step Δt (Frind, 1982). These two criteria corresponding to the x coordinate direction are:

$$Co_x = \frac{u_x \Delta t}{\Delta x} \leq 1 \tag{10}$$

$$Pe_x = \frac{u_x \Delta x}{D_{xx}} \leq 2 \tag{11}$$

The same criteria also apply to y and z coordinate directions. For multi-dimensional transport, stability criteria are functions of variables in all directions.

Modeling Saltwater Upconing Beneath Pumping Wells

To understand the basic characteristics of the upconing phenomenon and the interaction of water salinity under multi-well systems, we numerically simulated saltwater upconing under one, two, and three pumping wells. Because of limited field data, we encountered some difficulties in using geostatistic techniques for estimating the aquifer parameters. A sensitivity analysis is performed to investigate the effect of aquifer parameters on saltwater upconing. The numerical models are calibrated based on the measured profile of chloride concentration at the Siefkes site and then projected 10 years into the future to predict the salinity of the discharged ground water in terms of pumping rate and recharge. A second-order corrected central difference approximation in both time and space is used to eliminate numerical dispersion with carefully chosen grid size and time step during the simulations. It is important to note that in the simulations presented in this report, the pumpage employed was continuous during the simulation period even if the water pumped was highly saline in order to test the system responses. However, although the single- or two- or three-well simulations by themselves may be not correspond to real world pumping schedules, if one considers the large number of wells in the area pumping at different times, the cumulative result would be similar to the simulations presented here.

Sensitivity Analysis of Saltwater Upconing Beneath a Single Pumping Well

The sensitivity analysis is performed by adopting an axisymmetrical flow geometry using the density-dependent solute-transport SWIFT-II model; this model discretizes the partial-differential equations and boundary conditions in time and space into the cylindrical coordinate system to investigate the saltwater upconing under a single pumping well. The physical system of the simulated area is shown in Figs. 2A and 2B (Fig. 2B is the simulated area near the pumping well). With regards to the impact of clay layer stratigraphy on saltwater intrusion, we evaluated a continuous clay-layer, a discontinuous clay layer, and no clay layer. The physical system for the continuous clay-layer case and the discontinuous clay-layer case are shown in Figs. 2C and 2D,

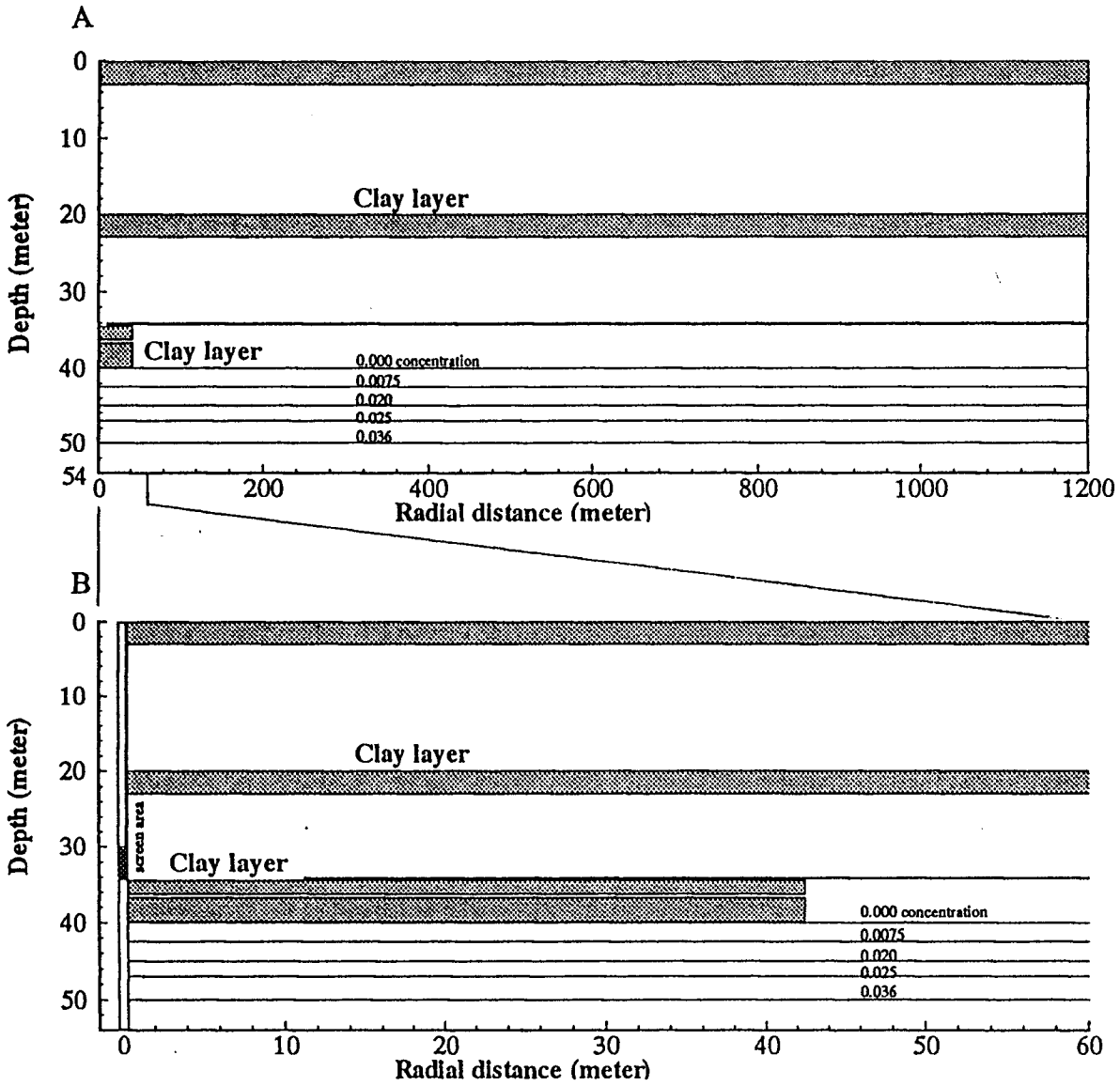

Figure 2. A. The physical system of the conceptual model with clay layers interspersed in the aquifer for salt water upconing simulation.
B. Area near the pumping well at an expanded scale.

C. Continuous clay layer

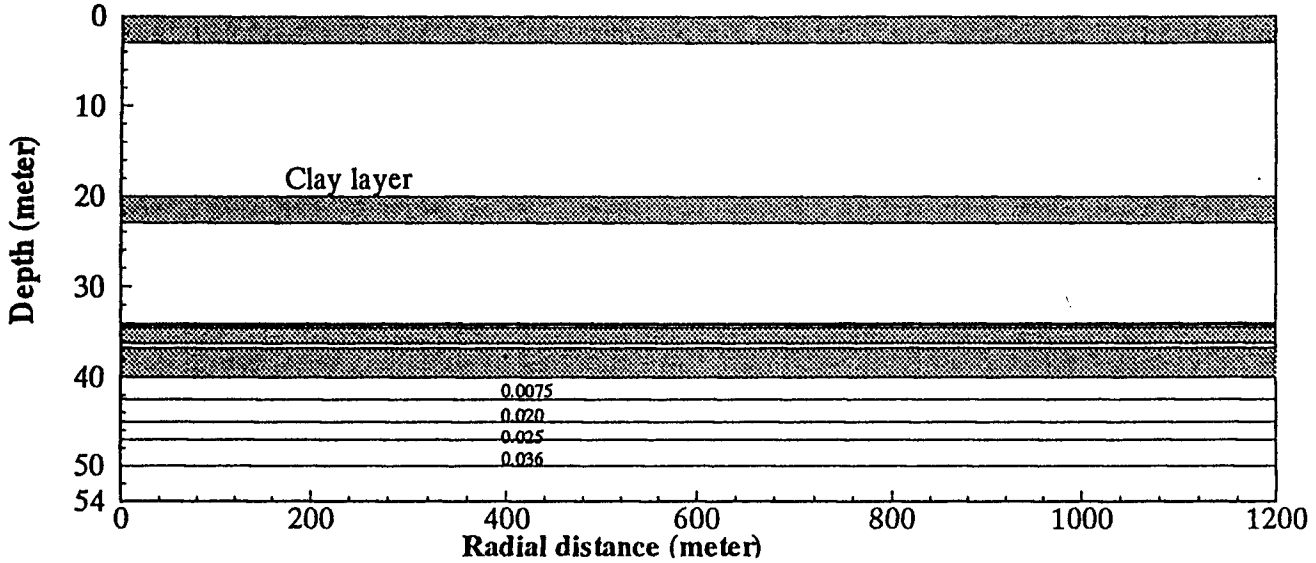

D. Discontinuous clay layer

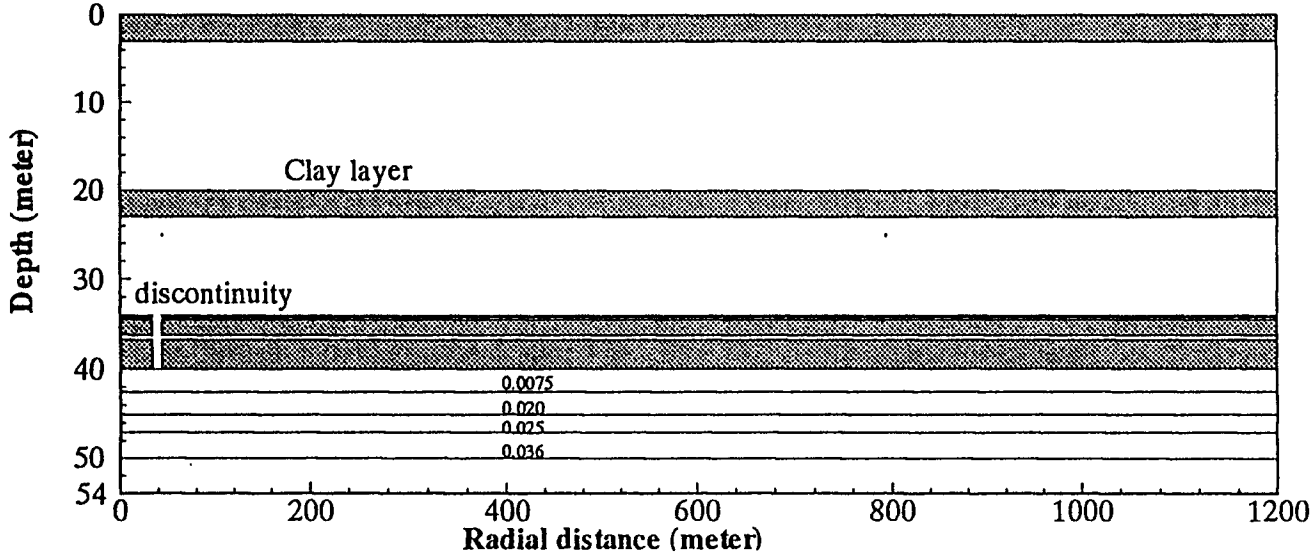

Figure 2. C. The physical system of the conceptual model with continuous clay layers.
D. The physical system of the conceptual model with discontinuous clay layers.

respectively. In the discontinuous clay-layer case, we assumed that there is a 10-meters-wide discontinuity located 33 meters from the pumping well. The whole area is 1200 meters by 54 meters with low-permeability clay layers interspersed in the aquifer. The mesh of the simulated area consisted of 34 rows by 95 columns (Fig. 3). In the radial direction, 34 nodes are used with variable spacing ranging from 0.4 meter to 200 meters. In the vertical z direction, 95 nodes are used with variable spacing composed of 1 meter in the top 24 rows, 0.5 meter in the following 12 rows, 0.25 meter in the next 30 rows, 0.5 meter in the following 10 rows, and 1 meter for the rest. The pumping well has a radius of 0.4 meter with the center at radius equal to zero. The well is screened from 30 to 34 meters below the initial water table. Results are presented graphically in terms of the average brine concentration versus time. Brine concentration is calculated by dividing the total mass of discharged salt during each time step by the total mass of pumpage during the same period. In the SWIFT model, freshwater concentration of density of 1,000 kg/m^3 is taken as zero, whereas the brine concentration of the Permian fluids in the area, which have an average density of 1,036 kg/m^3, is taken as 0.036. This brine concentration of 0.036 corresponds to a chloride concentration of 28,000 mg/L. Therefore, a fluid concentration of 500 mg/L chloride, which is the approximate limit of usable water concentration, would correspond to a brine concentration of 0.036 x (500/28,000) $\approx$ 0.00064.

Nine simulation cases are considered in this report and summarized in Table 2. Two different boundary conditions are assumed for each case. One assumes that the brine concentration and fluid pressure at the bottom of the aquifer are constant (bottom boundary condition). Brine concentration and fluid pressure also are assumed to be constant at the side (side boundary condition). The initial water-table condition is assumed to be horizontal and is allowed to vary due to the change of fluid pressure. Saltwater initially starts at 40 meters below the initial water table with depth-varying brine concentration from 0.0 to 0.036.

Case #1 is used as a reference model. The values of variables and parameters and the boundary conditions used in Case #1 are summarized in Table 3 and Table 4, respectively. The total simulation period is one year and a constant, continuous pumpage of 800 gpm is applied

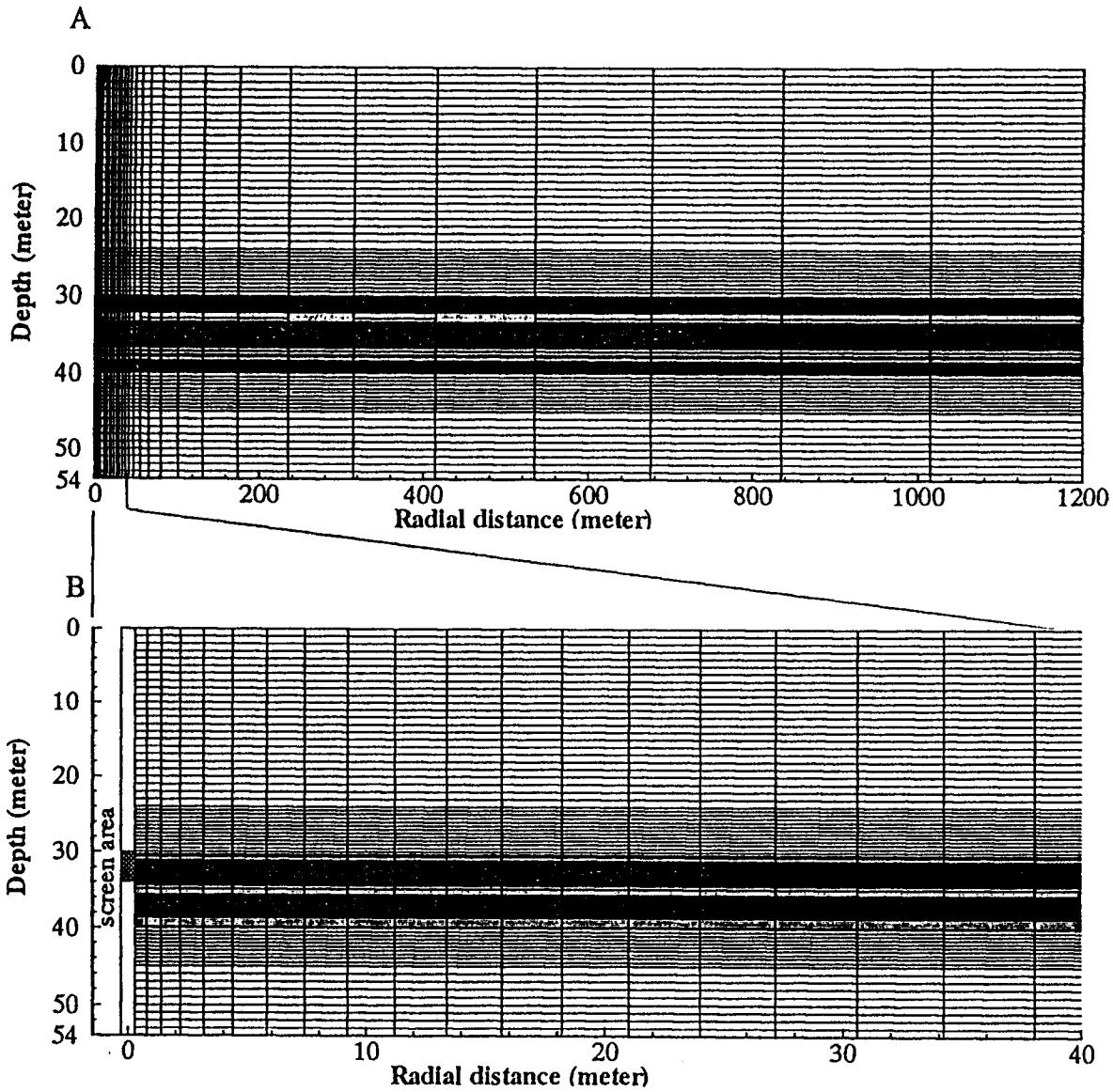

Figure 3. A. Mesh of the conceptual axisymmetrical model.
B. Mesh near the pumping well.

Table 2. Simulation cases in the axisymmetrical numerical model for saltwater-upconing simulation.

Case No.	Descriptions
1.	Single pumping well(reference case). The input parameters, variables, and boundary conditions are described in Tables 3 and 4, respectively.
2.	Investigation of the effect of the radial conductivity, Kr, by changing the Kr from 2.3 m/day to 230 m/day (7.5 ft/day to 750 ft/day).
3.	Investigation of the effect of the vertical conductivity, Kz, by changing the Kz from 0.23 m/day to 23 m/day (0.75 ft/day to 75 ft/day).
4.	Investigation of the effect of the longitudinal dispersivity, α_L, by changing the α_L from 0.1 m to 10 m (0.33 ft to 33 ft).
5.	Investigation of the effect of the transverse dispersivity, α_T, by changing the α_T from 0.01 m to 1 m (0.033 ft to 3.3 ft).
6.	Investigation of the effect of the location of well screen by elevating the location of well screen 10 m and 20 m from the reference model.
7.	Investigation of the effect of the porosity, ϕ, by changing the ϕ from 0.05 to 0.25.
8.	Investigation of the effect of various recharge amount by imposing 0.05 m/year and 0.127 m/year (2 in./year and 5 in./year) recharge to the aquifer.
9.	Investigation of the effect of the pumpage by changing the pumpage from 0.01 m^3/s to 0.09 m^3/s (160 gpm to 1440 gpm).
10.	Investigation of the effect of the spatial distribution of clay layers. A continuous clay layer, a discontinuous clay layer, and no clay layer are considered.

Table 3. Variables and parameters used in the numerical model (case # 1, Table 2) for saltwater upconing.

Aquifer, Fluid, and other Parameters	
radial hydraulic conductivity	Kr = 23 m/d (75 ft/d)
vertical hydraulic conductivity	Kz = 2.3 m/d (7.5 ft/d)
porosity	$\phi = 0.15$
bulk porous matrix compressibility	$\alpha = 2.58 \times 10^{-7}[kg/(m\ s^2)]^{-1}$
water compressibility	$\beta = 4.40 \times 10^{-10}[kg/(m\ s^2)]^{-1}$
solute molecular diffusivity	$D_m = 1.0 \times 10^{-10}\ m^2/s$
longitudinal dispersivity	$\alpha_L = 1$ m
transverse dispersivity	$\alpha_T = 0.1$ m
fluid (water) density	$\rho_o = 1{,}000\ kg/m^3$
brine density	$\rho = 1{,}036\ kg/m^3$
solid grain density	$\rho_s = 2{,}650\ kg/m^3$
fluid (water) viscosity	$\mu = 1.0 \times 10^{-3}\ kg/(m\ s)$
initial fluid (freshwater) salt concentration	$C_0 = 0$
initial brine fluid salt concentration	C (r,z,0); variable
initial specified pressure at the boundary	p(r, z, 0); variable
saturated thickness	b = 54 m
depth to freshwater/saltwater interface	40 m
depth to Permian boundary	54 m
volumetric pumping rate	$Q_p\ (m^3/s)$; variable
gravitational acceleration	$g = 9.81\ m/s^2$
total simulation time	1 yr.
recharge	no
well-screen depth location	30 to 34 m

Clay Layer Properties

Location (m)	Thickness (m)	Kr (m/s)	Kz (m/s)	Porosity
0-3	3	0.23	0.0023	0.25
20-23	3	0.23	0.023	0.25
34-34.25	0.25	0.0023	0.00023	0.25
34.75-36.25	1.5	0.46	0.028	0.25
37-40	3	4.6	0.092	0.25

Table 4. Two types of boundary conditions used in axisymmetrical saltwater-upconing model.

Type 1 (side-boundary condition)

Top	Bottom	Outer radius	Inner radius
streamline (no flow)	no flow	constant pressure & brine concentration	specified volumetric flux at well Q_p (m^3/s)

Type 2 (bottom-boundary condition)

Top	Bottom	Outer radius	Inner radius
streamline (no flow)	constant pressure & brine concentration	no flow	specified volumetric flux at well Q_p (m^3/s)

throughout the whole simulation period. The patterns of flow line under the above two boundary conditions at the 300th simulation day are compared and shown in Fig. 4. The brine concentration contours for both boundary conditions at the 300th simulation day are shown in Fig. 5 (note that the spatial scale in Fig. 5 is different from the one in Fig. 4). As can be seen, if the fluid pressure and brine concentration are fixed at the bottom of the aquifer, that is, the source of salt is from the local upward flux, the upward flux is more significant; consequently, the upward movement of saltwater upconing will become more significant.

Case #2 investigates the effect of radial conductivity by changing the values of radial conductivity from 2.3 m/d to 230 m/d. Case #3 investigates the effect of vertical conductivity by changing the values of vertical conductivity from 0.23 m/d to 23 m/d. The results for Cases #2 and #3 under two different boundary conditions are shown in Figs. 6 7, respectively. The hydraulic conductivity can vary several orders of magnitude in some cases and is usually considered as the most uncertain parameter. In Case #2, the mixing of freshwater and saltwater is dominated by the radial conductivity. The higher the radial conductivity, the more significant mixing of freshwater and saltwater. As can be seen in Fig. 6, the mixing process will dilute the brine concentration; this makes the upconing of saltwater less significant. Figs. 8 and 9 are the comparison of the brine-concentration contours of two radial-conductivity values, 2.3 m/d and 230 m/d, for the bottom and side boundary conditions, respectively. As can be seen, the lower radial conductivity causes the saltwater to advance more significant than the higher radial conductivity due to less mixing of freshwater and saltwater; therefore, the upconing of the saltwater is inversely controlled by the radial conductivity (also demonstrated in Fig. 6). In Case #3, increasing vertical conductivity will increase the vertical velocity; consequently, the velocity of saltwater upconing also will be increased. That is, the saltwater upconing is directly controlled by the vertical conductivity, and this is also demonstrated by the results shown in Fig. 7 .

Case #4 investigates the effect of longitudinal dispersivity, α_L, by changing the values of α_L from 0.1 m to 10 m. Case #5 investigates the effect of transverse dispersivity,

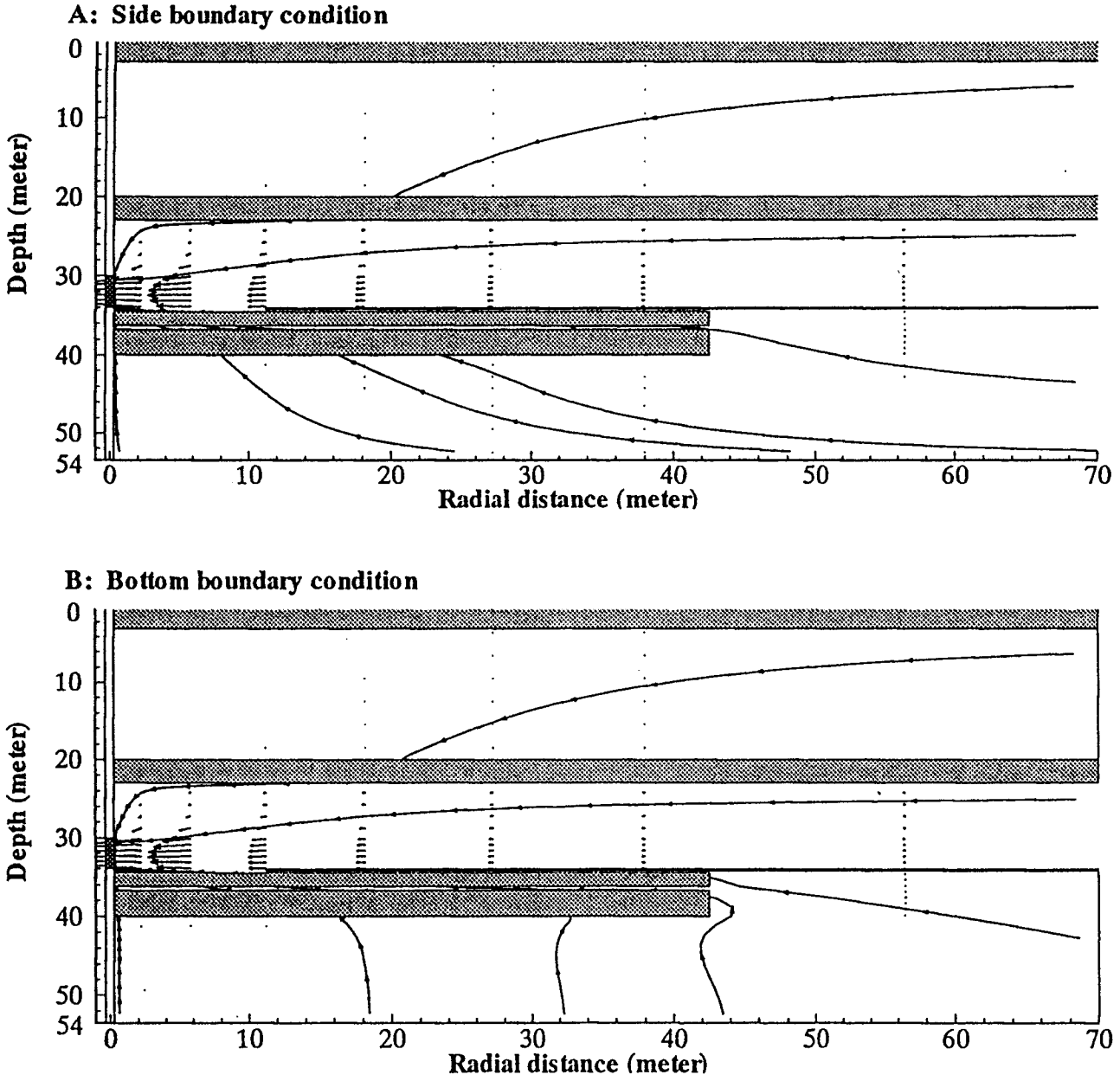

Figure 4. Comparison of flow line pattern under side and bottom boundary conditions at the 300th day after pumping started for case #1.

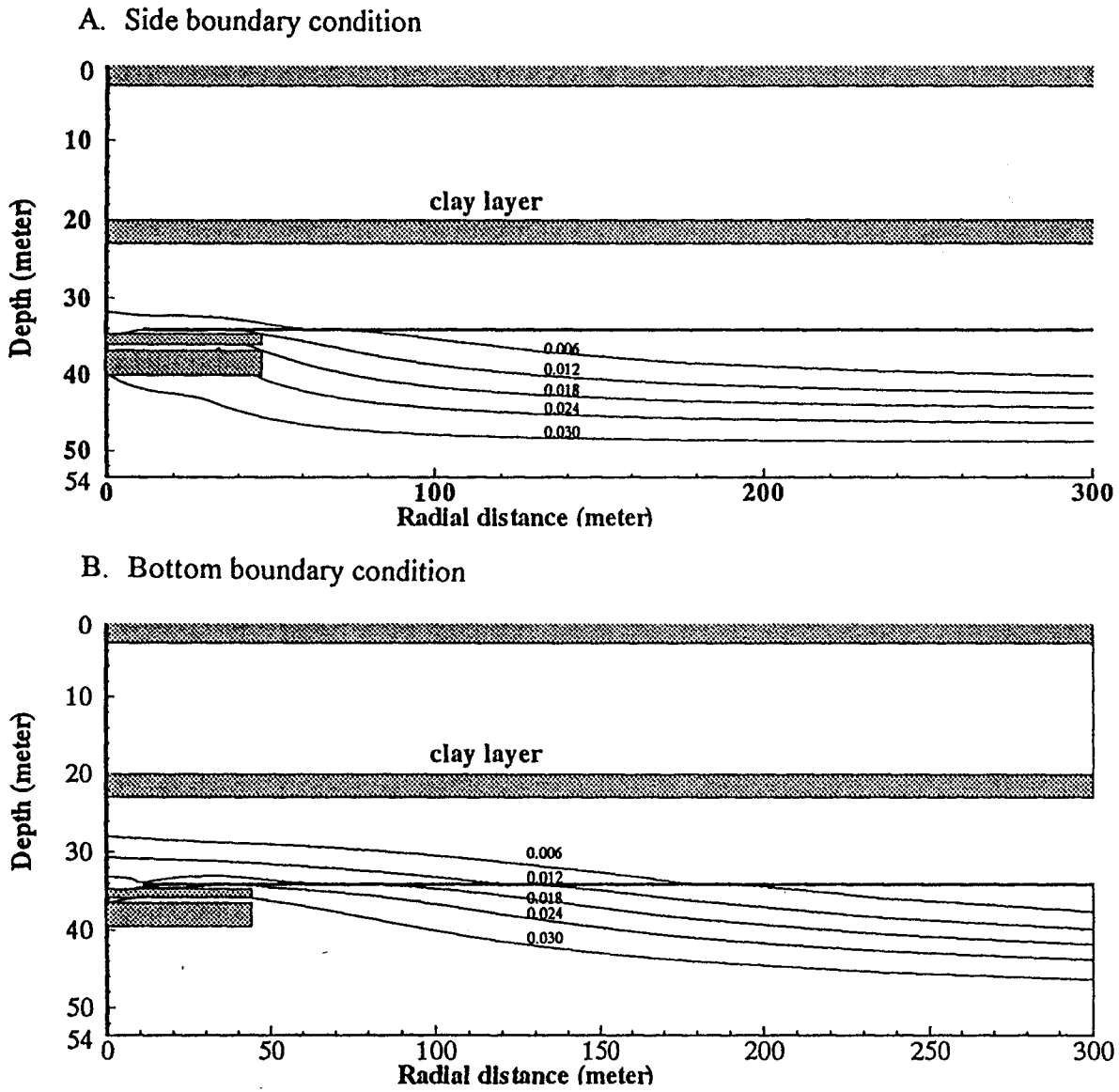

Figure 5. Comparison of brine-concentration contours for side and bottom boundary conditions at the 300th day after pumping started for Case #1 (0.036 brine concentration is equivalent to 28,000 mg/L chloride concentration).

A: Side boundary condition

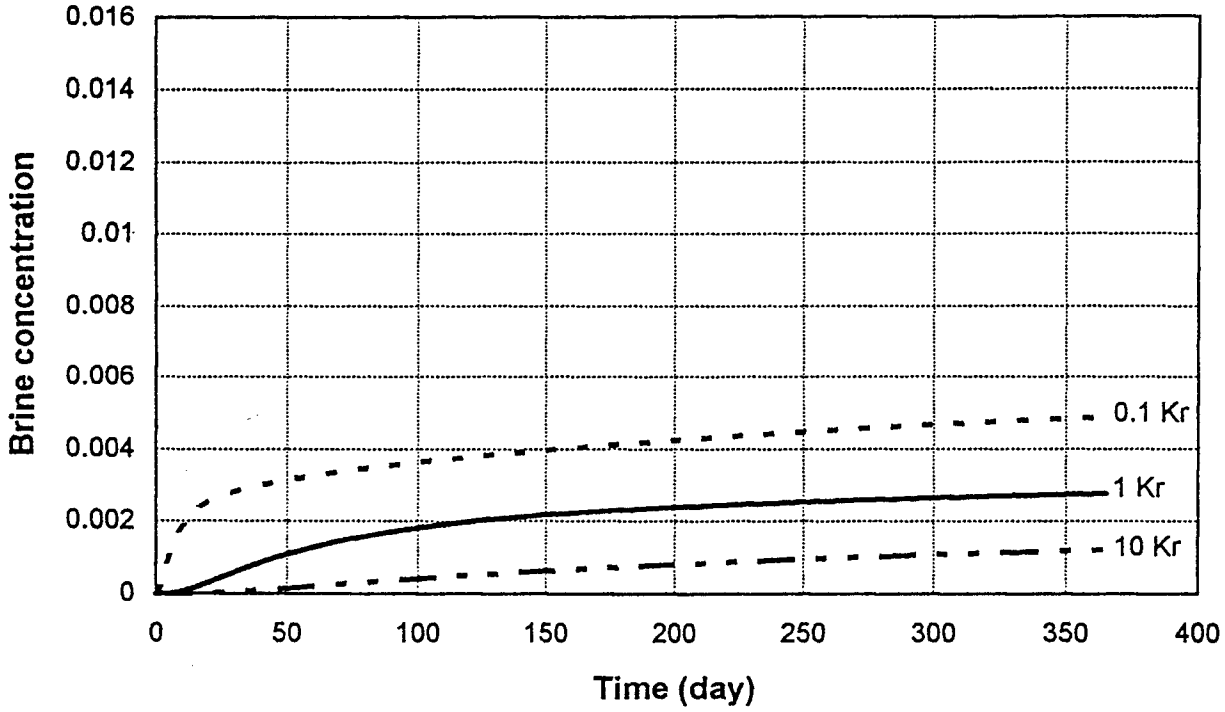

B: Bottom boundary condition

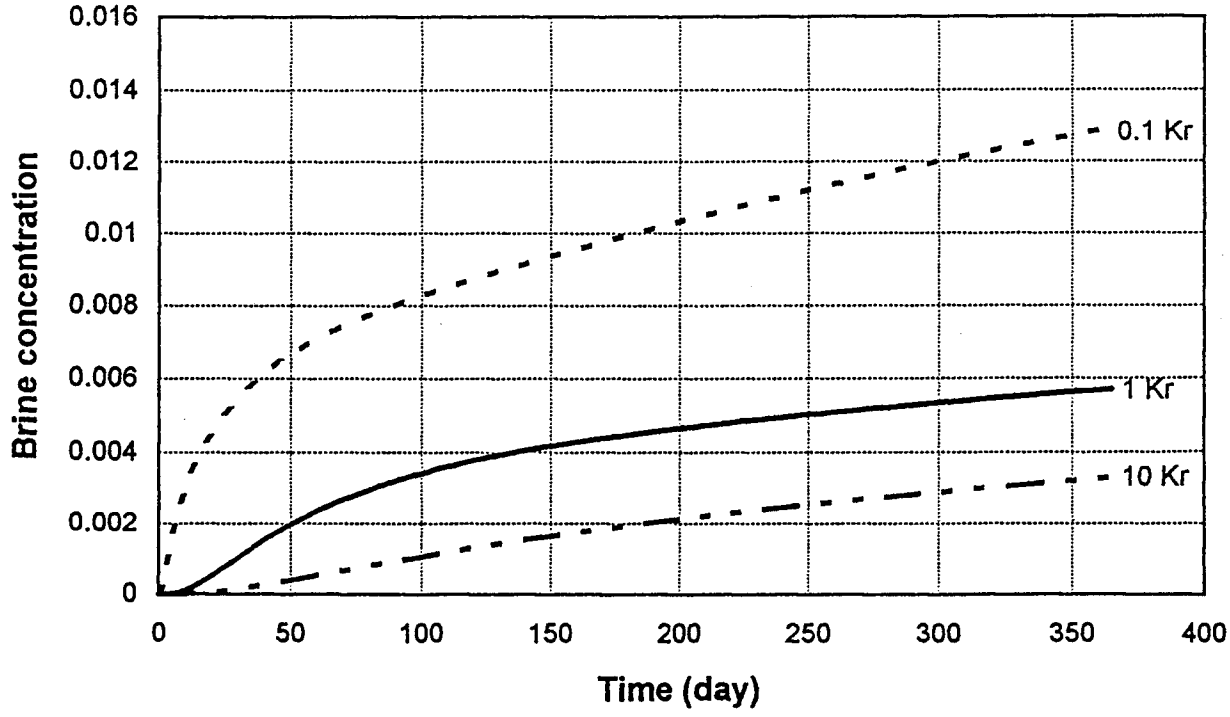

Figure 6. Comparison of discharged brine concentration vs. time for the simulated system with three different radial hydraulic conductivity values (Kr), where Kr = 23 m/d.
(0.036 brine concentration is equivalent to 28,000 mg/L chloride concentration)

A: Side boundary condition

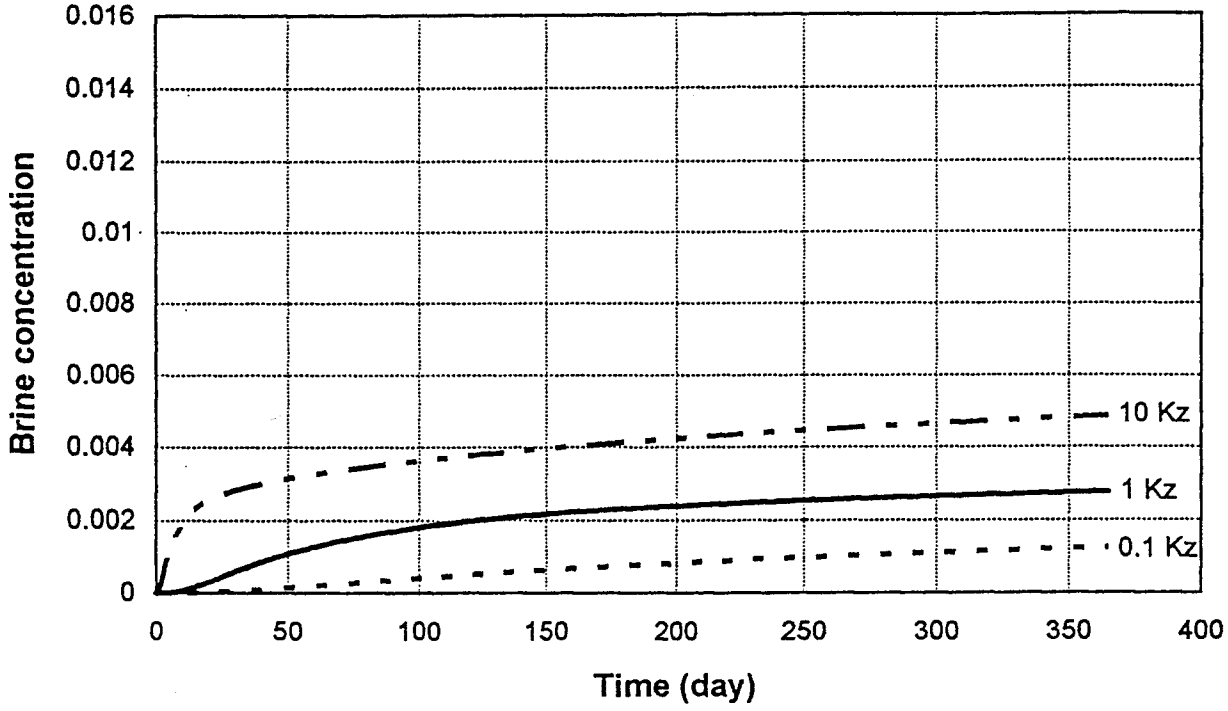

B: Bottom boundary condition

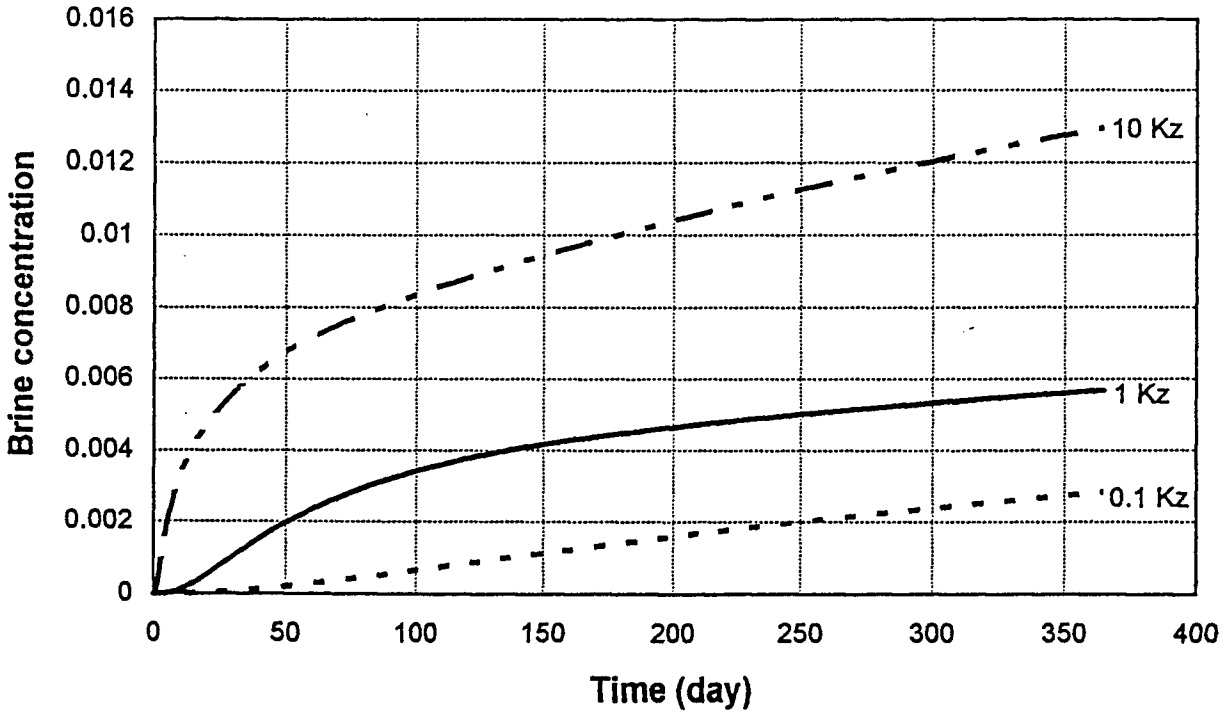

Figure 7. Comparison of discharged brine concentration vs. time for the simulated system with three different vertical hydraulic conductivity values (Kz), where Kz = 2.3 m/d.
(0.036 brine concentration is equivalent to 28,000 mg/L chloride concentration)

A. Radial hydraulic conductivity, Kr, = 2.3 m/d

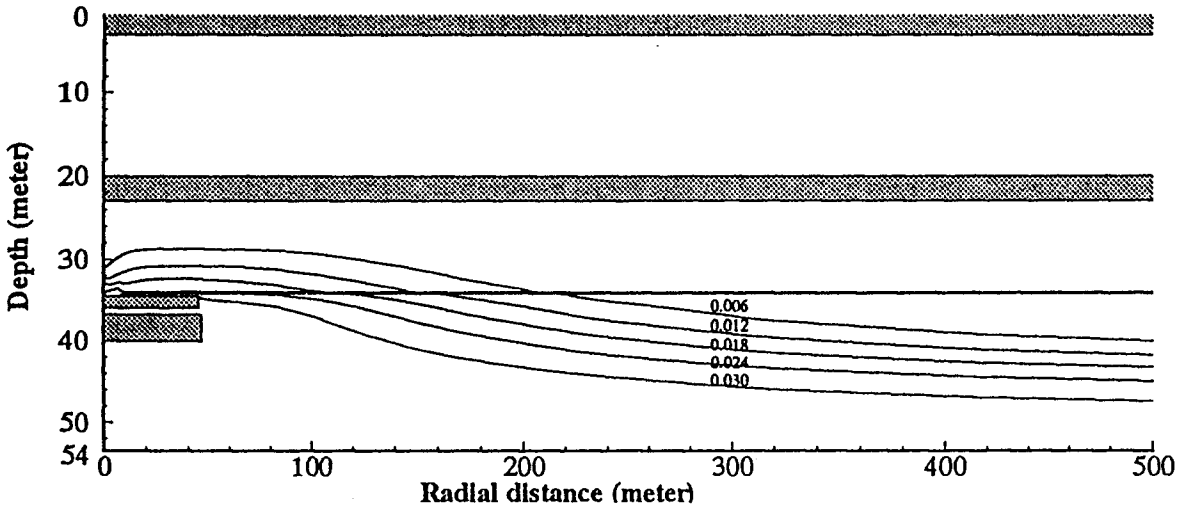

B. Radial hydraulic conductivity, Kr, = 230 m/d

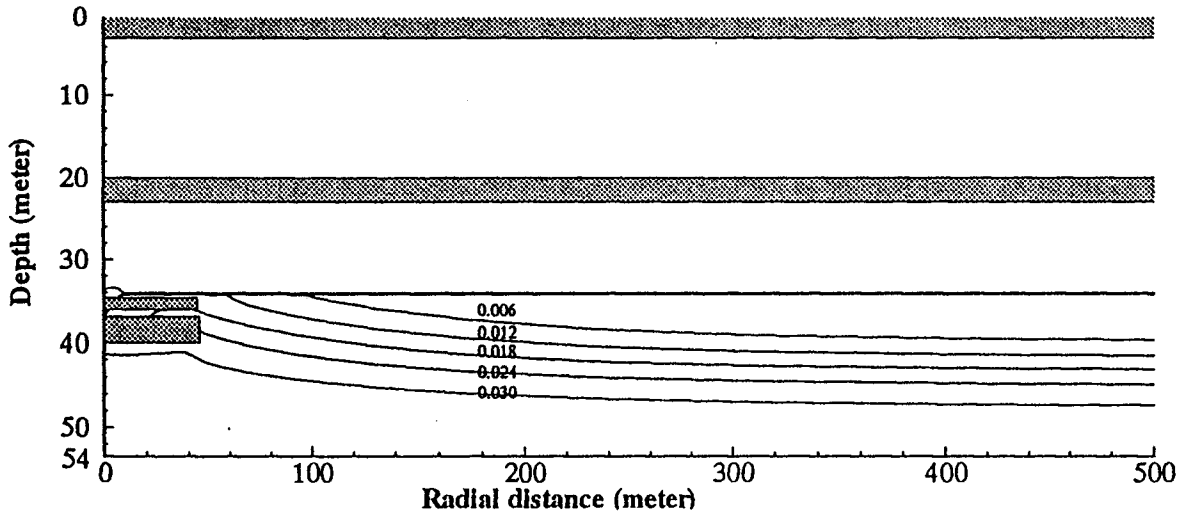

Figure 8. Comparison of brine concentration contours with two different radial hydraulic conductivity values, Kr, (2.3 m/d and 230 m/d) and the bottom boundary condition is assumed at the 300th day simulation for case #2.
(0.036 brine concentration is equivalent to 28,000 mg/L chloride concentration)

A. Radial hydraulic conductivity, Kr, = 2.3 m/d

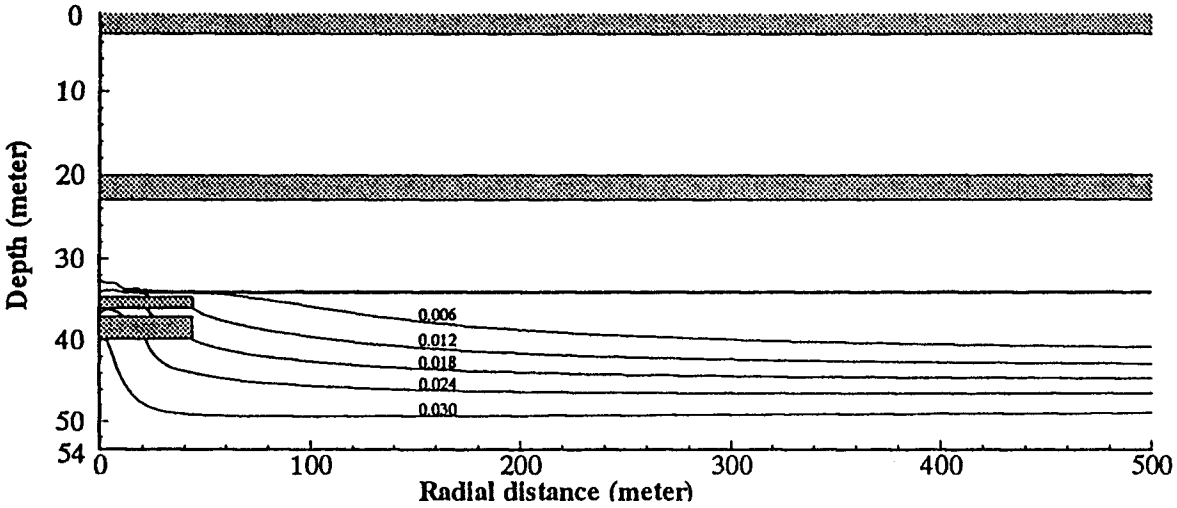

B. Radial hydraulic conductivity, Kr, = 230 m/d

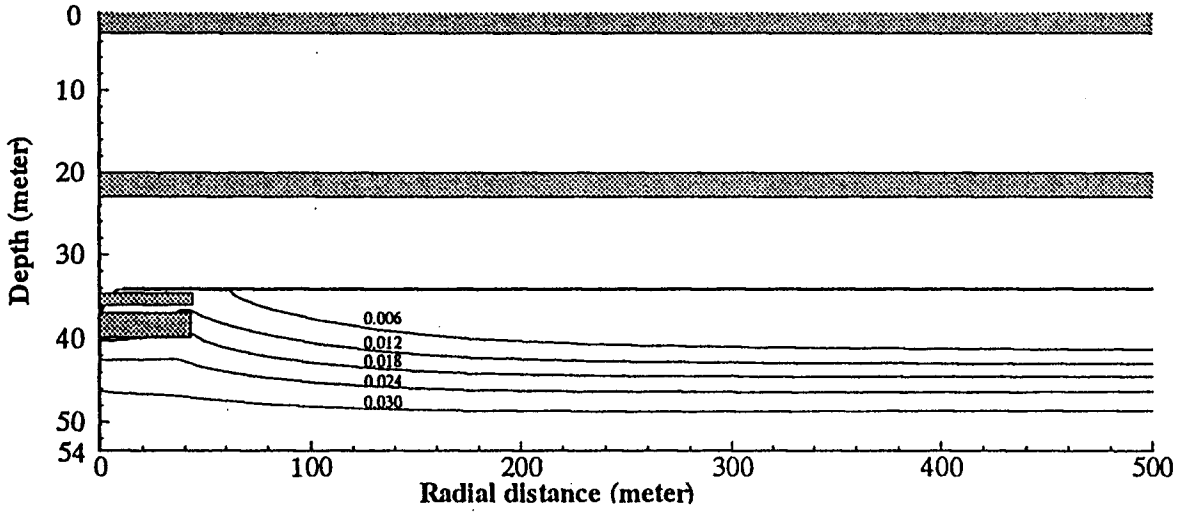

Figure 9. Comparison of brine concentration contours with two different radial hydraulic conductivity values, Kz, (2.3 m/d and 230 m/d) and the side boundary condition is assumed at the 300th day simulation for case #2.
(0.036 brine concentration is equivalent to 28,000 mg/L chloride concentration)

α_T, by changing the values of α_T from 0.01 m to 1 m. The results for Cases #4 and #5 are shown in Figs. 10 and 11, respectively. The migration of saltwater is controlled by the combination of advection, dispersion, and diffusion. The dispersion and diffusion are not critical in the saltwater-upconing simulation because the dominant factor is the advection. The dispersion tensor, D (Eq. 9), is a function of flow velocity and is used to represent the mixing of saltwater and freshwater. Higher values of α_L or α_T will result in more significant mixing of freshwater and saltwater.

Case #6 investigates the effect of well-screen location by elevating the location of well screen by 10 meters or 20 meters. The shifting of well-screen depth changes the distance from the well screen to the saltwater/freshwater interface, and flow velocity is inversely proportional to the distance to the pumping well; therefore, the upward movement of saltwater will become less significant if the distance between the well screen and the saltwater/freshwater interface becomes larger. This can be clearly demonstrated from the results shown in Fig. 12.

Case #7 investigates the effect of porosity, ϕ, by changing the values of ϕ from 0.05 to 0.25. The average velocity, V, is given by the specific discharge obtained from Darcy's law (Eq. 2) divided by the effective porosity, that is, V is inversely proportional to the porosity. The brine is mainly transported by advection; therefore, the saltwater-upconing problem will be less significant if a high-porosity value is used, and vice versa. This is demonstrated from the results shown in Fig. 13.

Case #8 investigates the effect of recharge by imposing 2-in./year and 5-in./year recharge into the aquifer. The annual recharge is uniformly distributed into the whole simulation period and is 115.5 gpm (2 in./year), which is much lower than the local pumping rate (800 gpm). Therefore, recharge should not significantly relax the saltwater upconing when the local pumping is active. The results for both boundary conditions are shown in Fig. 14.

Case #9 investigates the effect of pumpage by changing the pumping rate from 0.01 m^3/s to 0.09 m^3/s. A family of nonlinear relationships of the brine concentration versus time under

A: Side boundary condition

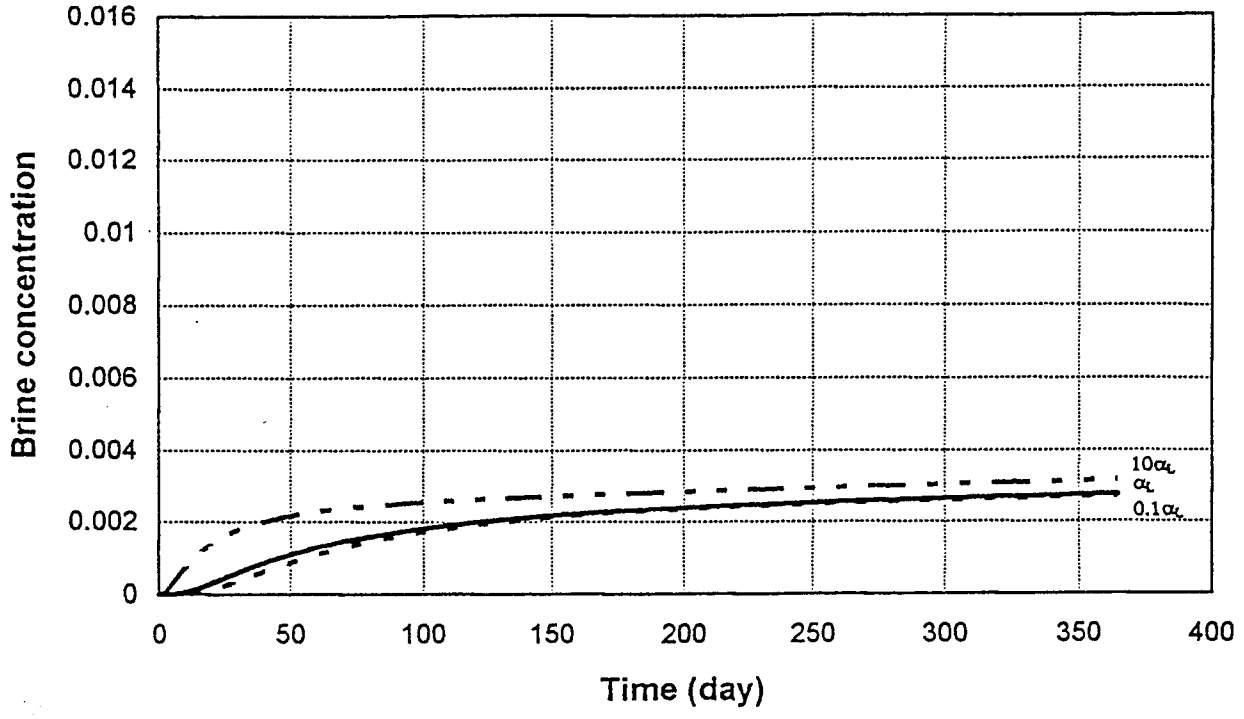

B: Bottom boundary condition

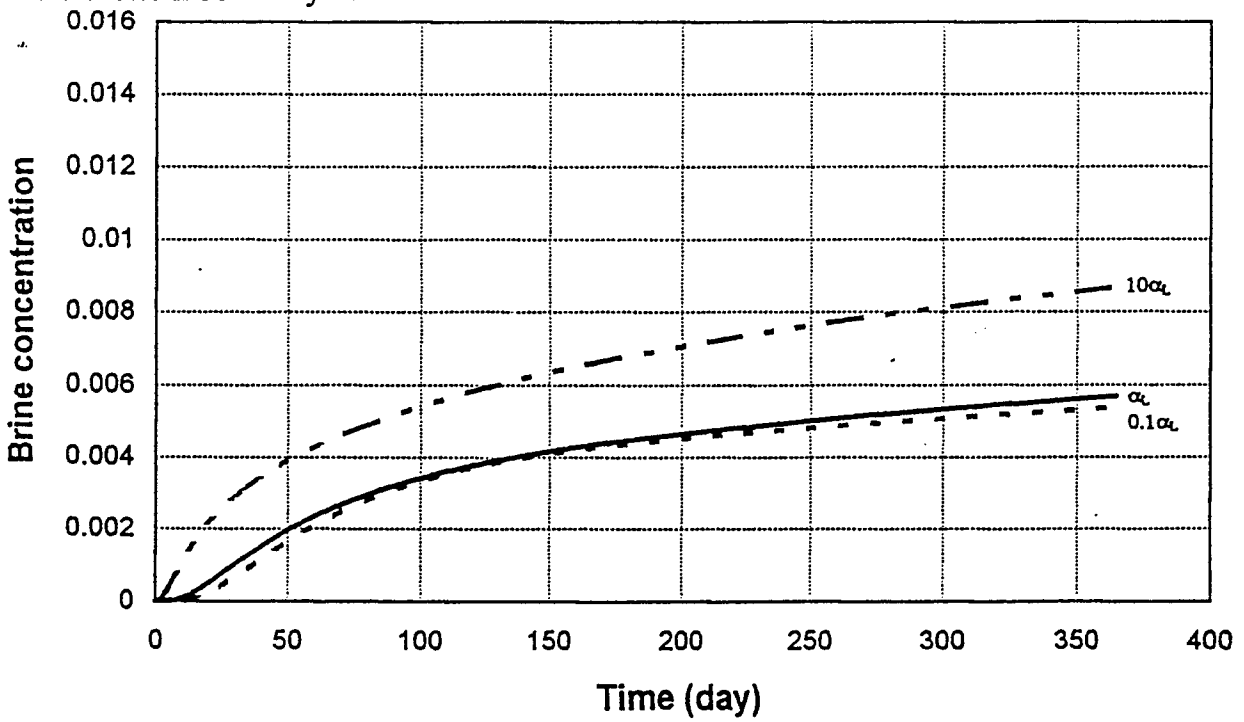

Figure 10. Comparison of discharged brine concentration vs. time for the simulated system with three different longitudinal dispersivity values (α_L), where α_L = 1 meter. (0.036 brine concentration is equivalent to 28,000 mg/L chloride concentration)

A: Side boundary condition

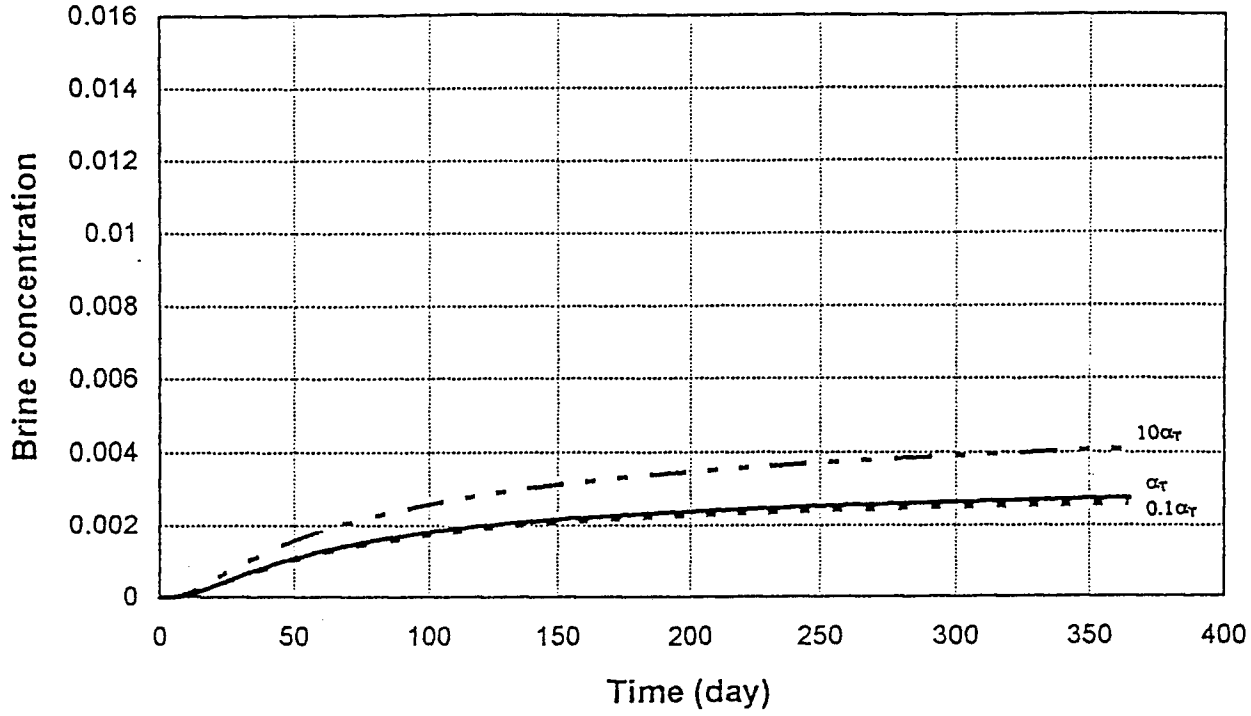

B: Bottom boundary condition

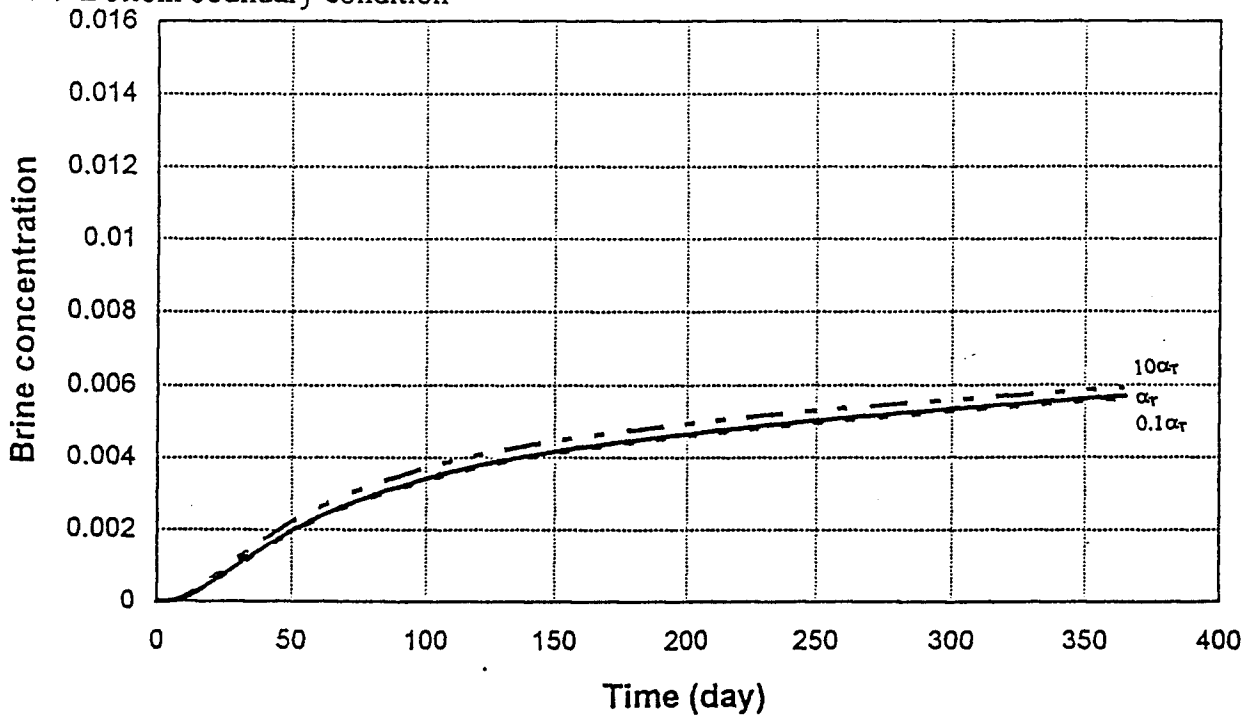

Figure 11. Comparison of discharged brine concentration vs. time for the simulated system with three different transverse dispersivity values (α_T), where α_T = 0.1 meter. (0.036 brine concentration is equivalent to 28,000 mg/L chloride concentration)

A: Side boundary condition

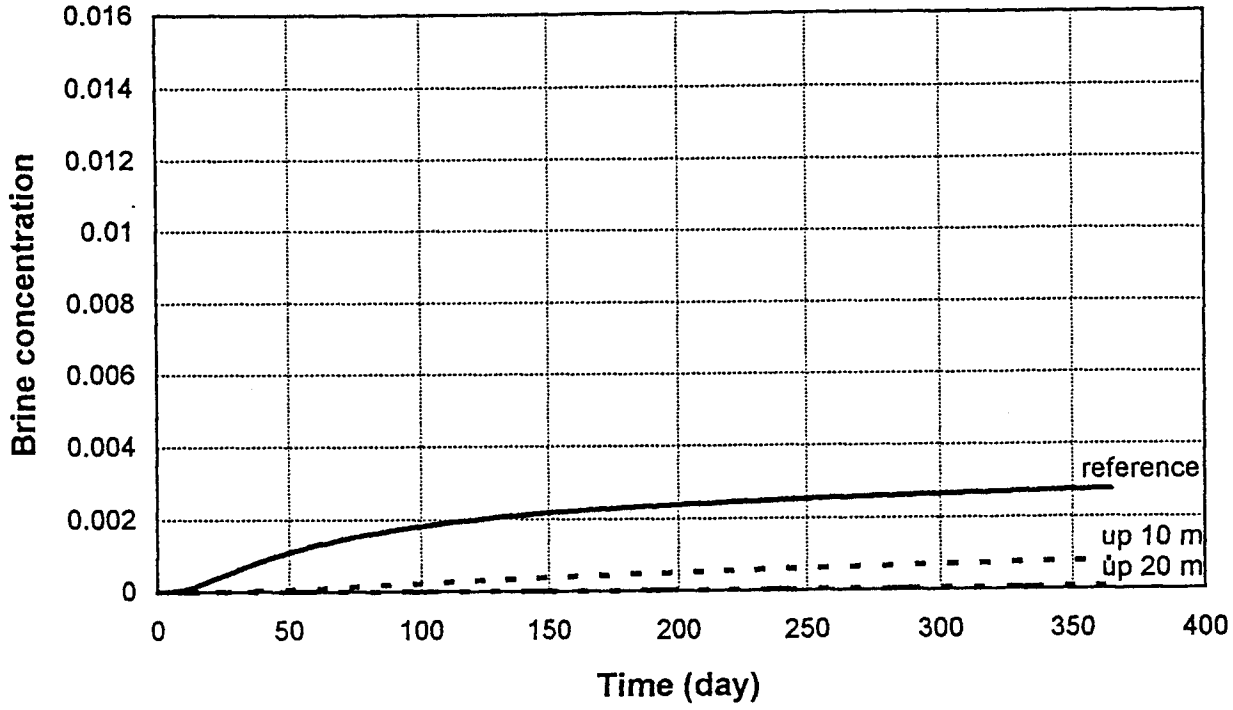

B: Bottom boundary condition

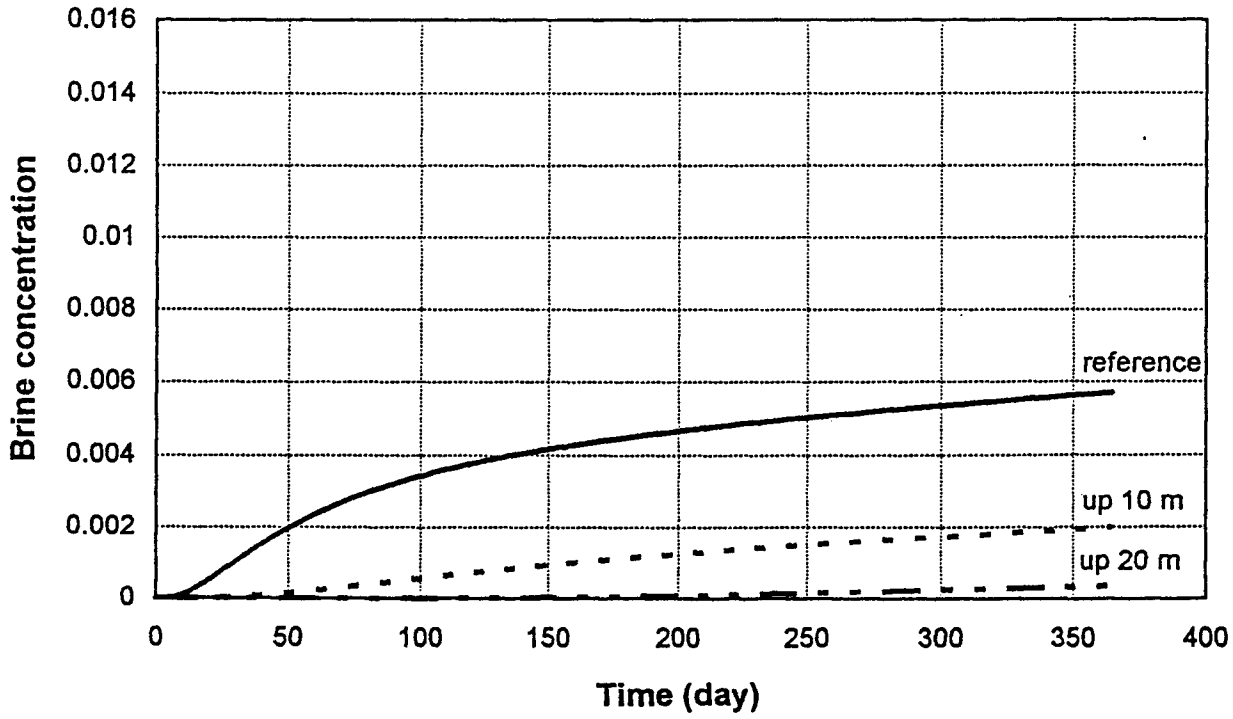

Figure 12. Comparison of discharged brine concentration vs. time for the simulated system with three different locations of well screen.
(0.036 brine concentration is equivalent to 28,000 mg/L chloride concentration)

A: Side boundary condition

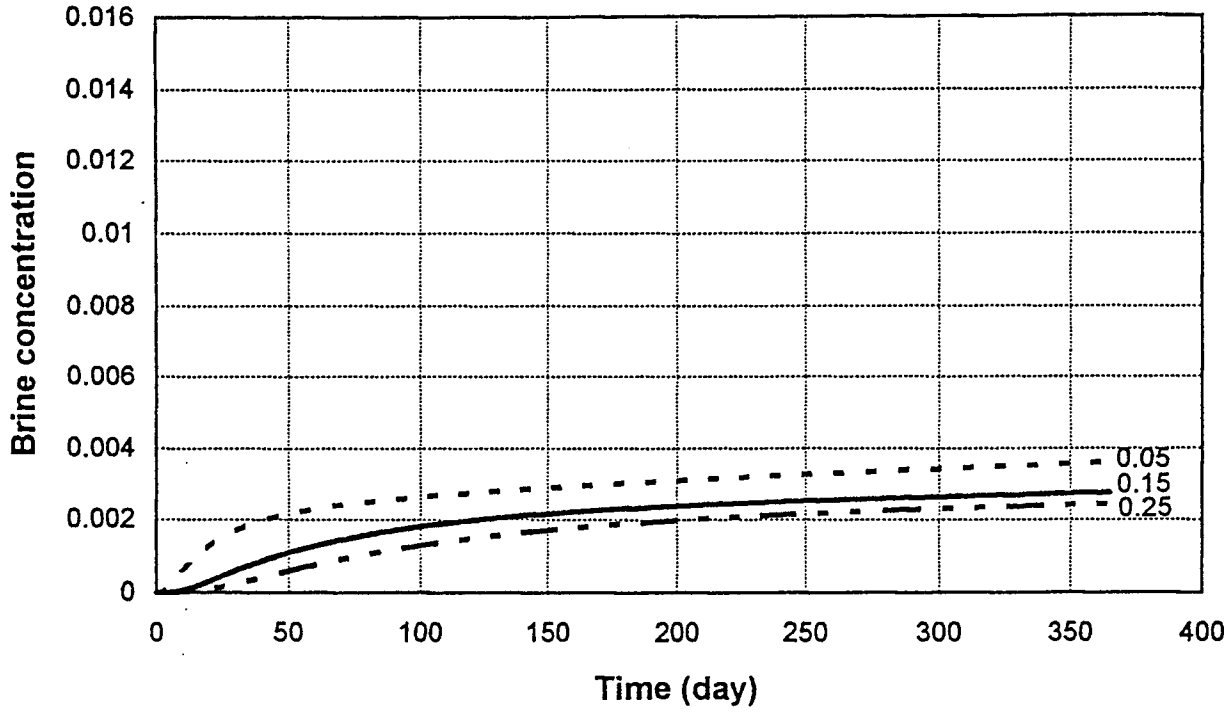

B: Bottom boundary condition

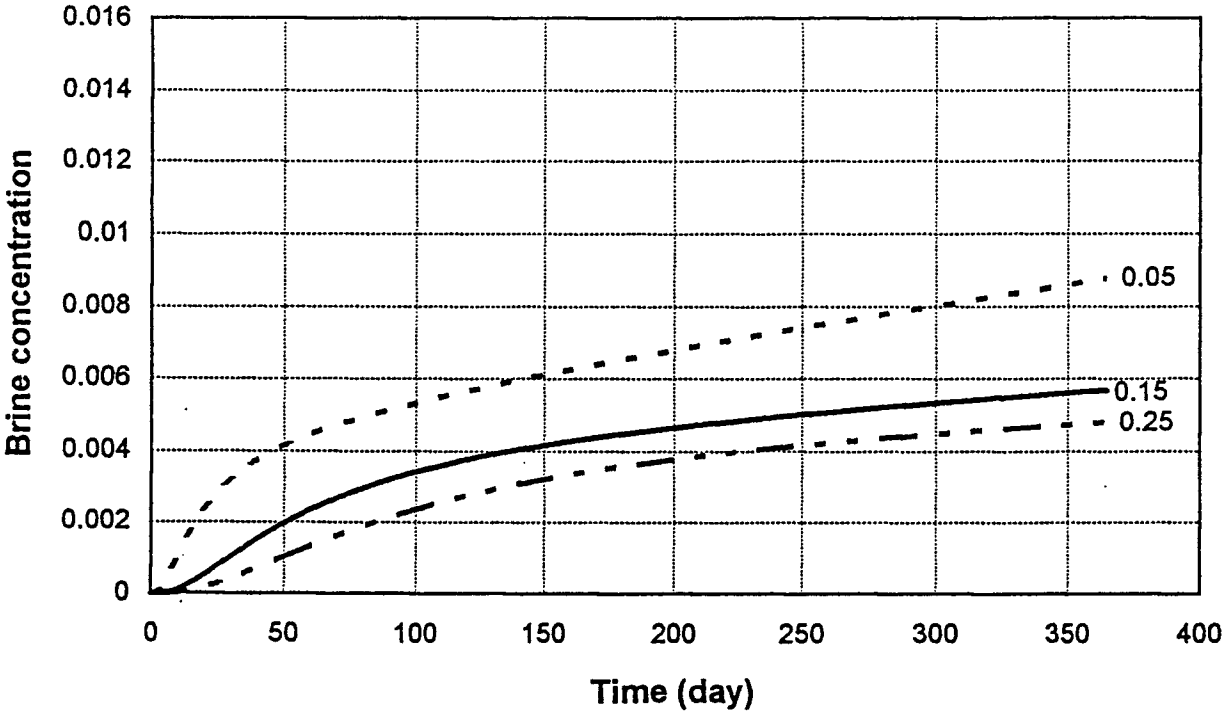

Figure 13. Comparison of discharged brine concentration vs. time for the simulated system with three different porosity values (0.05, 0.15, and 0.25).
(0.036 brine concentration is equivalent to 28,000 mg/L chrolide concentration)

A: Side boundary condition

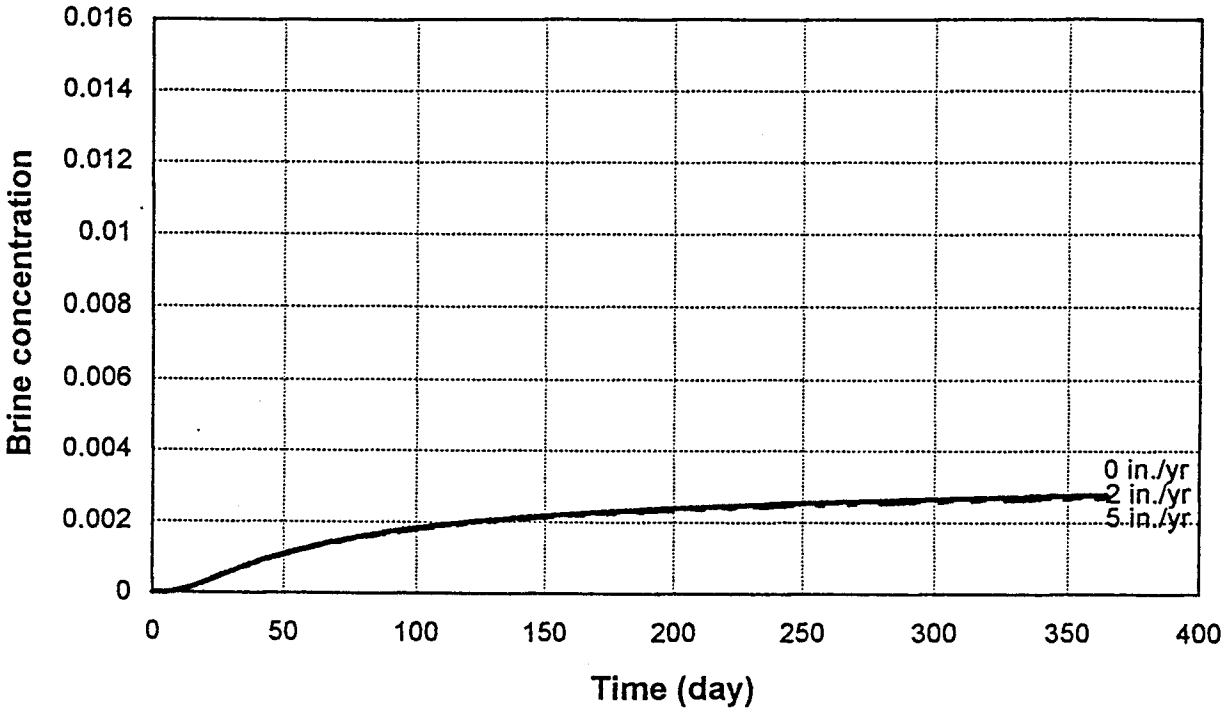

B: Bottom boundary condition

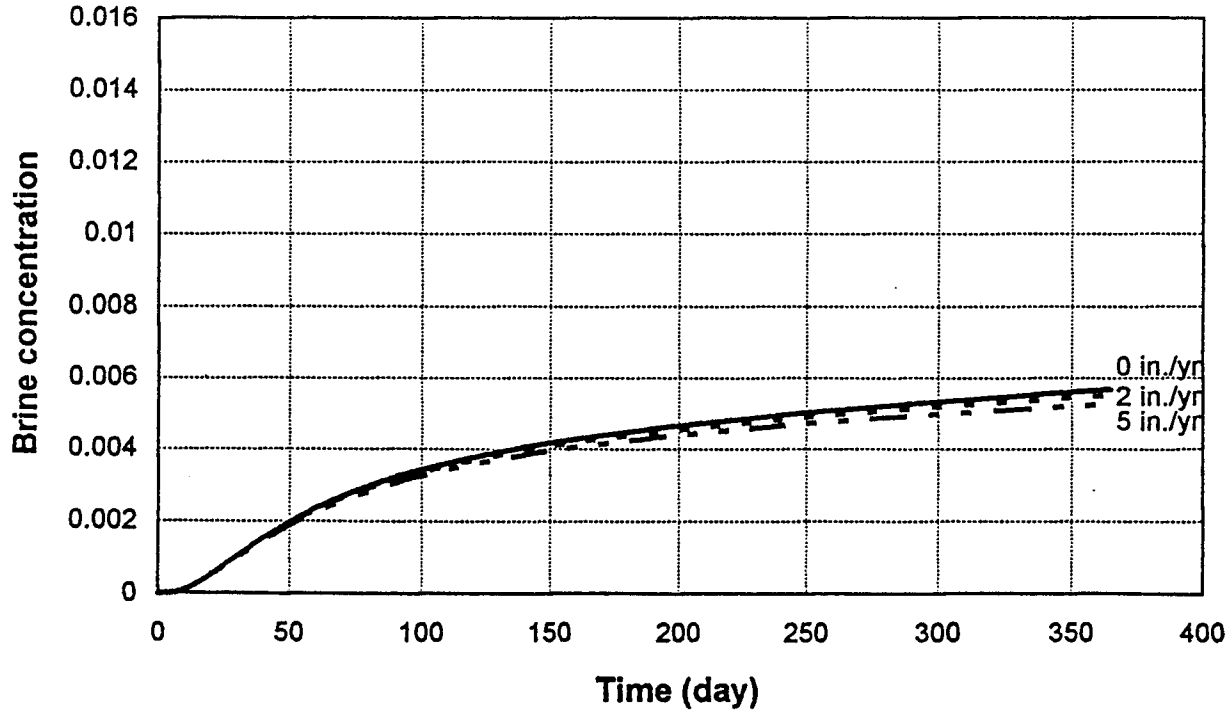

Figure 14. Comparison of discharged brine concentration vs. time for the simulated system with three different recharge values (0, 2, and 5 in./year 0.036 brine concentration is equivalent to 28,000 mg/L chloride concentration).

various pumpages is shown in Fig. 15. The results from this simulation can help determine appropriate safe-yield discharge.

Case #10 investigates the effect of the spatial distribution of clay layers. A continuous clay layer (Fig. 2C), a discontinuous clay layer (Fig. 2D), and no clay layer are considered and compared with the simulation Case #1. The results for both boundary conditions are shown in Fig. 16 (please note that the scale of brine concentration in Fig. 16 is different from the previous plots). As can be seen from the results, the upconing of saltwater can barely be observed with the protection of the continuous clay layer. A discontinuous clay does not offer much protection. However, without the protection of a clay layer, saltwater will be easily discharged and it is particularly significant if the source of salt is from the bottom (Fig. 16B). This simulation demonstrated that the clay layer is the most important factor dominating the migration of saltwater.

From the above investigation, saltwater upconing is sensitive to the pumping rate, radial and vertical hydraulic conductivity, location of well screen, and boundary conditions. This study provides information on the dynamic relationships between saltwater and freshwater in a ground-water system, helps guide the calibration of the numerical models, and provides insights for the study of more complex three-dimensional systems.

Calibration of Single Pumping-Well Model

Here we attempt to calibrate the single pumping-well model based on the observed brine concentrations at the Siefkes site. The size of the study area and mesh of the model adopted in this study is the same as the one used in the sensitivity analysis; however, the well is screened from 15 to 20 meters and 23 to 34 meters based on the irrigation well at the Siefkes site. A sample of the profile of the measured electrical conductance and drilling log for the Permian monitoring well at the Siefkes site is shown in Fig. 17 (Buddemeier et al., 1993). As can be seen, some clay layers are interspersed in the aquifer; however, the extenuation of the clay layers in not certain. The measured formation conductance (Cm′) can be converted to chloride percentage concentration (Cl%) by using

A: Side boundary condition

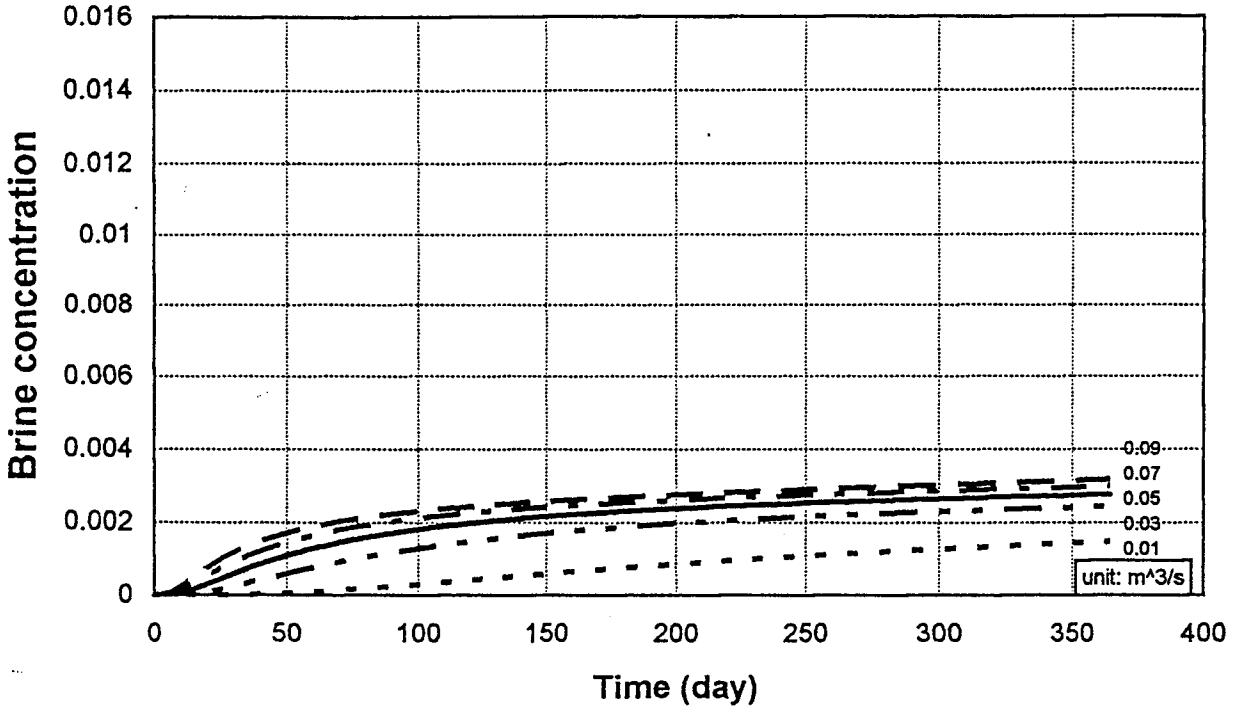

B: Bottom boundary condition

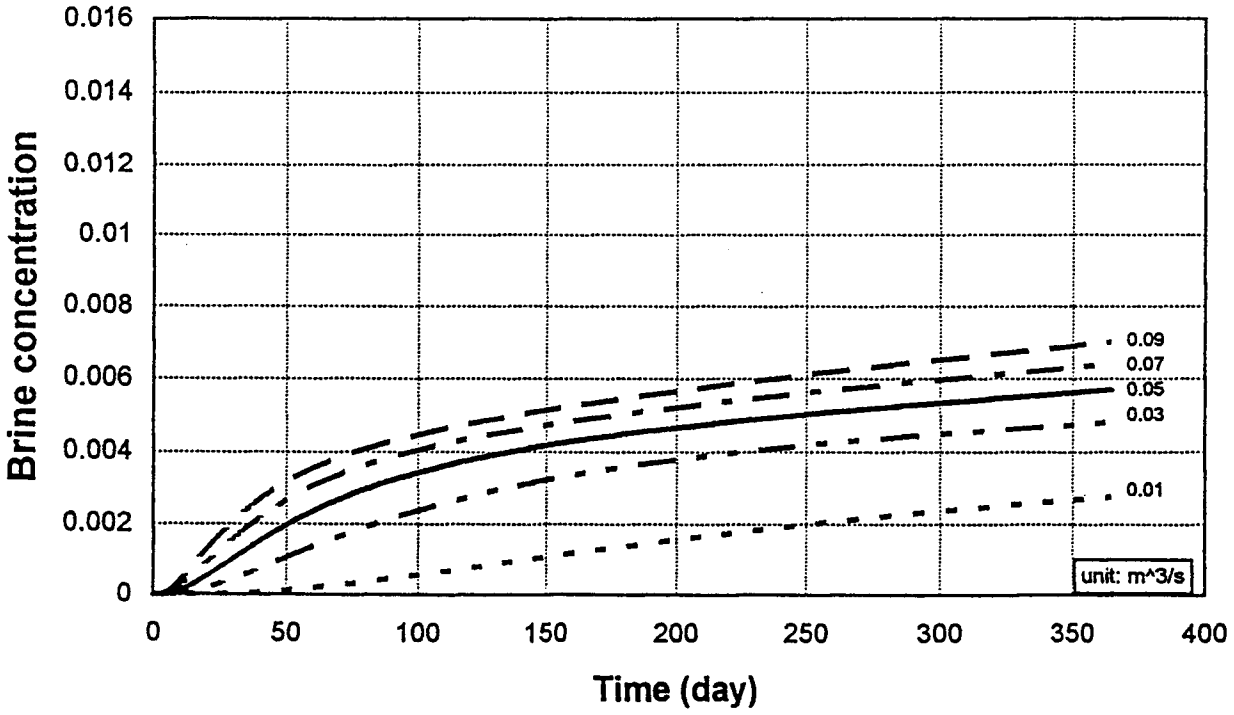

Figure 15. Comparison of discharged brine concentration vs. time for the simulated system with five different pumping rates (0.01- 0.09 m^3/s 0.036 brine concentration is equivalent to 28,000 mg/L chloride concentration).

A: Side boundary condition

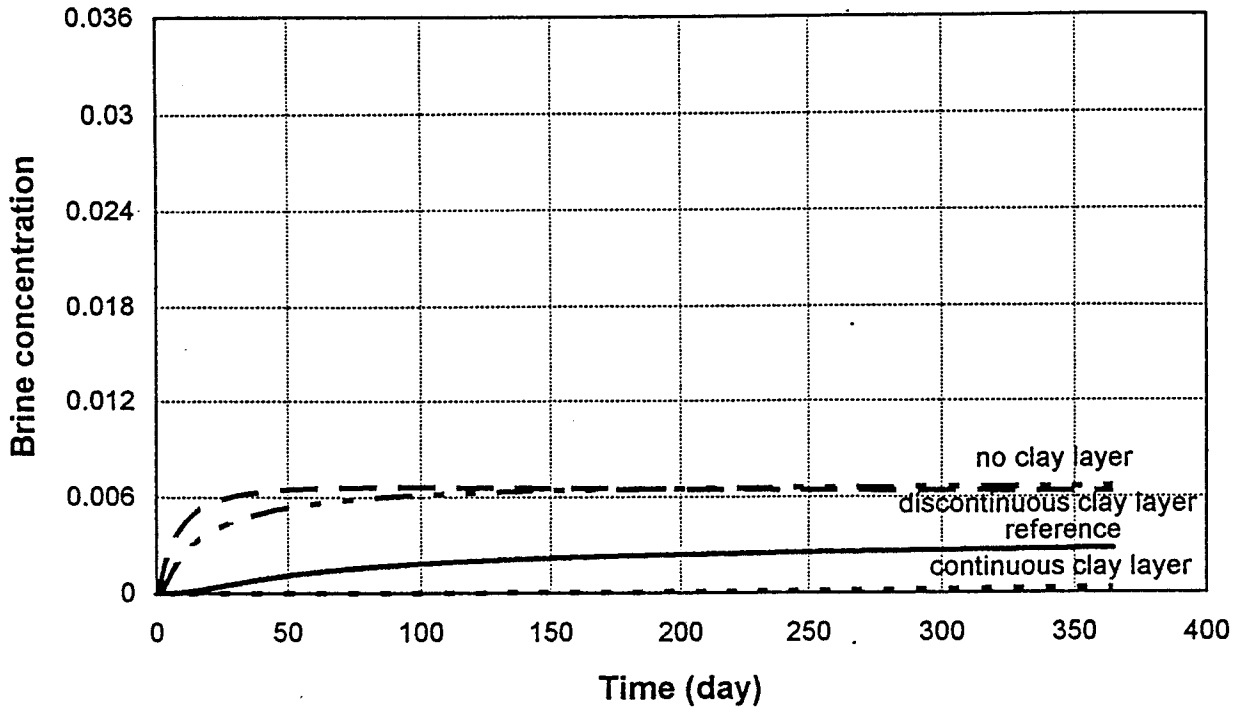

B: Bottom boundary condition

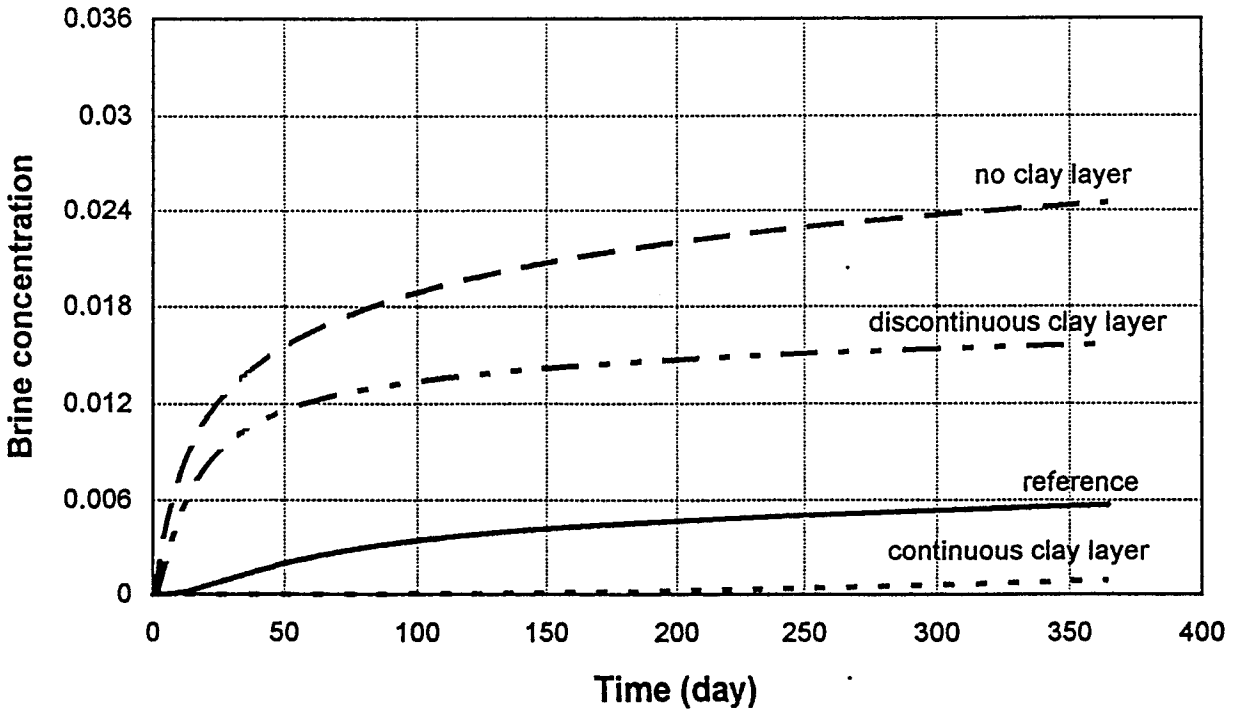

Figure 16. Comparison of discharged brine concentration vs. time for the simulated system with different spatial distribution of clay layers.
(0.036 brine concentration is equivalent to 28,000 mg/L chloride concentration)

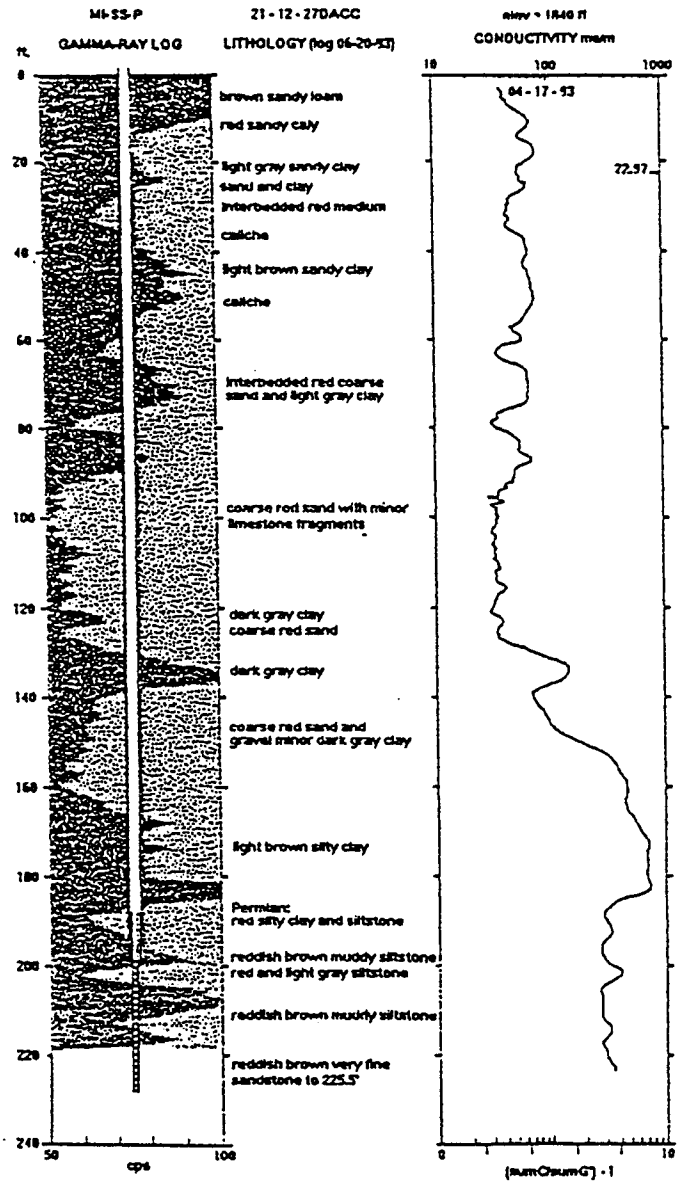

Figure 17. Gamma-ray, formation conductivity, and drilling log for the Permian monitoring well at the Siefkes site (Buddermeier et al., 1993).

the following equation (Garneau et al., 1994):

$$Cl\% = \text{Max}\,[40, (Cm'-18)/0.02388 + 40]/420 \qquad (11)$$

and the concentration can be converted to density by the following equation (Williams, 1962):

$$Y = 0.99931 + 0.0013444 * X \qquad (12)$$

where Y is the converted density of seawater at 15 deg. C, and X is the corresponding concentration.

The profile of the measured conductance on March 1994, at the deep aquifer monitoring well located about 35 meters away from the irrigation well is converted to its corresponding brine concentration by setting the brine concentration equal to zero for pure freshwater (with 1 g/cm^3 density). A converted brine concentration of 0.036 is equivalent to 28,000 mg/L chloride concentration. The saltwater/freshwater interface is assumed to start from 40 meters below the initial water table, and this position is used as the initial saltwater condition in the numerical model. The plot of profiles of the converted brine concentration at different time periods at the deep aquifer monitoring well is shown in Fig. 18A, and the initial saltwater condition in the numerical model is shown in Fig. 18B. The purpose of model calibration is to reproduce a simulated brine concentration similar to the measured profile. The pumping rate of the irrigation well at the Siefkes site is 800 gpm; however, the schedule of pumping depends on many factors, such as weather conditions, type of crop, etc. The exact pumping schedule at the Siefkes site is not certain; therefore, the total accumulated volume of pumpage at the Siefkes site is uniformly distributed over the irrigation season. The 1994 accumulated volume of pumpage at the Siefkes site is shown in Fig. 19. The irrigation season in 1994 started in April and ended in September, and the average pumping rate during the irrigation season was approximately 210 gpm. Sophocleous (1993) estimated the annual

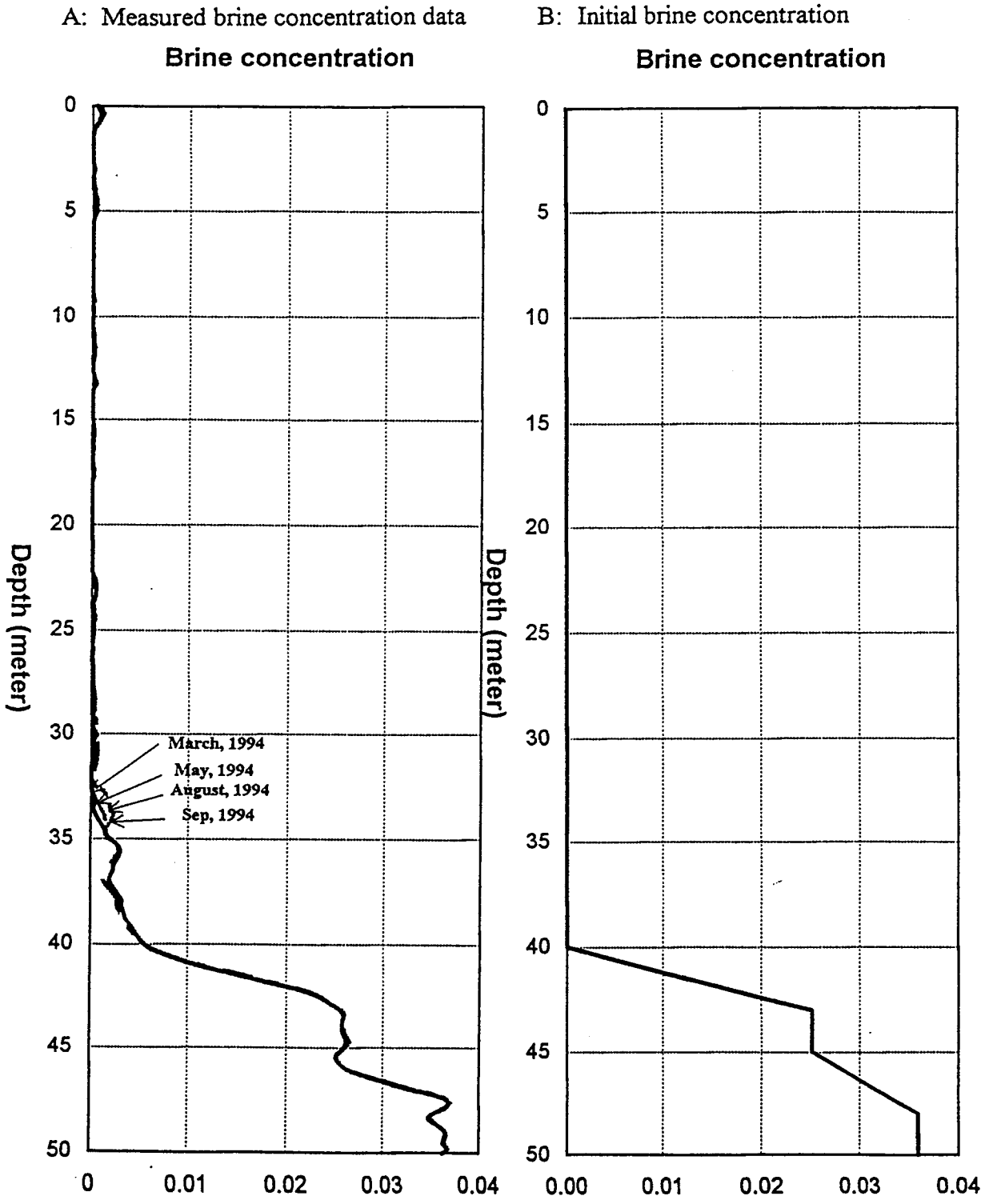

Figure 18. The plot of profiles of the converted brine concentration at different times in the deep aquifer monitoring well (A) and the initial brine concentration profile employed in the numerical model (B).
(0.036 brine concentration is equivalent to 28,000 mg/L chloride concentration)

Date	gallons	Date	gallons	Date	gallons	Date	gallons
4/1/94	680000	5/26/94	9293000	8/3/94	35398000	9/16/94	56063000
4/8/94	3476000	6/21/94	16236000	8/4/94	36078000	10/6/94	58658000
4/13/94	4050000	7/5/94	21775000	8/9/94	39955000	10/13/94	59328000
4/19/94	4050000	7/8/94	21842000	8/10/94	40690000	10/26/94	59328000
4/21/94	4426000	7/19/94	27488000	8/12/94	41224000	11/9/94	59328000
4/22/94	5183000	7/20/94	27488000	8/17/94	45373000	11/16/94	59328000
5/16/94	5772000	7/21/94	27545000	8/24/94	48915000	11/17/94	59328000

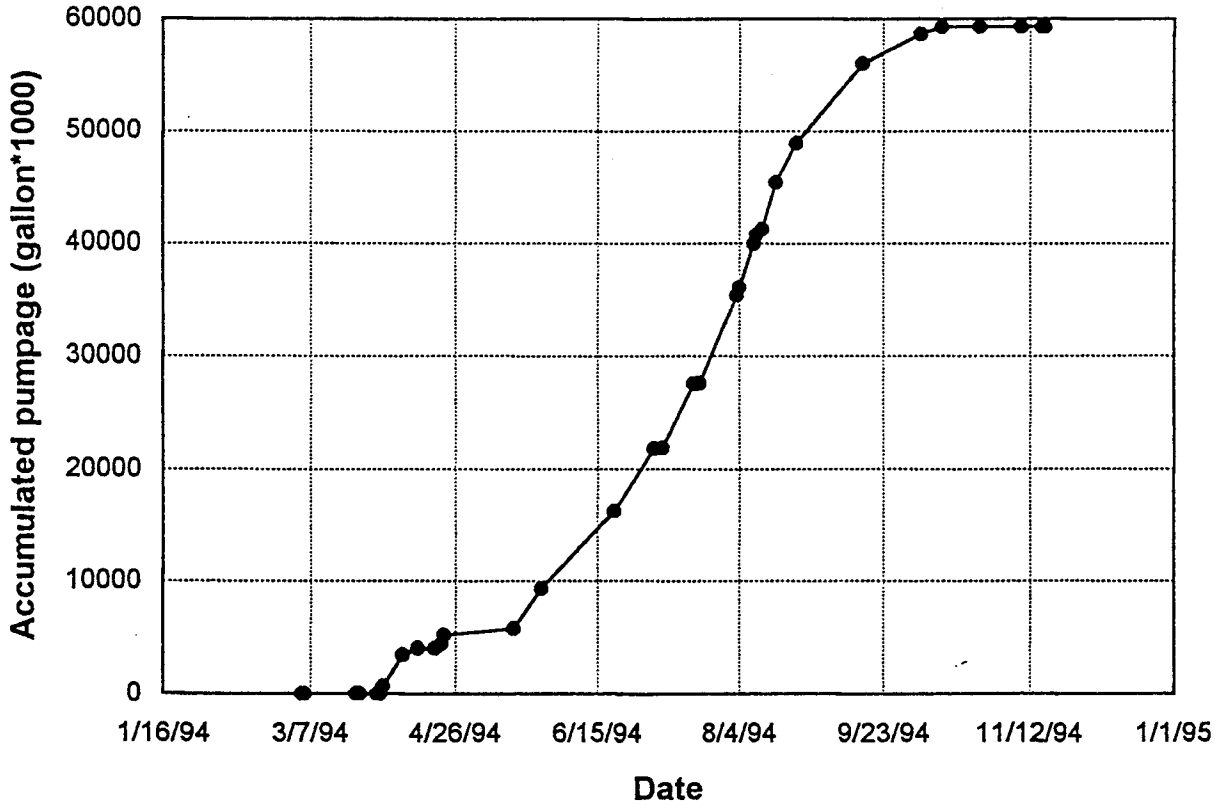

Figure 19. The 1994 accumulated volume of pumpage at the Siefkes site.

recharge ranges as 1 to 3 inches, which is approximately 10% of the annual precipitation. Two annual recharge values (2 in./year and 5 in./year) are considered in the simulation and uniformly distributed into the whole year. The location and characteristics of clay layers are determined by trial and error. Two types of boundary conditions are considered: the constant brine concentration and fluid pressure at the bottom of the aquifer and the constant brine concentration and fluid pressure at the edge. The physical system for the calibration of the numerical model is shown in Fig. 20, and the values of input parameters are listed in Table 5.

The simulated brine concentration is taken at a location about 35 meters away from the pumping well and displayed as the brine-concentration profile at the 90th, 150th, 240th, and 270th simulation day. Because of the uncertainty of the aquifer parameters and distribution of clay layers, and the simplification of pumping schedule and recharge, a near- perfect match of the simulated results to the measured data is an extremely difficult task.

Figs. 21 and 22 are the time-series results of brine-concentration profiles with recharge values of 2 in./year and 5 in./year, respectively, for two different boundary conditions. The simulated brine-concentration profiles with bottom boundary condition are considered to have a good match with the measured data (Fig. 18A); however, the results from the models with side boundary condition do not match the measured data well.

The calibrated model is projected 10 years into the future using different recharge and pumping rates, so that the relationship of pumping rate and discharged brine concentration can be obtained. For the 10 years simulation, pumping is activated from May to October in each year and no pumping was assumed for the rest of the time (January to April, November, and December). The above four calibrated models are adopted and projected into a 10-year time horizon. The pumping rate is modified to 400 gpm and 800 gpm and two different recharge values (2 in./yr and 5 in./yr) are considered. The ground-water chloride concentration of 500 mg/L or less is suitable for most general uses and is considered as the target for sustainable ground water. A converted brine

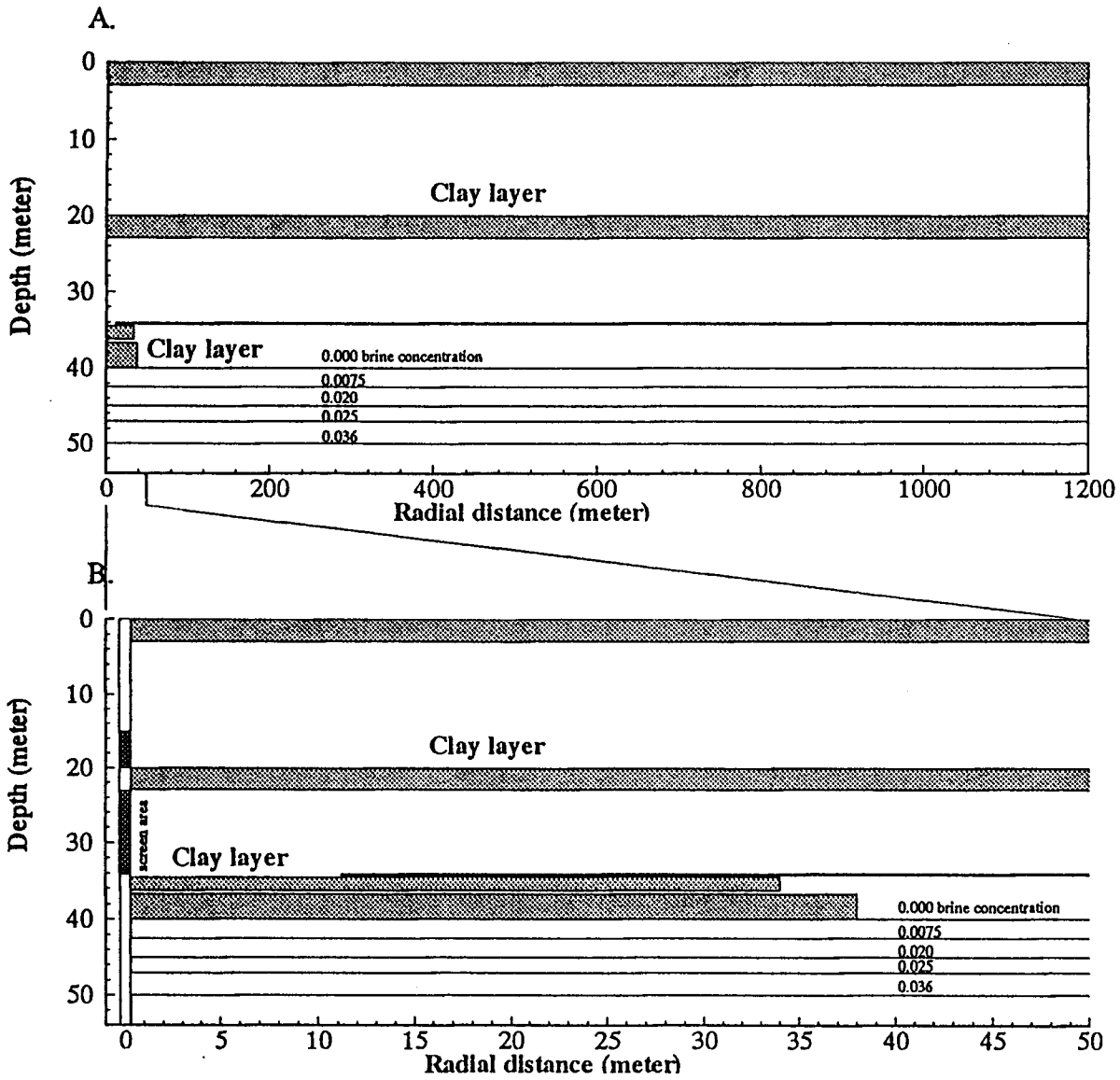

Figure 20. A. The physical system of the numerical model with clay layers interspersed in the aquifer for the salt water upconing simulation.
B. Area near the pumping well.

Table 5. Variables and parameters used in the numerical model for saltwater upconing.

Aquifer, Fluid, and other Parameters

radial hydraulic conductivity	(0-40 meter)	Kr = 23 m/d (75 ft/d)
radial hydraulic conductivity	(40-54 meter)	Kr = 2.3 m/d (75 ft/d)
vertical hydraulic conductivity	(0-40 meter)	Kz = 2.3 m/d (7.5 ft/d)
vertical hydraulic conductivity	(40-54 meter)	Kz = 0.23 m/d (7.5 ft/d)
porosity		$\phi = 0.15$
bulk porous matrix compressibility		$\alpha = 2.58 \times 10^{-7}[kg/(m\ s^2)]^{-1}$
water compressibility		$\beta = 4.40 \times 10^{-10}[kg/(m\ s^2)]^{-1}$
solute molecular diffusivity		$D_m = 1.0 \times 10^{-12}\ m^2/s$
longitudinal dispersivity		$\alpha_L = 1$ m
transverse dispersivity		$\alpha_T = 0.1$ m
fluid (water) density		$\rho_o = 1{,}000\ kg/m^3$
brine density		$\rho = 1{,}036\ kg/m^3$
solid grain density		$\rho_s = 2{,}650\ kg/m^3$
fluid (water) viscosity		$\mu = 1.0 \times 10^{-3}\ kg/(m\ s)$
initial fluid (freshwater) salt concentration		$C_0 = 0$
initial brine fluid salt concentration		C (r,z,0); variable
initial specified pressure at the boundary		p(r, z, 0); variable
saturated thickness		b = 54 m
depth to freshwater/saltwater interface		40 m
depth to Permian boundary		54 m
volumetric pumping rate		$Q_p\ (m^3/s)$; variable
gravitational acceleration		$g = 9.81\ m/s^2$
well-screen depth location		15 to 20 m and 23 to 34 m
total simulation time		10 yr.

Clay Layer Properties

Location (m)	Thickness (m)	Kr (m/s)	Kz (m/s)	Porosity
0-3	3	0.023	0.023	0.25
20-23	3	0.23	0.23	0.25
34-34.25	0.25	0.0023	0.0023	0.25
34.75-36.25	1.5	0.00184	0.00184	0.25
37-40	3	0.23	0.23	0.25

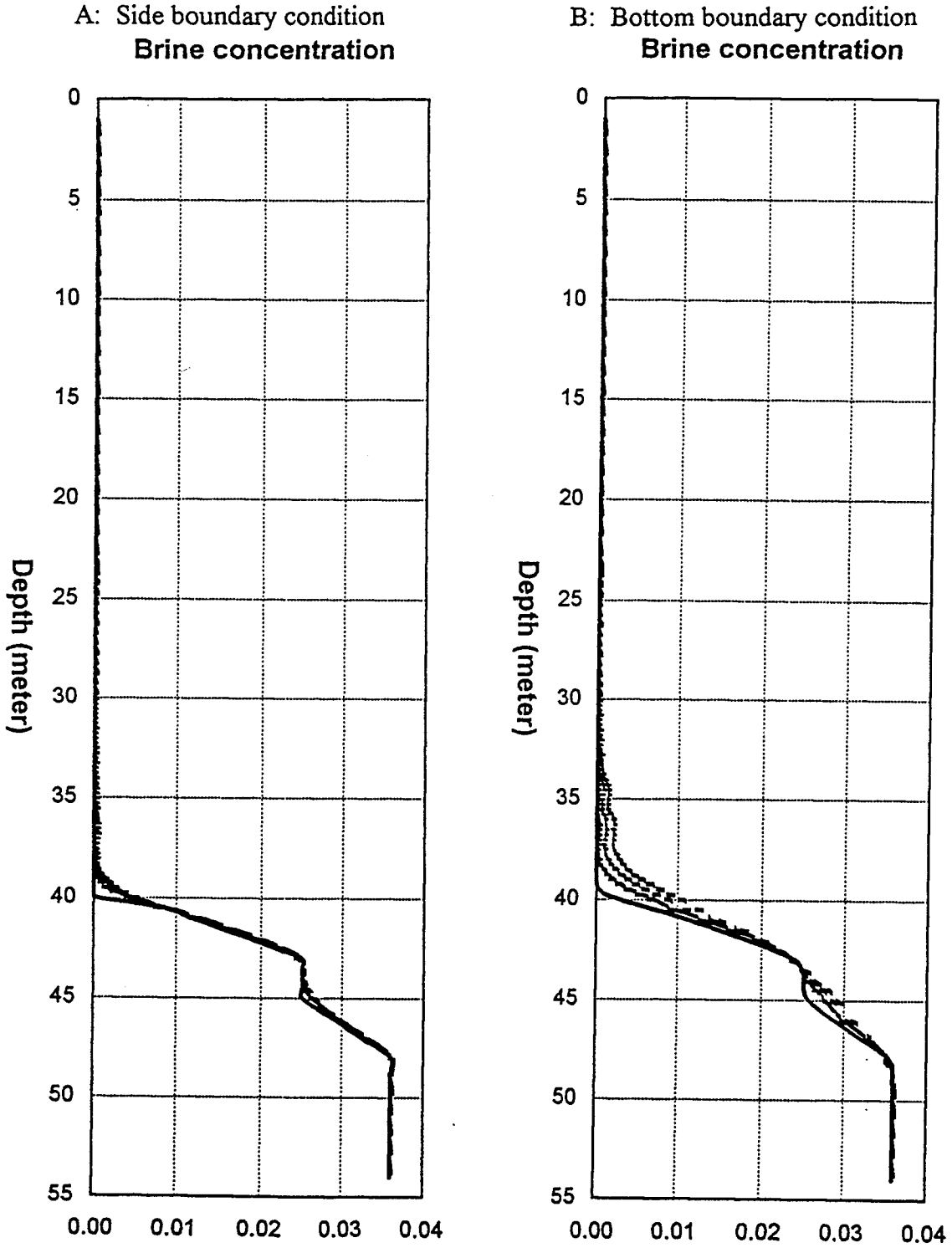

Figure 21. The time series results (90th, 150th, 240th, and 270th day of simulation) of brine concentration profile for side and bottom boundary conditions. Pumping rate is 210 gpm and recharge is 2 in./yr.
(0.036 brine concentration is equivalent to 28,000 mg/L chloride concentration)

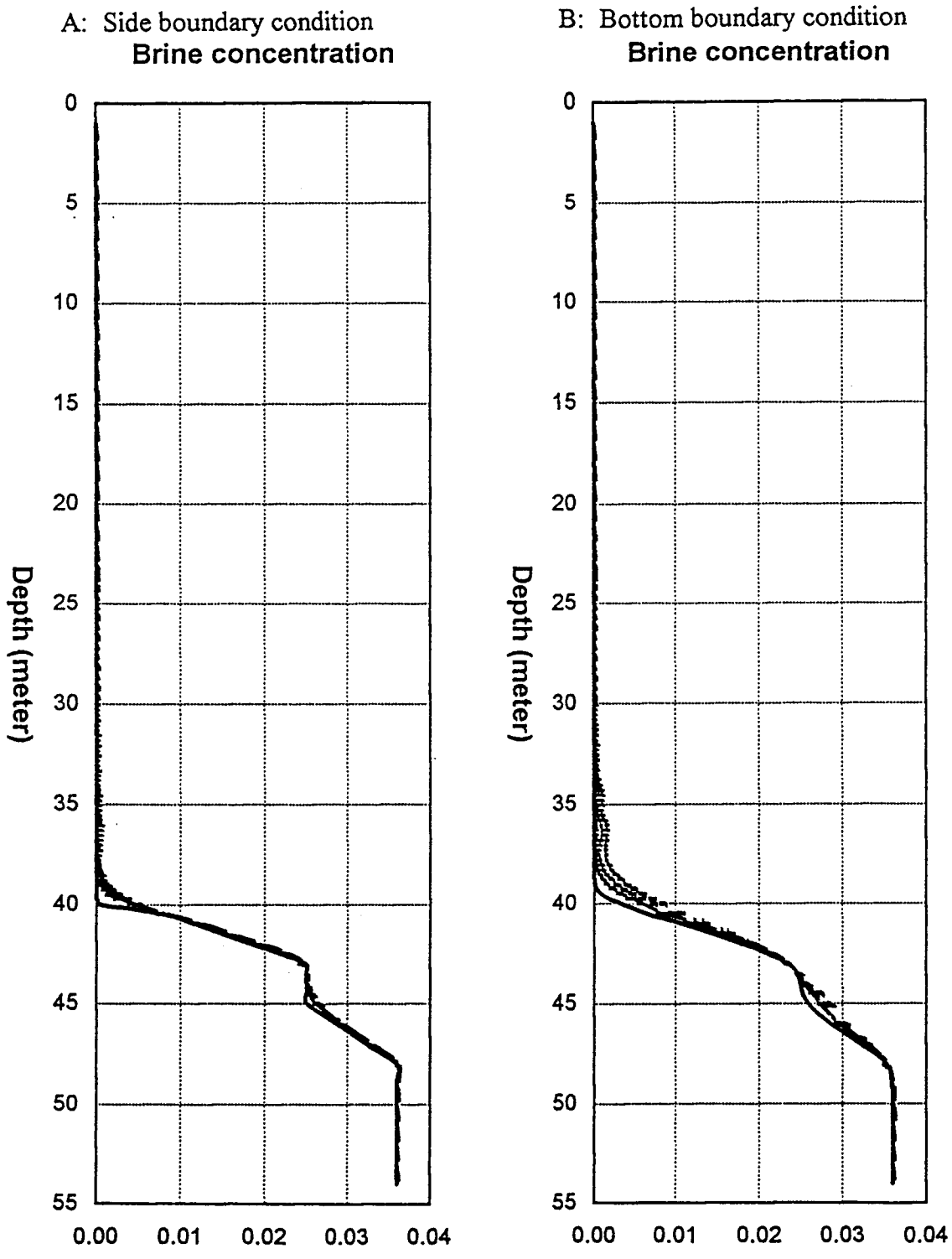

Figure 22. The time series results (90th, 150th, 240th, and 270th day of simulation) of brine concentration profile for side and bottom boundary conditions. Pumping rate is 210 gpm and recharge is 5 in./yr.
(0.036 brine concentration is equivalent to 28,000 mg/L chloride concentration)

concentration of 0.00065 is equivalent to 500 mg/L chloride concentration. The relationships of the discharged brine concentration versus time are presented in Figs. 23 to 26. As can be seen, high recharge and low pumping rate will alleviate the problem of saltwater upconing, and the recovery of saltwater intrusion will be significant with the help of recharge during the nonpumping season. In addition, if the source of salt is provided from the side, the salinity of discharged water can meet water-quality standards and last for a longer period of time. However, if the source of salt is provided from the bottom of the aquifer, the problem of saltwater intrusion that would be encountered in the projected time period will depend on the pumping rate and recharge. The Permian bedrock at the Siefkes site is highly mineralized and the aquifer is directly in contact with the Permian bedrock; therefore, the model with constant brine concentration at the bottom of the aquifer is closer to the real situation and is preferred. In these 10-year simulations, the result shown in Fig. 25A with pumping rate of 400 gpm, 5 in./year of recharge, and the side boundary condition has the least problem of saltwater intrusion; however, the case of Fig. 24B with pumping rate of 800 gpm, 2 in./year of recharge, and the bottom boundary condition has the worst problem of saltwater intrusion.

Saltwater Upconing Beneath Two and Three Pumping Wells

The objective here is to investigate the interaction of water salinity under a multi-well pumping system. The simulation area we considered is 2110 meters by 2110 meters, and the total aquifer depth is 54 meters. The model grid (shown in Fig. 27) is meshed as 33x33x11 cells. In the X-Y direction, the variable spacing employed ranges from a maximum of 150 meters to a minimum of 50 meters. In the vertical direction, Z, a uniform spacing of 5 meters is discretized in the top 10 rows, with 4 meters in the last row. The initial water table is assumed to be horizontal, and the saltwater initially starts at 40 meters below the initial water table with linearly varying brine concentration from 0.0 to 0.036. A constant fluid pressure and brine concentration at the bottom of the aquifer are assumed, and no clay layers are considered. The physical system of the two-well case is shown in Fig. 28. As can be seen, well #1 is always placed at the center of the simulation area;

A: Side boundary condition

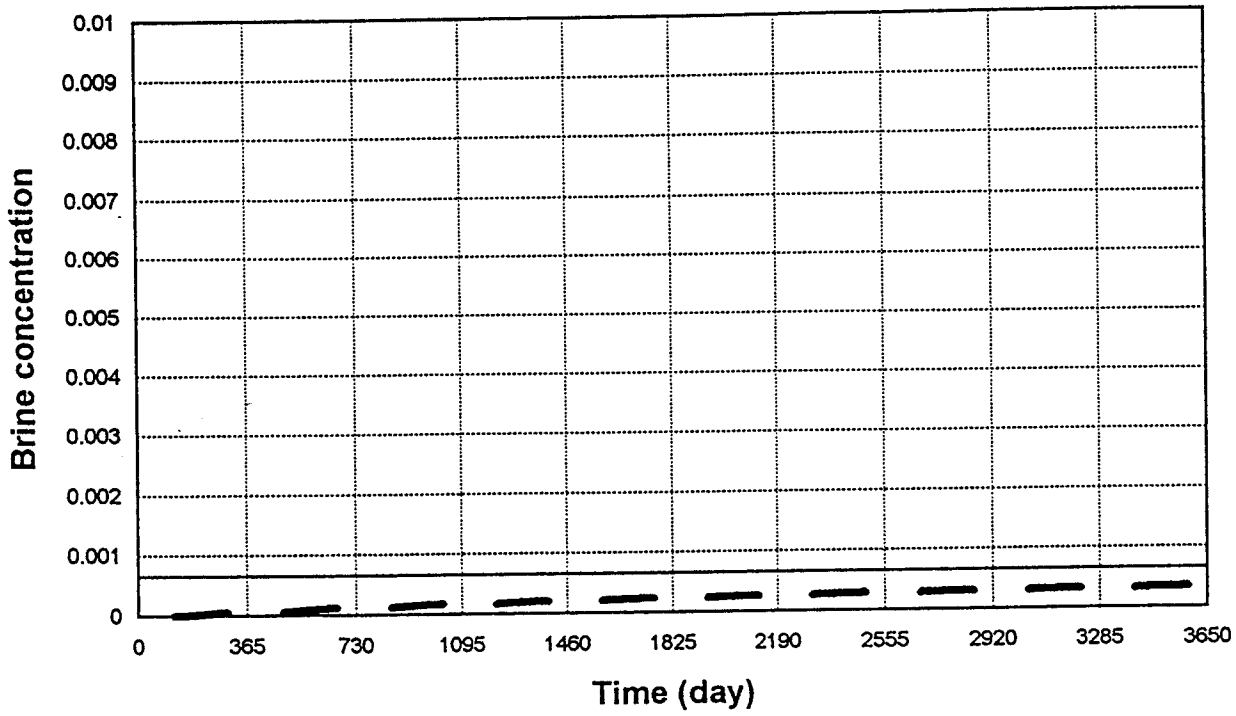

B: Bottom boundary condition

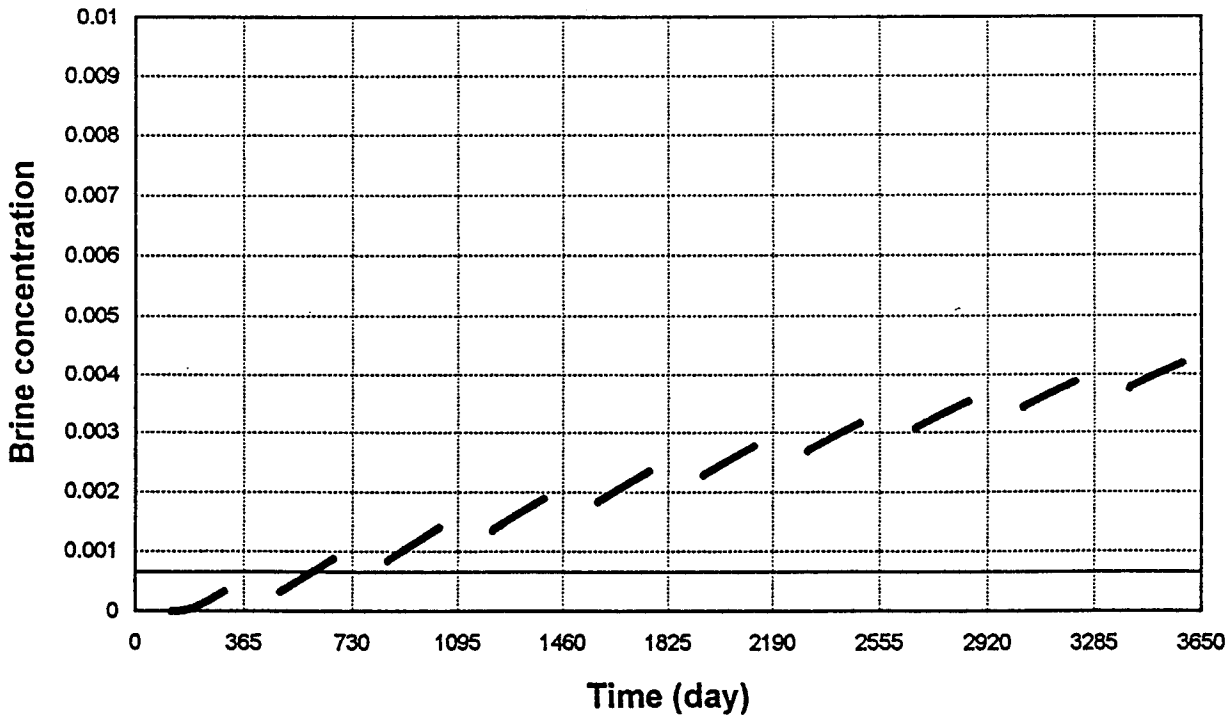

Figure 23. The relationship of discharged brine concentration versus time for side and bottom boundary conditions from the 10 years simulation. Pumping rate is 400 gpm and recharge is 2 in./yr. Chloride concentration of 500 mg/L is represented by the solid horizontal line.
(0.036 brine concentration is equivalent to 28,000 mg/L chloride concentration)

A: Side boundary condition

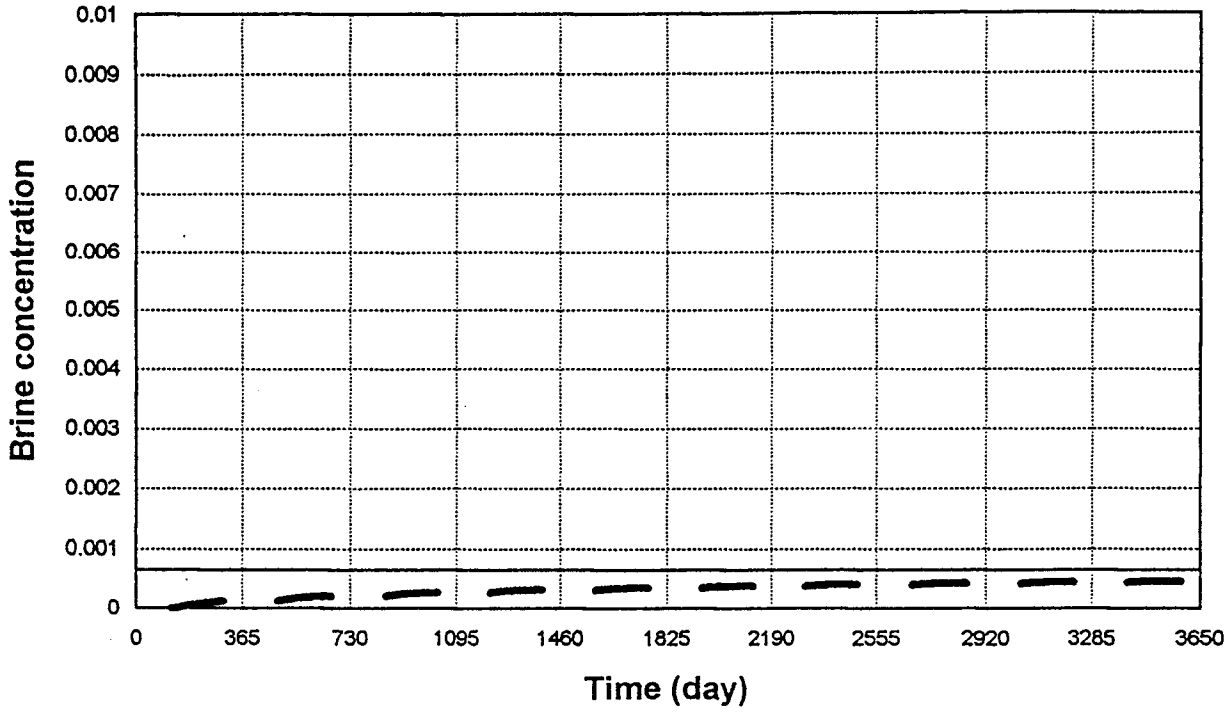

B: Bottom boundary condition

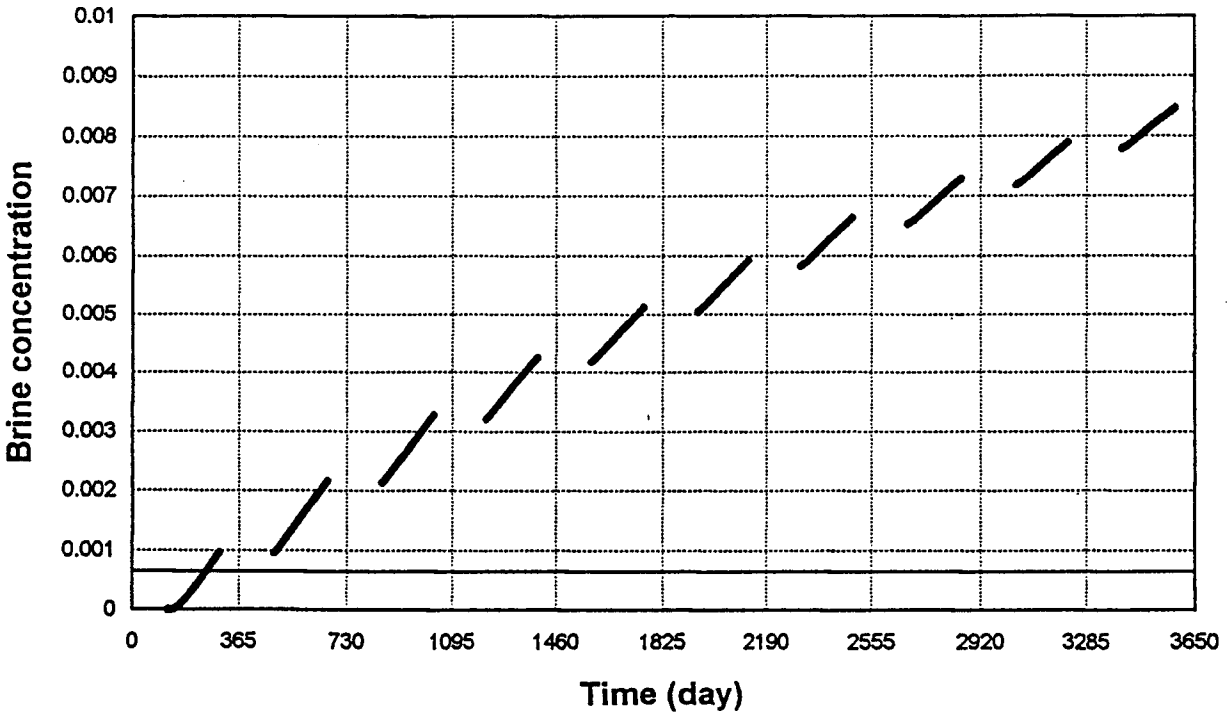

Figure 24. The relationship of discharged brine concentration versus time for side and bottom boundary conditions from the 10 years simulation. Pumping rate is 800 gpm and recharge is 2 in./yr. Chloride concentration of 500 mg/L is represented by the solid horizontal line
(0.036 brine concentration is equivalent to 28,000 mg/L chloride concentration)

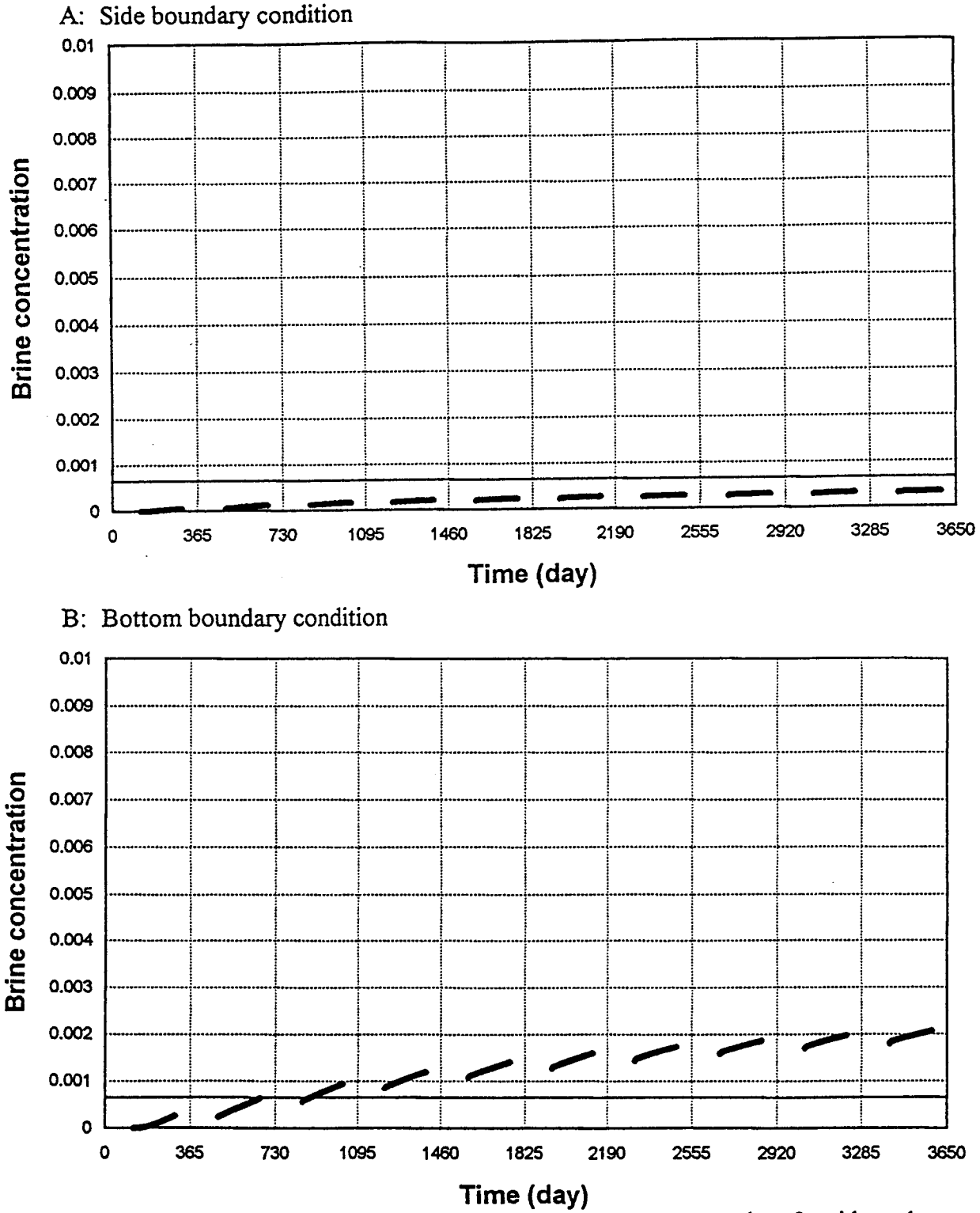

Figure 25. The relationship of discharged brine concentration versus time for side and bottom boundary conditions from the 10 years simulation. Pumping rate is 400 gpm and recharge is 5 in./yr. Chloride concentration of 500 mg/L is represented by the solid horizontal line
(0.036 brine concentration is equivalent to 28,000 mg/L chloride concentration)

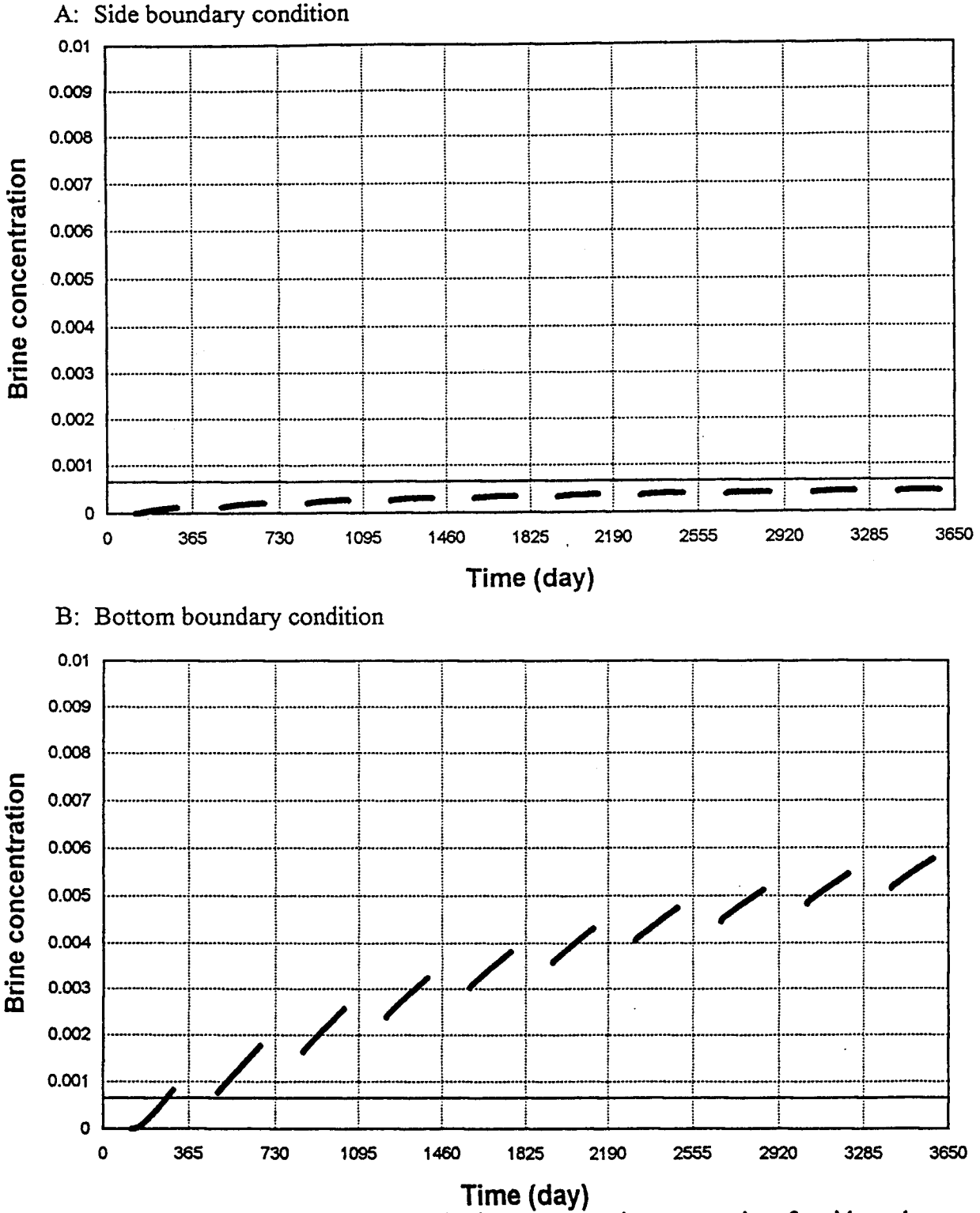

Figure 26. The relationship of discharged brine concentration versus time for side and bottom boundary conditions from the 10 years simulation. Pumping rate is 800 gpm and recharge is 5 in./yr. Chloride concentration of 500 mg/L is represented by the solid-horizontal line
(0.036 brine concentration is equivalent to 28,000 mg/L chloride concentration)

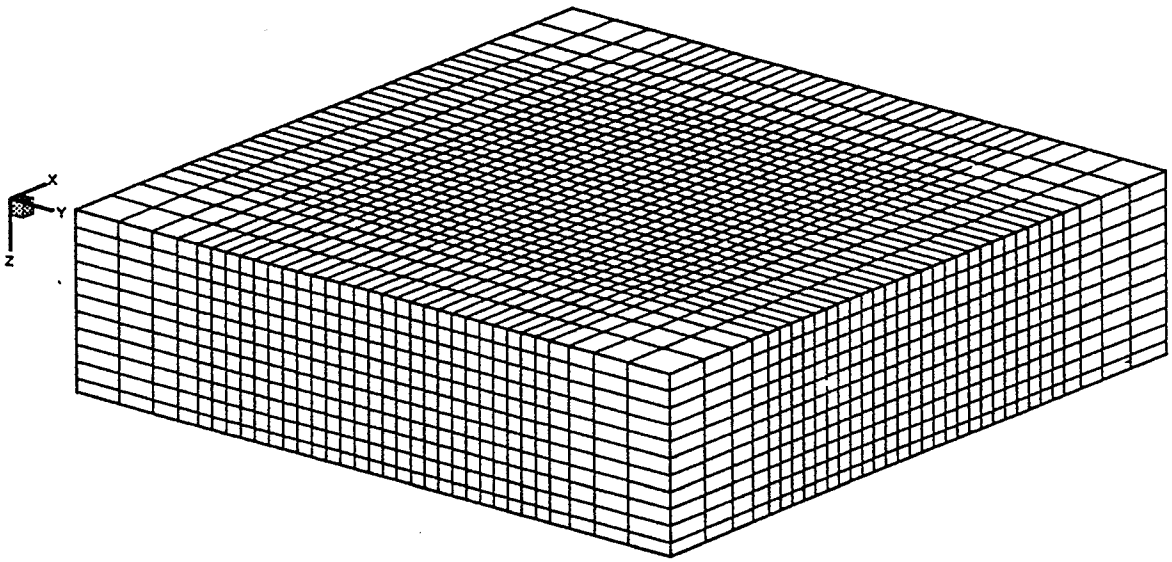

Figure 27. A three-dimensional mesh of the study area with variable spacing in X, Y, and Z directions.

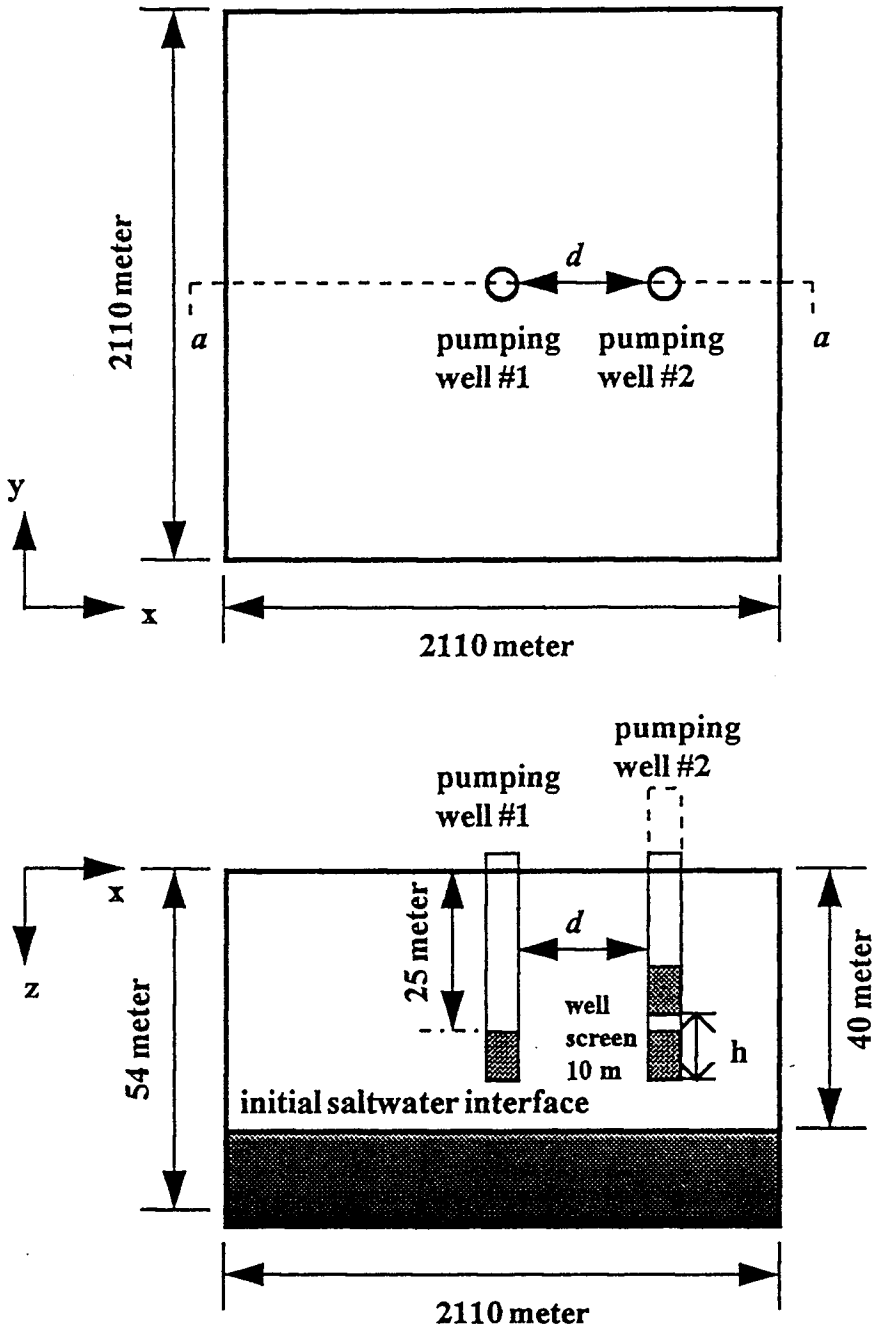

Figure 28. A conceptual two-pumping-well system for saltwater upconing simulation with variable separation distance, *d*, and location of well screen, *h*, by changing the position of pumping well #2.

however, well #2 is placed with separation distance, *d*, 100 m, 300 m, and 500 m away from the #1 well. The physical system of the three-well case is shown in Fig. 29, where wells #2 and #3 are placed symmetrically with separation distance, *d*, 100 m, 300 m, and 500 m on both sides of well #1. The total simulation period is one year with time-step equal to 5 days. Three different pumpage rates, 400 gpm, 800 gpm, and 1600 gpm, are applied throughout the simulation period. All the wells are screened from 25 to 35 meters below the initial water table. Results are presented in terms of the average brine concentration versus time. Table 6 shows the values of variables and parameters used in the simulation, and seven basic simulation cases are considered and briefly summarized in Table 7.

Case #1 is the simulation of the saltwater upconing under a single pumping well with three different pumpage rates. The simulation results are used as the reference for later comparisons. Case #2 is the simulation of the saltwater upconing under two pumping wells with separation distances, *d*, of 100 meters, 300 meters, and 500 meters between the two pumping wells. Case #3 is the simulation of the saltwater upconing under three pumping wells, where wells #2 and #3 are placed symmetrically on both sides of well #1 with separation distances, *d*, of 100 meters, 300 meters, and 500 meters. All the above simulations are performed with three different pumpage rates (400 gpm, 800 gpm, and 1600 gpm) to investigate how the water salinity on well #1 is affected by pumping well #2 and the combination of pumping wells #2 and #3. Simulation results are presented graphically by plotting brine concentration versus time; the brine concentration is calculated from well #1 by taking a five-day total mass of discharged salt divided by the total mass of pumpage during the same time period.

Without the protection of a clay layer, the upconing of saltwater will be significant. The results of single-well, two-well, and three-well systems under 400 gpm continuous pumpage are shown in Figs. 30A and B. Similarly, Figs. 31A and B and Figs. 32A and B are the simulation results with 800 gpm and 1600 gpm pumpage, respectively. As can be seen from these results, the interactions of water salinity between two wells and three wells are inversely proportional to their separation distance, *d*. The two-well and three- well systems considered in this study show that when

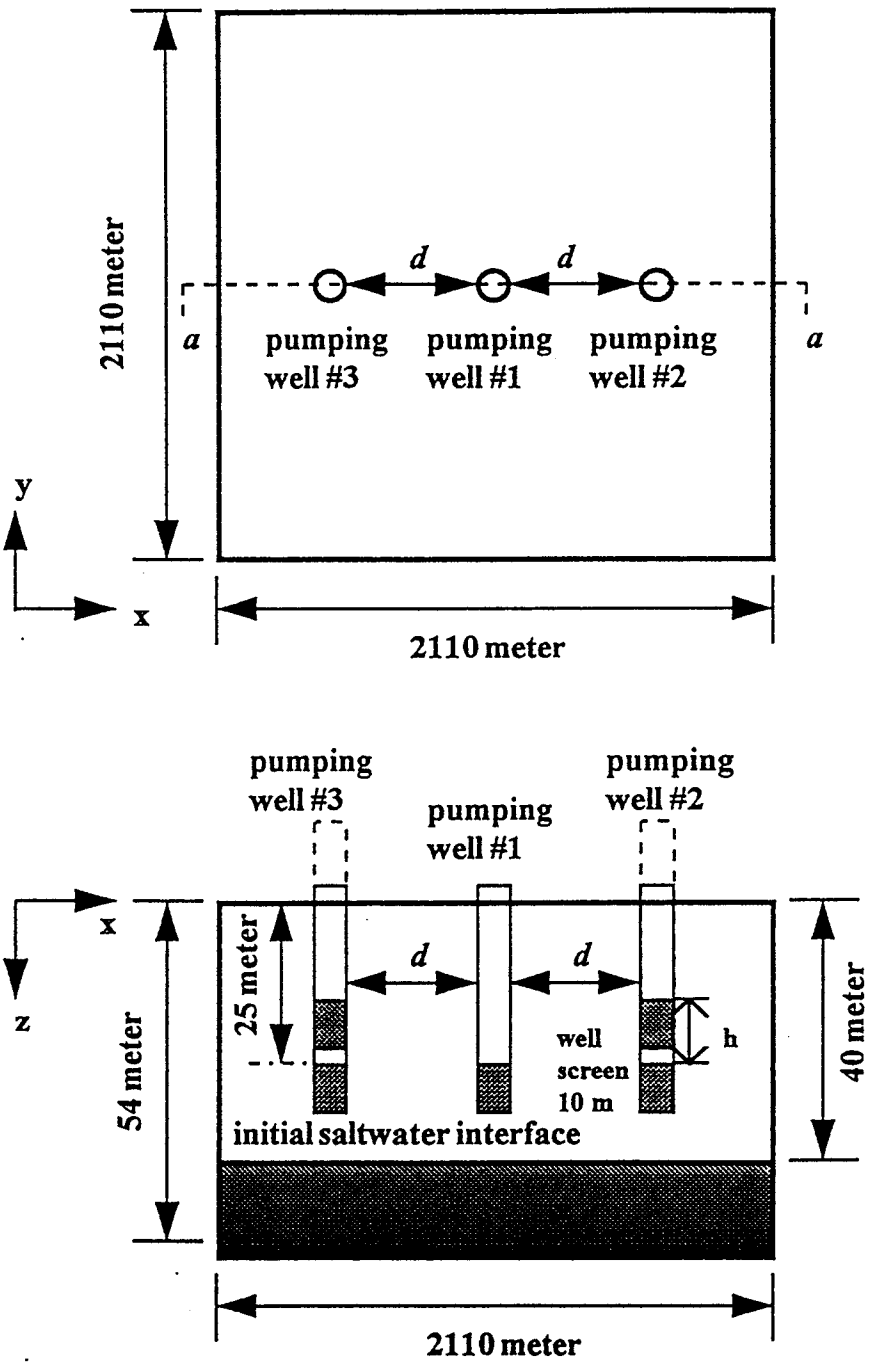

Figure 29. A conceptual three-pumping-well system for saltwater upconing simulation with variable separation distance, *d*, and location of well screen, *h*, by symmetrically changing the positions of pumping wells #2 and #3.

Table 6. Variables and parameters used in three-dimensional, multi-well system for saltwater-upconing simulation.

Aquifer, Fluid, and other Parameters	
horizontal hydraulic conductivity	Kh = 23 m/d (75 ft/d)
vertical hydraulic conductivity	Kz = 2.3 m/d (7.5 ft/d)
porosity	$\phi = 0.15$
bulk porous matrix compressibility	$\alpha = 2.58 \times 10^{-7}[kg/(m\ s^2)]^{-1}$
water compressibility	$\beta = 4.40 \times 10^{-10}[kg/(m\ s^2)]^{-1}$
solute molecular diffusivity	$D_m = 1.0 \times 10^{-10}\ m^2/s$
longitudinal dispersivity	$\alpha_L = 8$ m
transverse dispersivity	$\alpha_T = 1$ m
fluid (water) density	$\rho_o = 1{,}000\ kg/m^3$
brine density	$\rho = 1{,}036\ kg/m^3$
solid grain density	$\rho_s = 2{,}650\ kg/m^3$
fluid (water) viscosity	$\mu = 1.0 \times 10^{-3}\ kg/(m\ s)$
initial fluid (freshwater) salt concentration	$C_0 = 0$
initial brine fluid salt concentration	C (x,y,z,0); variable
initial specified pressure at the boundary	p(x, y, z, 0); variable
saturated thickness	b = 54 m
depth to freshwater/saltwater interface	40 m
depth to Permian boundary	54 m
pumping rate	$Q_p\ (m^3/s)$; variable
gravitational acceleration	$g = 9.81\ m/s^2$
total simulation time	1 yr
well screen depth location	25 to 35 m
clay layer	no

Table 7. Case scenarios in three-dimensional saltwater-upconing simulation.

Case No.	Description
1.	Single-well system with three different pumpage rates, 0.025 m^3/s, 0.05 m^3/s, and 0.1 m^3/s (400 gpm, 800 gpm, and 1600 gpm). Simulation area: 2110 m by 2110 m; depth dimension: 54 m.
2.	Two-well system with separation distances, *d*, between two wells equal to 100 m, 300 m, and 500 m (Fig. 28). Three different pumpage rates, 0.025 m^3/s, 0.05 m^3/s, and 0.1 m^3/s (400 gpm, 800 gpm, and 1600 gpm), are used.
3.	Three-well system with two wells placed symmetrically on both sides of the central well with separation distances, *d*, between wells equal to 100 m, 300 m, and 500 m (Fig. 29). Three different pumpage rates, 0.025 m^3/s, 0.05 m^3/s, and 0.1 m^3/s (400 gpm, 800 gpm, and 1600 gpm), are used.
4.	Two-well system with separation distances, *d*, between two wells equal to 100 m, 300 m, and 500 m (Fig. 28). The screen location of well #2 is shifted up 15 meters; two different pumpage rates, 0.025 m^3/s and 0.05 m^3/s (400 gpm and 800 gpm), are used.
5.	Three-well system with two wells placed symmetrically on both sides of the central well with separation distances, *d*, between wells equal to 100 m, 300 m, and 500 m (Fig. 29). The screen location of wells #2 and #3 are shifted up 15 meters and two different pumpage rates, 0.025 m^3/s and 0.05 m^3/s (400 gpm and 800 gpm), are used.
6.	Same as Case #1, but simulation area is reduced to 1250 m x 1250 m and only one pumpage, 0.05 m^3/s (800 gpm), is applied for the entire simulation.
7.	Same as Case #3, but simulation area is reduced to 1250 m x 1250 m, and only one separation distance (d = 500 m) and one pumpage rate, 0.05 m^3/s (800 gpm), are used.

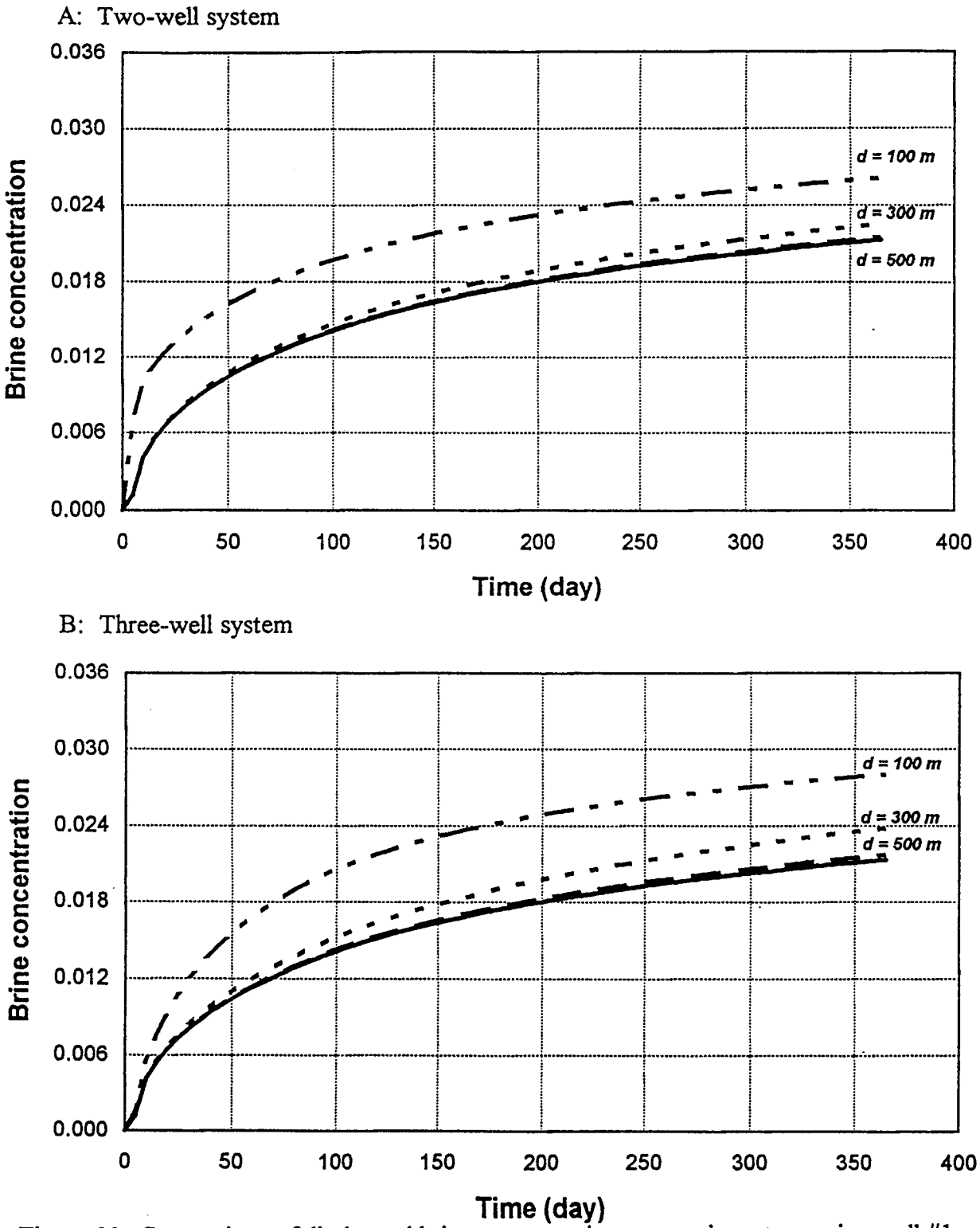

Figure 30. Comparison of discharged brine concentration versus time at pumping well #1 with 400 gpm continuous pumping rate and three different separation distances (100m, 300m, and 500m). The solid line is the result of a single-well system with same pumping rate.
(0.036 brine concentration is equivalent to 28,000 mg/L chloride concentration)

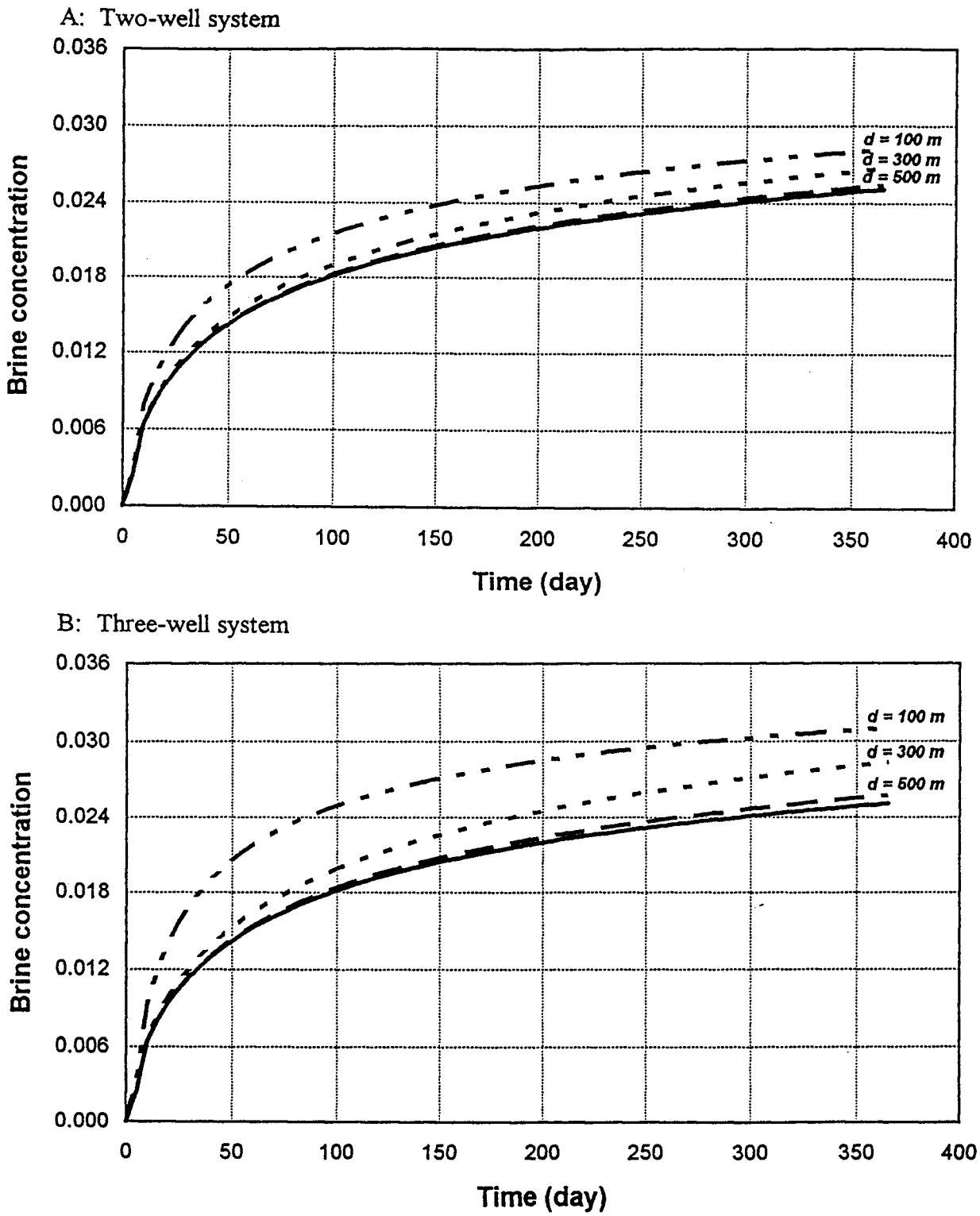

Figure 31. Comparison of discharged brine concentration versus time at pumping well #1 with 800 gpm continuous pumping rate and three different separation distances (100m, 300m, and 500m). The solid line is the result of a single-well system with same pumping rate.
(0.036 brine concentration is equivalent to 28,000 mg/L chloride concentration)

A: Two-well system

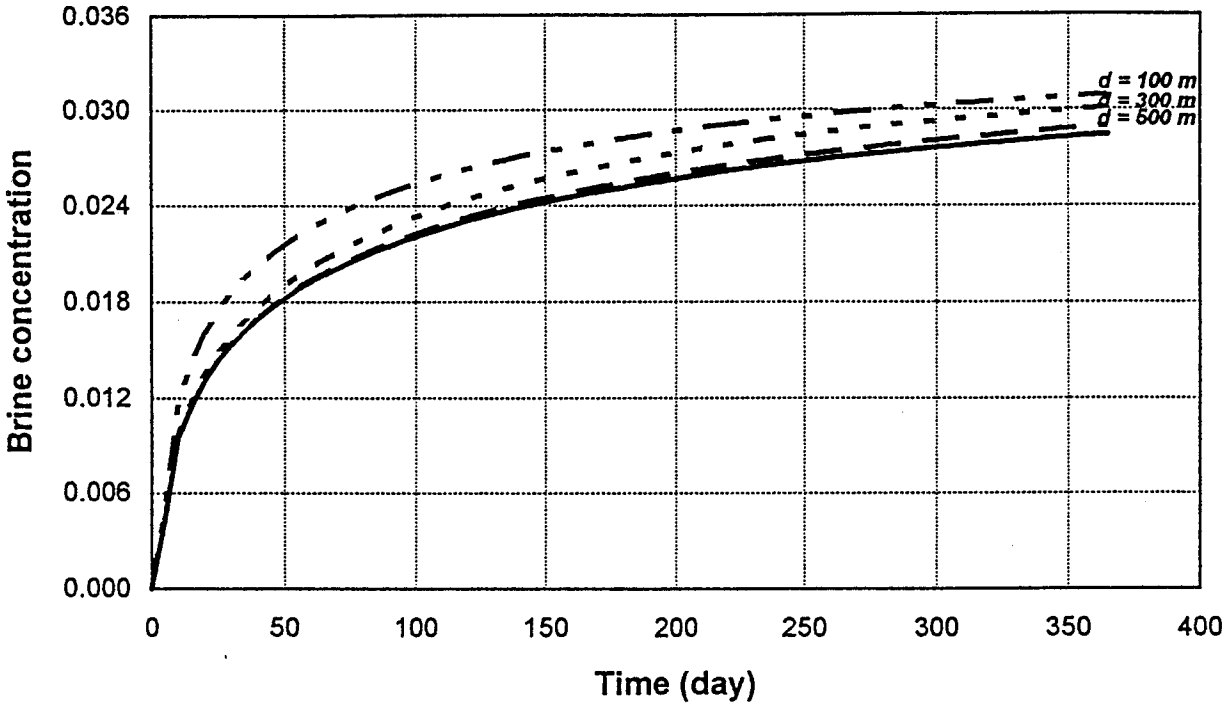

B: Three-well system

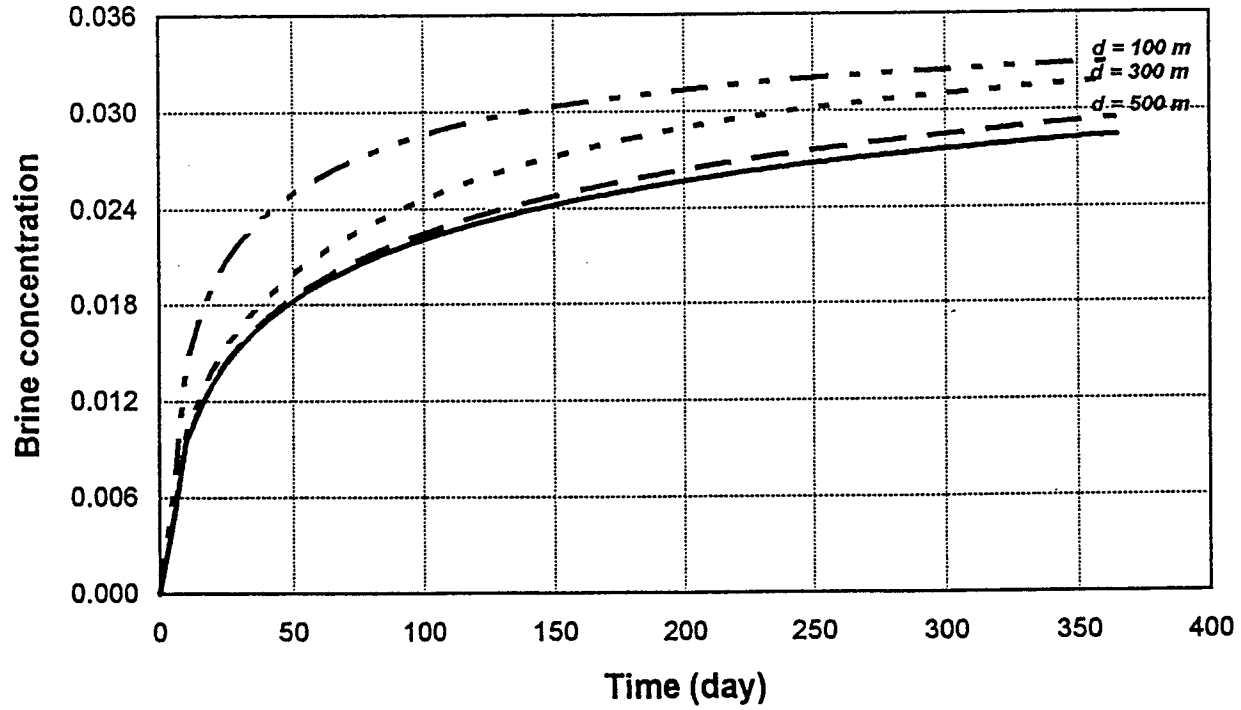

Figure 32. Comparison of discharged brine concentration versus time at pumping well #1 with 1600 gpm continuous pumping rate and three different separation distances (100m, 300m, and 500m). The solid line is the result of a single-well system with same pumping rate.
(0.036 brine concentration is equivalent to 28,000 mg/L chloride concentration)

the separation distance, d, is 500 meters, the interactions become insignificant. This implies that as the separation distance increases to a critical distance, each well will behave independently. However, the determination of the critical distance depends on many factors, such as aquifer parameters, recharge, pumping rate, etc. As expected, the interaction of water salinity on the three-well system is more significant than the two-well system; this is verified from the result that the average brine concentration on the three-well system is higher than the two-well system under the same pumpage.

Case #4 studies the well-screen location on the two-well system. Well #1 is pumped at a constant rate, 800 gpm, and screened from 25 m to 35 m below the initial water table. Well #2 is placed at three separation distances (100 m, 300 m, and 500 m), the well screen is elevated by 15 meters, and two pumping rates, 400 gpm and 800 gpm, are considered. Case #5 studies the location of well screen in a three-well system. It is similar to Case #4, except that well #3 is symmetrically placed at the opposite side of well #1 with three separation distances (100 m, 300 m, and 500 m); the well screen is also elevated by 15 meters, and two pumping rates, 400 gpm and 800 gpm, are considered. The results of two- and three-well systems at separation distances 100 m, 300 m, and 500 m are shown in Figs. 33, 34, and 35, respectively. The discharged brine concentration on well #1 from the result of Fig. 33A (800 gpm pumping rate and 100 meters separation distance from the nearby irrigation wells) is significantly increased as a result of the additional pumping wells. However, the increase of the separation distance or the decrease of the pumping rate of the nearby irrigation wells will reduce the saltwater problem, as is indicated in the case of lower pumping rate in combination with the larger separation distance (400-gpm pumping rate and 500-meters separation distance of the nearby irrigation wells, Fig. 35B), which shows the least influence on well #1.

Case #6 studies the influence of brine concentration in a single-well system using side boundary conditions by reducing the simulation area size from 2110 m x 2110 m to 1250 m x 1250 m; however, the depth is still 54 meters. The new simulation area is meshed as 25x25x11, with uniform spacing of 50 meters in the X-Y direction and the same grid spacing in the Z

A: 800 gpm pumping rate for wells #2 and #3

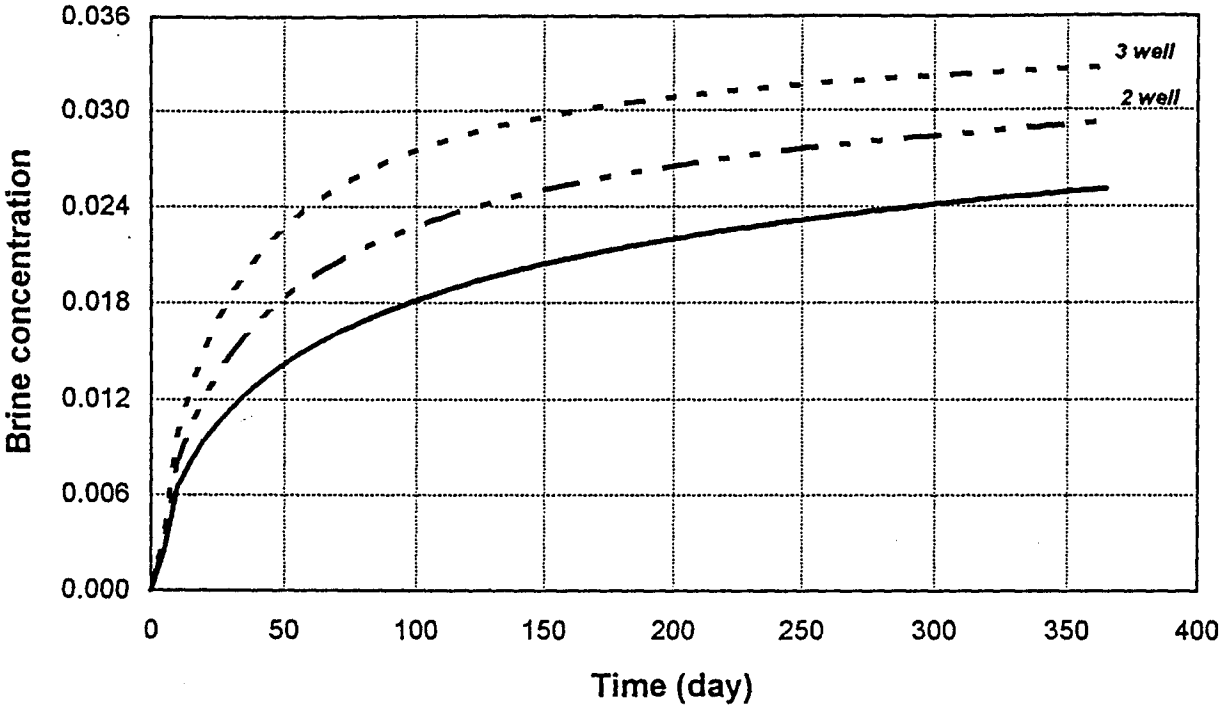

B: 400 gpm pumping rate for wells #2 and #3

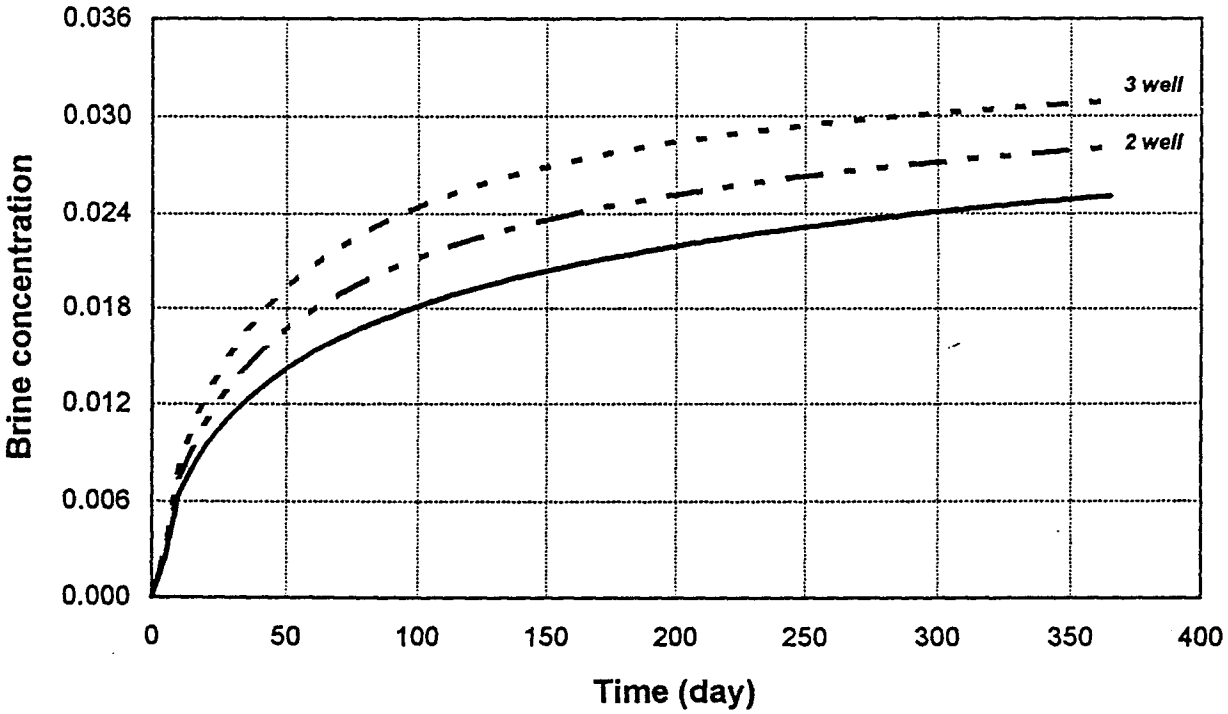

Figure 33. Comparison of discharged brine concentration versus time at pumping well #1 with 800 gpm continuous pumping rate. Two different pumping rates (400 gpm and 800 gpm) at wells #2 and #3. Separation distance is 100 meters and wells #2 and #3 are elevated by 15 meters. The solid line is the result of a single-well system with 800 gpm pumping rate.
(0.036 brine concentration is equivalent to 28,000 mg/L chloride concentration)

A: 800 gpm pumping rate for wells #2 and #3

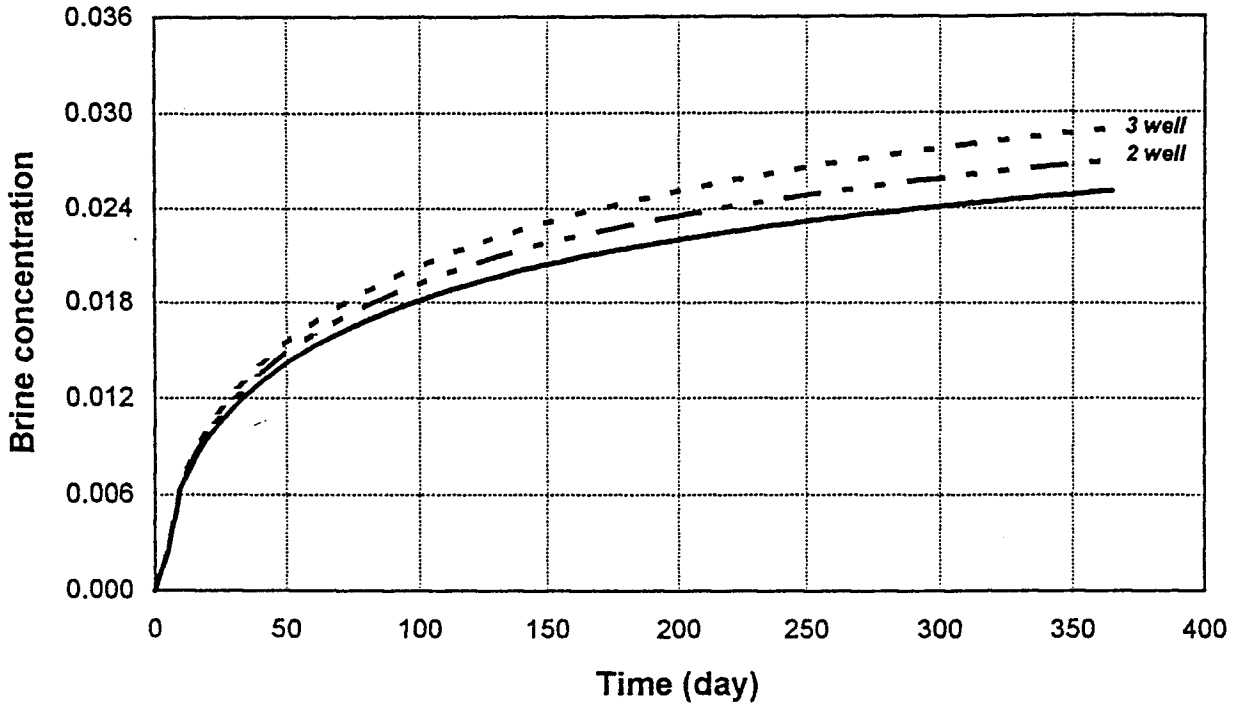

B: 400 gpm pumping rate for wells #2 and #3

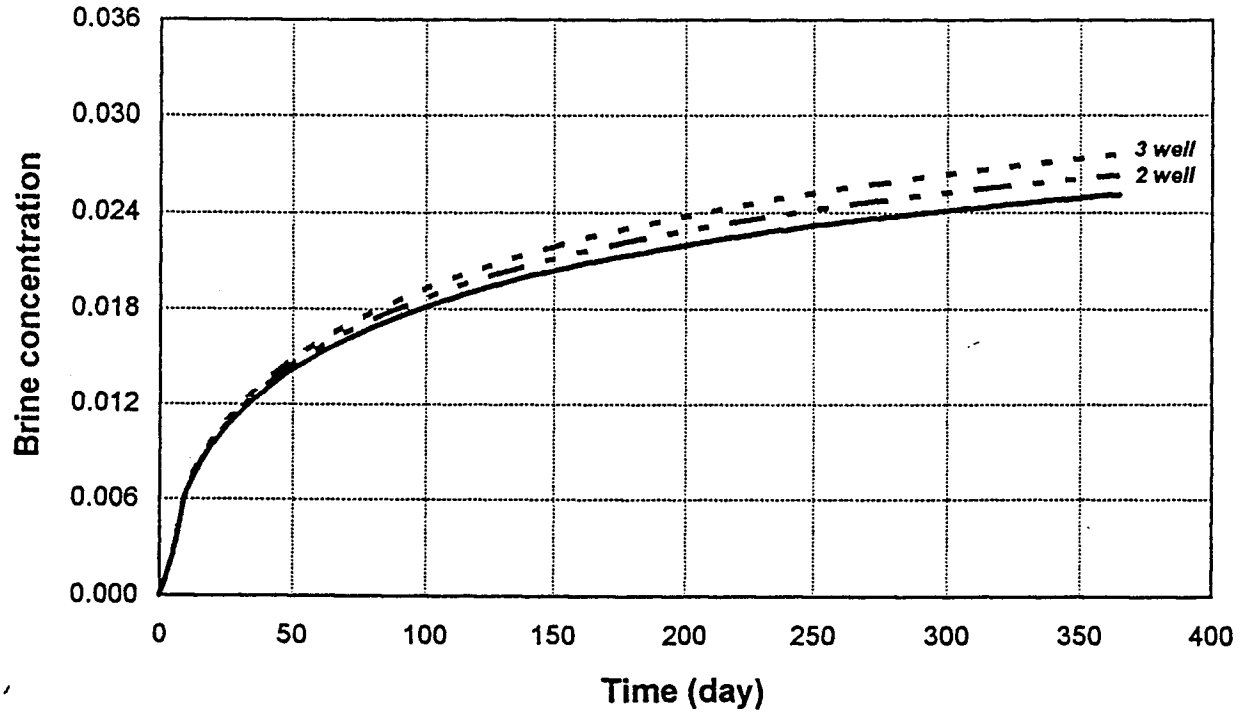

Figure 34. Comparison of discharged brine concentration versus time at pumping well #1 with 800 gpm continuous pumping rate. Two different pumping rates (400 gpm and 800 gpm) at wells #2 and #3. Separation distance is 300 meters and wells #2 and #3 are elevated by 15 meters. The solid line is the result of a single-well system with 800 gpm pumping rate.
(0.036 brine concentration is equivalent to 28,000 mg/L chloride concentration)

A: 800 gpm pumping rate for wells #2 and #3

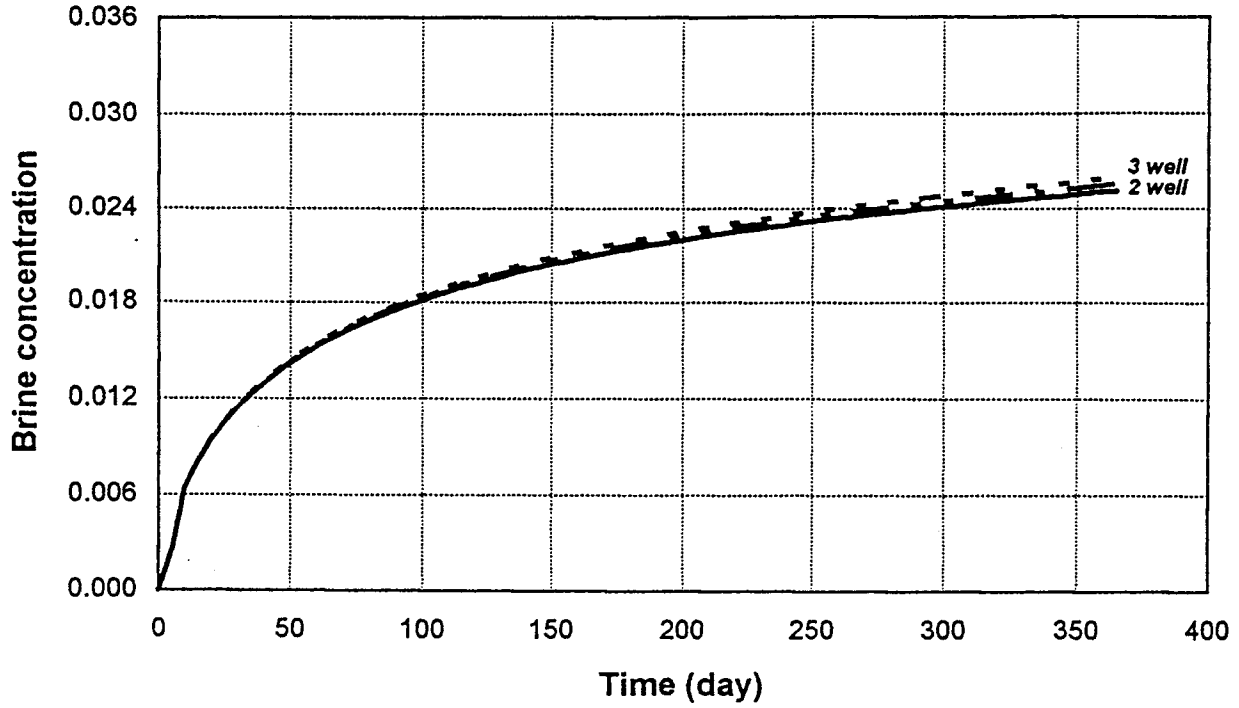

B: 400 gpm pumping rate for wells #2 and #3

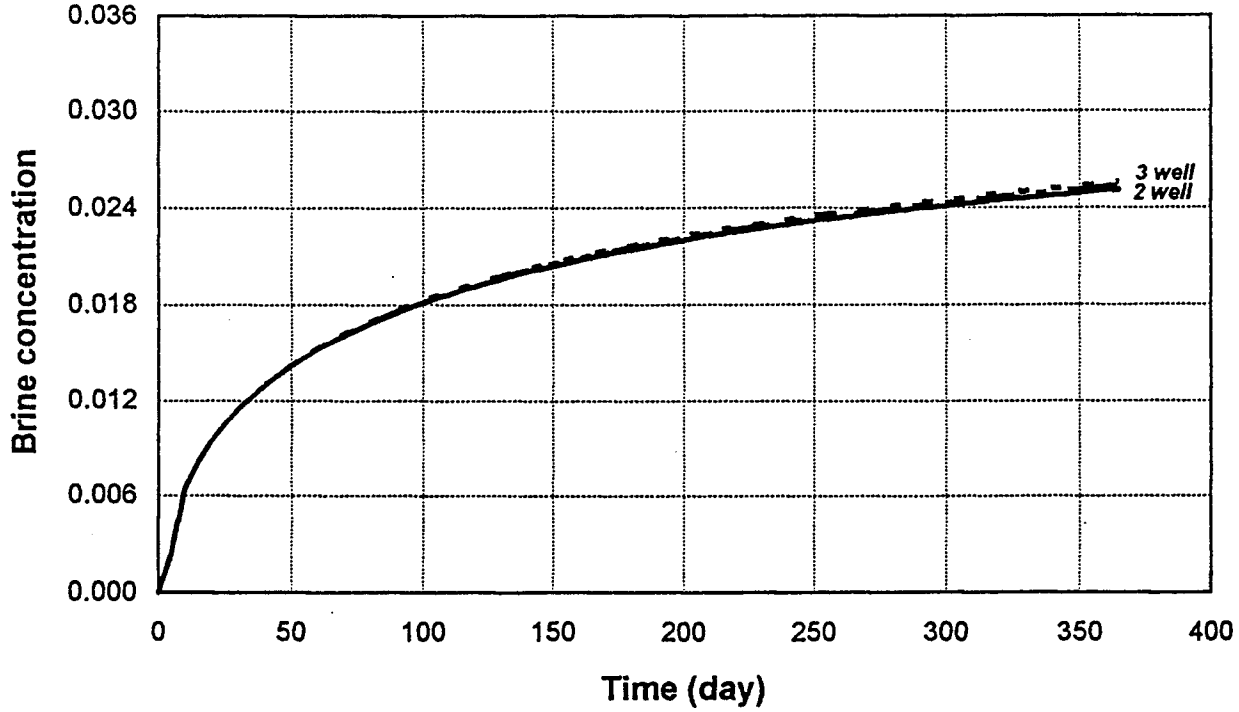

Figure 35. Comparison of discharged brine concentration versus time at pumping well #1 with 800 gpm continuous pumping rate. Two different pumping rates (400 gpm and 800 gpm) at wells #2 and #3. Separation distance is 500 meters and wells #2 and #3 are elevated by 15 meters. The solid line is the result of a single-well system with 800 gpm pumping rate.
(0.036 brine concentration is equivalent to 28,000 mg/L chloride concentration)

direction as the previous cases. Similarly, Case #7 studies the three-well system and the separation distance, *d*, is 500 meters. A continuous pumpage of 800 gpm is used for both cases. The results are displayed as the 0.01, 0.015, and 0.02 isobar-concentration contours at the 300th simulation day by taking the simulated values of brine concentration from the central cross section, *a-a*, of the models (Figs. 28 and 29). Figs. 36A and B are the brine-concentration contours of the original single-well system and the reduced size system, respectively. Similarly, Figs. 37A and B are the brine-concentration contours of the original three-well system and the reduced-size system. For Case #6, the pumping well is 600 meters away from both edges. The similarity of the results from Figs. 36A and B indicates that the edge effect is insignificant. For Case #7, wells #2 and #3 are only 100 meters away from the edge (i.e., they are very close to the edge). As can be seen in Fig. 37B, the strong influence from the edge effects deteriorates the simulation results. However, the results in Fig. 37A are unaffected from edge effects because pumping wells #2 and the #3 are still far away from the edge.

Calibration of Three-Dimensional Model

Because of computer-storage limitations and stability considerations for the numerical model, the study area for three-dimensional simulation is chosen to be approximately 2 mi x2 mi, with the Siefkes site located at the center. The locations and annual maximum pumpage of wells at the Siefkes site are shown in Fig. 38. The purpose of this study is to simulate the migration of saltwater under the influence of regional flow, pumpage, and recharge. A three-dimensional finite difference model is adopted for this numerical simulation.

The initial water level, topography of the bedrock, and the location of saltwater/freshwater interface can be estimated using geostatistic techniques as described in the 1994 progress report of the mineral intrusion project (Ma and Sophocleous, 1994). The aquifer parameters (hydraulic conductivity, porosity, dispersivity, etc.) and the distribution of clay layers are uncertain due to the limited field data. Therefore, the determination of the aquifer parameters and the distribution of clay layers will be performed by numerous trial and error approaches before the numerical model can

A. Larger single-well system (2110 m x 2110 m x 60 m)

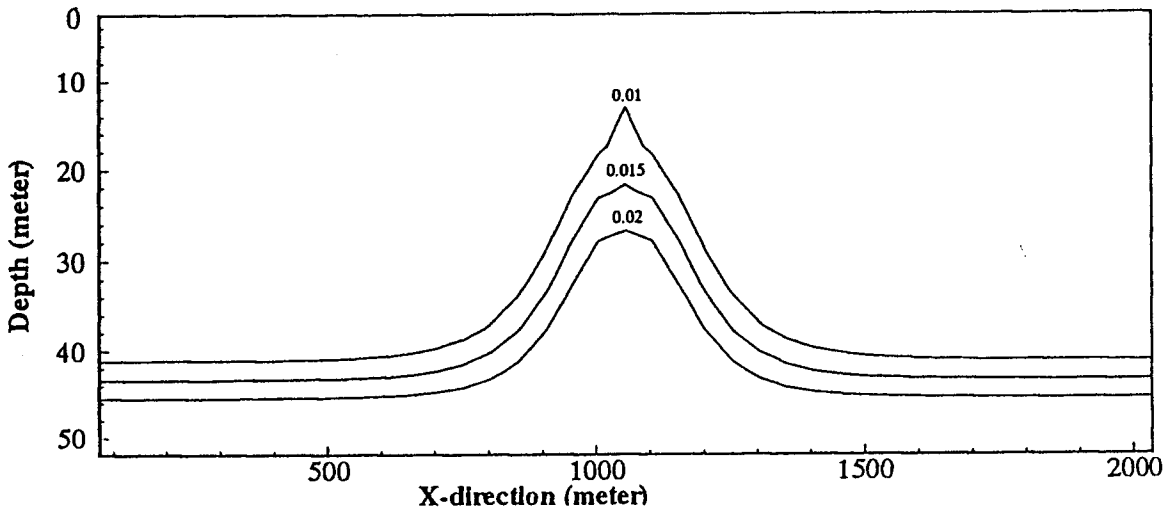

B. Smaller single-well system (1250 m x 1250 m x 60 m)

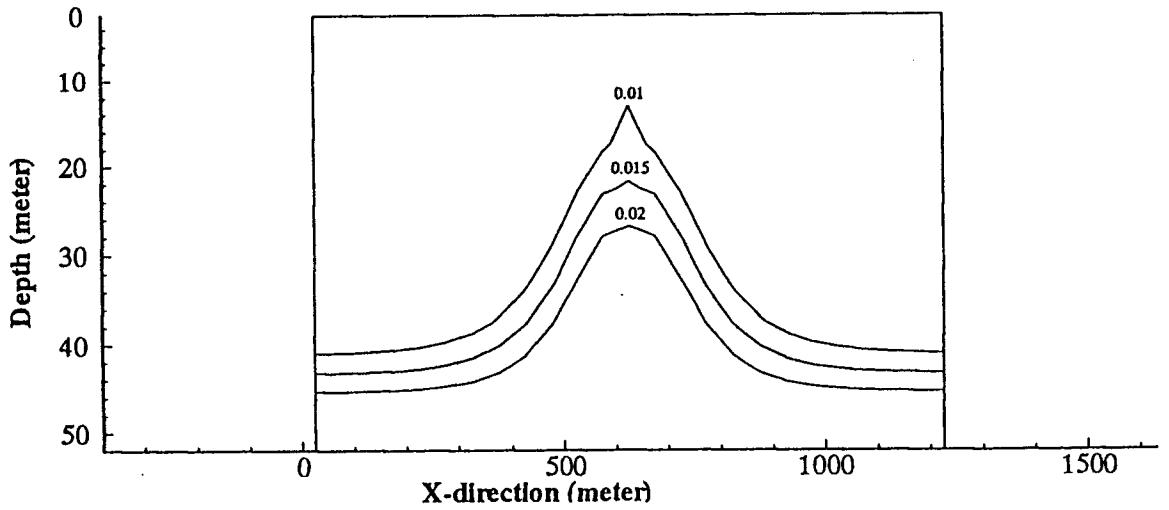

Figure 36. Isolines of brine concentration of single-well system at the 300th day of simulation with continuous 800-gpm pumping rate resulting from the central cross section, *a-a*, in Fig. 27 of conceptual model (0.036 brine concentration is equivalent to 28,000 mg/L chloride concentration).

A. Larger three-well system (2110 m x 2110 m x 60 m)

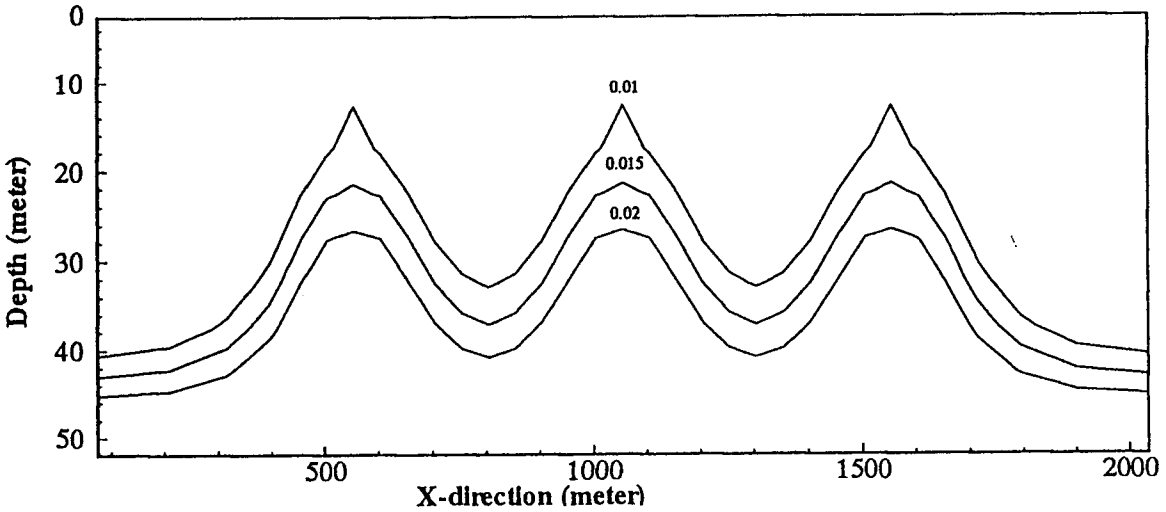

B. Smaller three-well system (1250 m x 1250 m x 60 m)

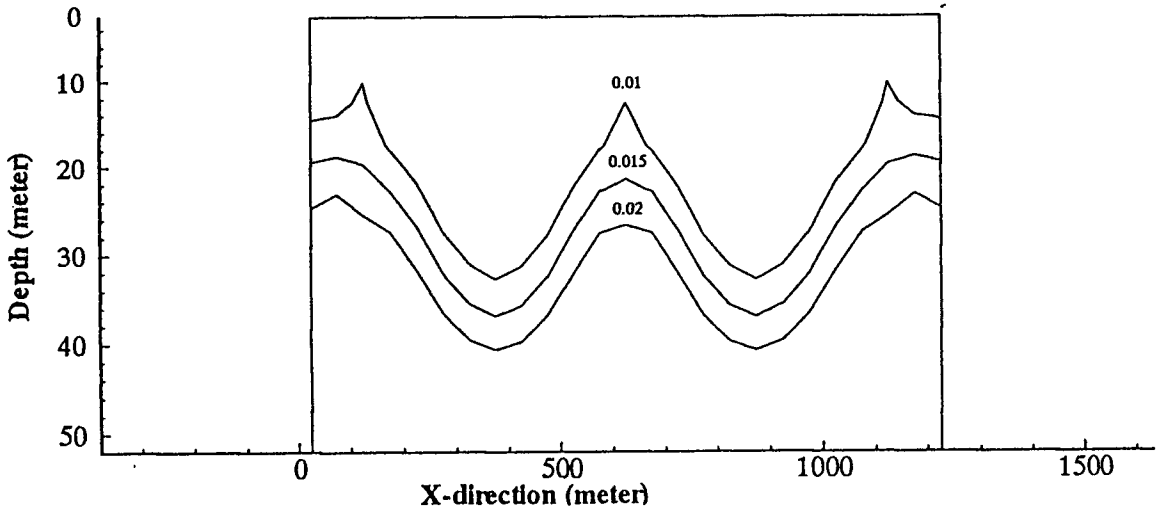

Figure 37. Isolines of brine concentration of three-well system at the 300th day of simulation with continuous 800-gpm pumping rate resulting from the central cross section, *a-a,* in Fig. 28 of conceptual model. The separation distance between wells is 500 meters (0.036 brine concentration is equivalent to 28,000 mg/L chloride concentration).

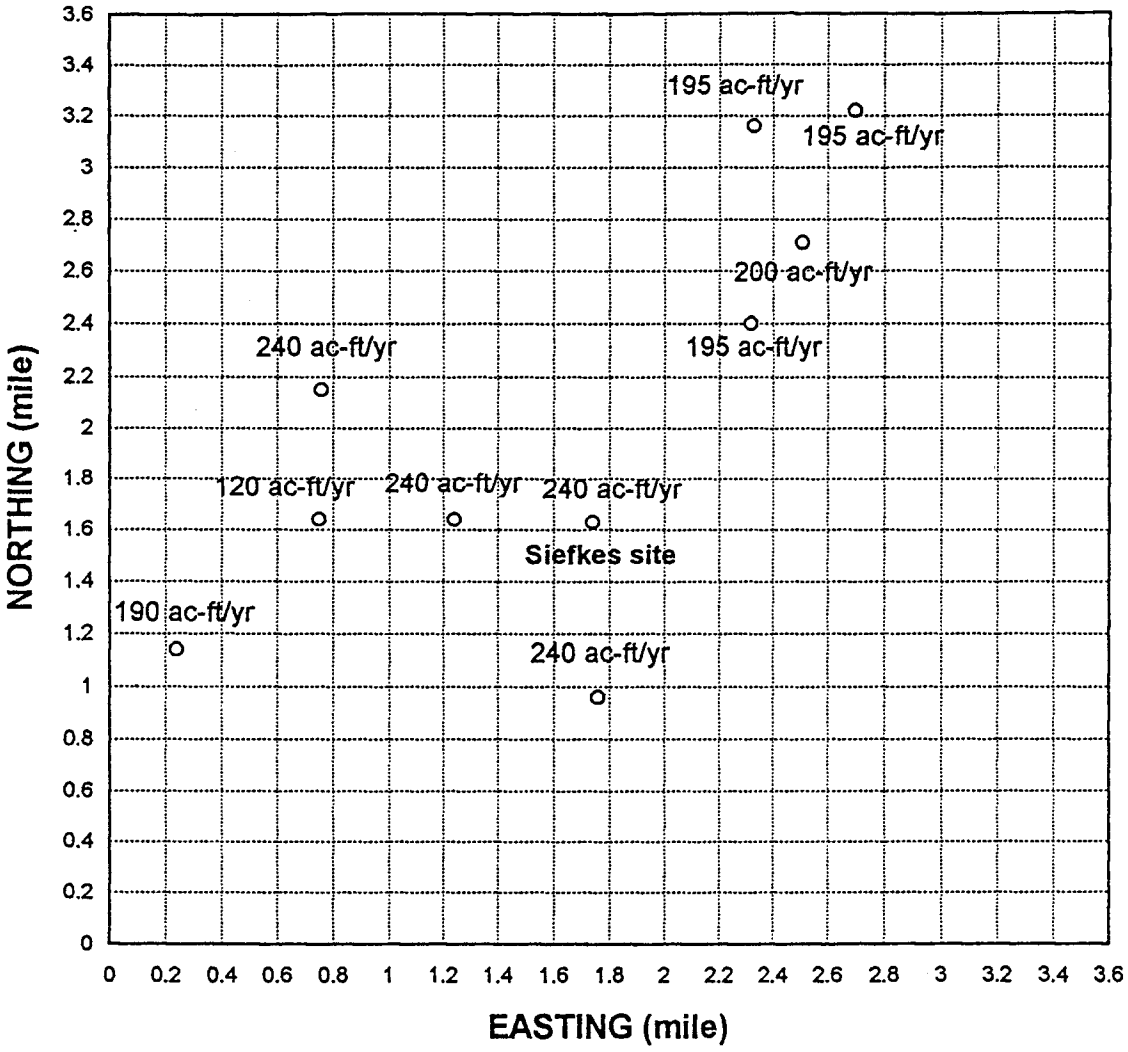

Figure 38. The locations and yearly maximum pumpages of wells at the Siefkes site.

reasonably describe the flow and saltwater movement in the simulation area. Because no natural boundaries exist for the 2 mi x 2 mi simulation area, the following approach is proposed to handle the boundary conditions for the model area. Water-level data from predevelopment to 1994 will be compiled. A statistical analysis will be conducted to investigate the variation of water levels over the years, and the most appropriate boundary conditions will be determined. The source of salt is assumed to be derived from the highly mineralized Permian bedrock.

With all the considerations discussed above, calibration of the three-dimensional model will be an extremely cumbersome and time-consuming task. In this study, the three-dimensional model will be simplified to predict the general trend of saltwater movement in the study area. The results will be presented based on the relationship between pumping rate and discharged brine concentration at the Siefkes site. This investigation is still in progress and the final results will be discussed in a later report.

Conclusions

The investigation of saltwater intrusion was studied in this report. The use of the axisymmetrical model to simulate the single-well system provides great detail in terms of the influence of aquifer parameters and the location of clay layers. However, the actual aquifer system is not axisymmetrical, and the interaction of the saltwater upconing from nearby pumping activities may be significant depending on the separation distance and pumping rate of the nearby pumping wells. This situation makes a three-dimensional saltwater-intrusion model the more appropriate approach. The following are some conclusions from the above study:

1. The saltwater upconing is sensitive to the pumping rate, hydraulic conductivity, and the location of well screen.

2. The influence of the recharge may not be noticeable when the local pumping is activated, however, the recovery from the saltwater upconing will become significant during the nonpumping period and enhanced by recharge.

3. The clay layer serves as a protection that greatly retards the upward movement of the saltwater under pumping stress.

4. The degree of saltwater upconing is greatly influenced by the boundary conditions. In other words, the source of salt is from local bedrock or lateral inflow.

5. The interaction of nearby pumping wells is proportional to the pumping rate and is inversely proportional to the separation distance.

6. Without consideration of recharge, the saltwater upconing will eventually affect the well if the well pumping is extended to a period of time. However, the problem of saltwater intrusion can be alleviated or even disappear if appreciable amounts of recharge can be received by the aquifer.

7. The three-dimensional model provides a better approach to describing the natural process of saltwater intrusion, and the use of the three-dimensional model for predicting the movement of the saltwater and the effect of multipumping will be emphasized in our next report.

References

Bear, J., "On the Tensor Form of Dispersion," Journal of Geophysical Research, Vol. 66, No. 4, 1961, pp. 1185-1197.

Buddemeier, R. W., Garneau, G., Healey, J. M., Ma, T. S., Sophocleous, M. A., Whittemore, D. O., Young, D., and Zehr, D., "The Mineral Intrusion Project: Report of Progress During Fiscal Year," 1993, 157 pp.

Frind, E. O., "The Principal Direction Technique: A New Approach to Groundwater Contaminant Transport Modeling. In: Finite Elements in Water Resources," Proceedings of the 4th International Conference, Hanover, Springer-Verlag, Berlin, 1982, pp. 13/25-13/42.

Garneau, G. W., Buddemeier, R. W., and Young, D. P., "Characterization of the Saltwater Interface and Related Parameters," Kansas Geological Survey, Open-File Report 94-28b, 1994.

Ma, T. S., and Sophocleous, M. A., "Simulations of Saltwater Upconing in the Great Bend Prairie Unconfined Aquifer," Kansas Geological Survey, Open-File Report 94-28f, 1994.

Price, H. S., Varga, R. S., and Warren, J. E., "Application of Oscillation Matrices to Diffusion-Convection Equations," Journal of Mathematics and Physics, Vol. 45, No. 3, 1966, pp. 301-311.

Reeves, M., Ward, D. S., Johns, N. D., and Cranwell, R. M., "Theory and Implementation for SWIFT II, the Sandia Water-Isolation Flow and Transport Model for Fractured Media," Rep. NUREG/CR-3328 and SAND83-1159, Sandia National Lab., Albuquerque, N. M., 1986.

Scheidegger, A. E., "General Theory of Dispersion in Porous Media," Journal of Geophysical Research, Vol. 66, No. 10, 1961, pp. 153-162.

Sophocleous, M. A., "Comparative Review and Synthesis of Ground-Water Recharge Estimates for the Great Bend Prairie Aquifer of Kansas," Kansas Geological Survey Bulletin 235, 1993, pp. 41-54.

Varga, R. S., "Matrix Iterative Analysis," Prentice-Hall, Inc., Englewood Cliffs, N. J., 1962, 322 pp.

Williams, J., "Oceanography," Little, Brown and Co., Boston, 1962.